SIGNAL TIMING OPTIMIZATION TO IMPROVE AIR QUALITY

A Dissertation

by

JINPENG LV

Submitted to the Office of Graduate Studies of
Texas A&M University
in partial fulfillment of the requirements for the degree of

DOCTOR OF PHILOSOPHY

Approved by:

Chair of Committee,	Yunlong Zhang
Committee Members,	Sergiy Butenko
	Luca Quadrifglio
	Cliff Spiegelman
	Joe Zietsman
Head of Department,	John Niedzwecki

December 2012

Major Subject: Civil Engineering

ABSTRACT

This study develops an optimization methodology for signal timing at intersections to reduce emissions based on MOVES, the latest emission model released by U.S. Environmental Protection Agency (EPA). The primary objective of this study is to bridge the gap that the research on signal optimization at intersections lags behind the development of emissions models. The methodology development includes four levels: the vehicle level, the movement level, the intersection level, and the arterial level.

At the vehicle level, the emission function with respect to delay is derived for a vehicle driving through an intersection. Multiple acceleration models are evaluated, and the best one is selected in terms of emission estimations at an intersection. Piecewise functions are used to describe the relationship between emissions and intersection delay.

At the movement level, emissions are modeled if the green time and red time of a movement are given. To account for randomness, the number of vehicle arrivals during a cycle is assumed to follow Poisson distributions. According to the numerical results, the relative difference of emission estimations with and without considering randomness is usually smaller than 5.0% at a typical intersection of two urban arterials.

At the intersection level, an optimization problem is formulated to consider emissions at an intersection. The objective function is a linear combination of delay and emissions at an intersection, so that the tradeoff between the two could be examined with the optimization problem. In addition, a convex approximation is proposed to approximate the emission calculation; accordingly, the optimization problem can be

solved more efficiently using the interior point algorithm (IPA). The case study proves that the optimization problem with this convex approximation can still find appropriate optimal signal timing plans when considering traffic emissions.

At the arterial level, emissions are minimized at multiple intersections along an arterial. First, discrete models are developed to describe the bandwidth, stops, delay, and emissions at a particular intersection. Second, based on these discrete models, an optimization problem is formulized with the intersection offsets as decision variables. The simulation results indicate that the benefit of emission reduction become more and more significant as the number of intersections along the arterial increases.

ACKNOWLEDGEMENTS

I would like to express my sincere gratitude and appreciation to my committee chair, Dr. Yunlong Zhang, for his guidance and support in the past years, without which this work cannot be made possible. I would also like to thank Dr. Sergiy Butenko, Dr. Luca Quadrifoglio, Dr. Cliff Spiegelman, and Dr. Joe Zietsman for serving in my Ph.D. committee and for their precious comments on this dissertation.

I also want to extend my gratitude to Dr. Bruce Wang and Mr. Kai Yin for the discussion on optimization methods and MATLAB programming. In addition, I would like to thank Mr. David Zeng, Mr. Qing Miao, Mr. Yajie Zou, and Mr. Zhi Chen for their help with VISSIM simulation, data collection, and data reduction.

Thanks also go to my friends and colleagues and the department faculty and staff for making my time at Texas A&M University a great experience.

Finally, many thanks to my parents for their encouragement and sustaining love.

TABLE OF CONTENTS

Page

LIST OF FIGURES

Page

LIST OF TABLES

Page

Page

Page

1. INTRODUCTION

In the U.S., traffic has become a major cause of emissions. According to an Environmental Protection Agency (EPA) report in 2005, on road traffic contributes 58.8% of Carbon Monoxide (CO), 35.5% of Nitrogen Oxides (NO), and 25.8% of Volatile Organic Compounds (VOCs) to the total emissions (Environmental Protection Agency, 2005).

Especially in urban areas, major intersections along arterials typically involve the highest traffic density, the longest vehicle idling time, and the most deceleration and acceleration. These intersections are often "hot spots" of air pollution and have negative environmental and health impacts on vulnerable objects such as hospitals, schools, and office buildings in the vicinity. Reducing traffic at these intersections is often infeasible, but properly timing signals can often provide air quality benefits by reducing vehicle stops and speed changes and emissions accordingly.

Therefore, the objective of this study is to develop an optimization methodology for signal timing at intersections to reduce emissions. Such signal timing needs emission models that can estimate emissions from such parameters describing traffic dynamics (as speed, delay, stops, acceleration time, etc.). The rest of this section reviews emission models and emission related studies at intersections in details.

1.1 Emission Models

1.1.1 MOBILE

The development of traffic emission models dates back to the 1970s. The oldest version of MOBILE models was developed in 1978 (Environmental Protection Agency, 2003). After that, EPA devoted continuous efforts to update and improve MOBILE models based on the increasing availability of computer technology and emission data, and its latest version is MOBILE6.2.

MOBILE6.2 was widely accepted in practices for two reasons. First, all on road traffic types were included in MOBILE6.2, including light-duty cars and trucks, heavy-duty trucks, motorcycles, and buses. Second, MOBILE6.2 could estimate various types of emissions such as CO, Hydrocarbon (HC), NO, particulates, and greenhouse gases. MOBILE6.2 had been used to generate state implementation plan (SIP) inventories for conformity determinations, emissions trend predictions, environmental impact studies, and emission reduction strategy development. For example, Figure 1 illustrates the overview of CO SIP emission modeling. Both on and off road emissions could be estimated by MOBILE6.2. In addition, considering point source emissions and the emission dispersion, the emission concentration was estimated with the attainment threshold, and the conformity could be determined. However, MOBILE6.2 was not very interactive because it mainly worked in the DOS system. An input file must be prepared in DOS text format, and inputs needed to be placed in the correct columns.

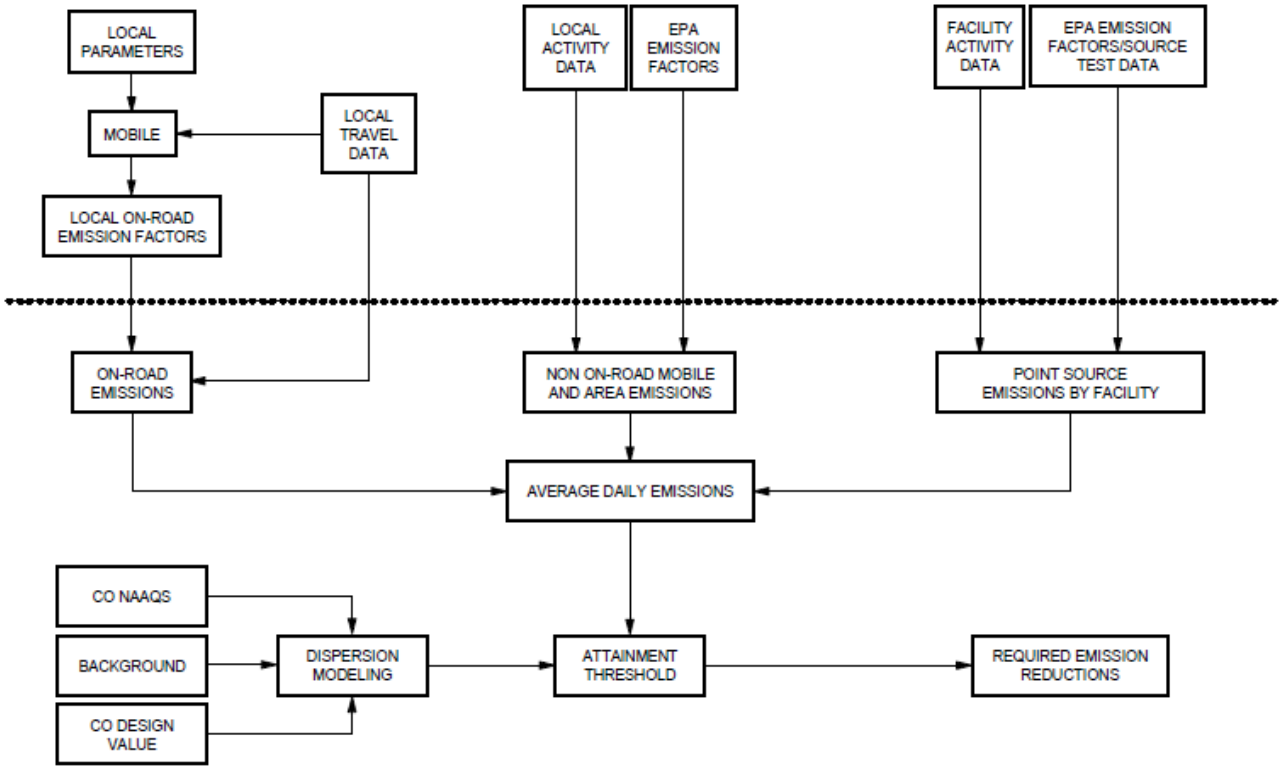

Figure 1 Overview of CO SIP emissions modeling (Environmental Protection Agency, 2001)

For the on road emission estimation, the most important input for MOBILE6.2 was the vehicle speed. MOBILE6.2 defined 14 speed bins with the lowest nominal speed equal to 2.5 mph and the highest nominal speed equal to 65 mph, as shown in Table 1. Figure 2 provides an example of emission estimations (CO) based on these speed bins (Zhang et al., 2010). As the speed increases, the emission rate first decreases and then gradually increases. The optimal speed with the minimum emission rate is around 30 mph. In MOBILE6.2, all emission rates were reported ultimately in terms of grams per mile (g/mi).

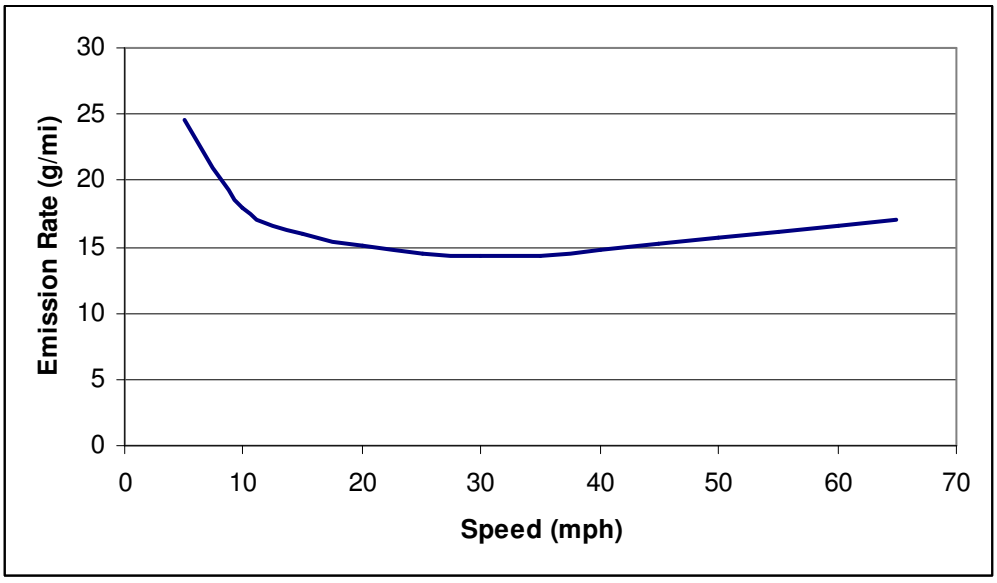

Figure 2 An example of emission estimations according to speed bins

Table 1 Average speed ranges for speed bins (Environmental Protection Agency, 2003)

Number	Abbreviation	Description
1	2.5 mph	Miles with average speed 0-2.5 mph
2	5 mph	Miles with average speed 2.5-7.5 mph
3	10 mph	Miles with average speed 7.5-12.5 mph
4	15 mph	Miles with average speed 12.5-17.5 mph
5	20 mph	Miles with average speed 17.5-22.5 mph
6	25 mph	Miles with average speed 22.5-27.5 mph
7	30 mph	Miles with average speed 27.5-32.5 mph
8	35 mph	Miles with average speed 32.5-37.5 mph
9	40 mph	Miles with average speed 37.5-42.5 mph
10	45 mph	Miles with average speed 42.5-47.5 mph
11	50 mph	Miles with average speed 47.5-52.5 mph
12	55 mph	Miles with average speed 52.5-57.5 mph
13	60 mph	Miles with average speed 57.5-62.5 mph
14	65 mph	Miles with average speed >62.5 mph

Many studies implemented MOBILE6.2 to evaluate or control on road emissions. For example, Lin and Ge (2006) used the cell-transmission model to capture traffic characteristic, MOBILE6.2 to estimate emissions, and the Gaussian dispersion model to predict roadside emission concentrations. Zhang et al. (2010) presented a methodology for regulating traffic flows under air quality constraints in metropolitan areas, where air quality was assessed using MOBILE6.2.

However, one shortcoming of MOBILE6.2 made these studies less convincing: MOBILE6.2 is macroscopic. It estimates emissions based on only one parameter of traffic dynamics that is average speeds, so the emission estimations neglect the impact of individual vehicle stops and accelerations. Accordingly, such estimations lose accuracy in microscopic scenarios, e.g., at an intersection. Recognizing this deficiency, modern emission models were developed in the microscopic view such as Comprehensive Modal Emission Model (CMEM), North Carolina State University emission model (NCSU model), and MOtor Vehicle Emission Simulator (MOVES).

1.1.2 CMEM

CMEM was developed by the University of California at Riverside (UC-Riverside). It was funded by the National Cooperative Highway Research Program (NCHRP) and the EPA. CMEM was considered microscopic because it can provide emission estimations for individual vehicles second-by-second (Barth et al., 2000). CMEM classified vehicles into 26 categories, as shown in Table 2. In each category, the emission rate was determined by the vehicle speed and acceleration. The lookup tables

of CO, NO, and HC could be generated from CMEM's basic core modal emissions model. The CMEM vehicle category 11 represents the light duty vehicles. An example of CO lookup table is presented in Figure 3.

Table 2 Vehicle categories in CMEM (Barth et al., 2000)

Category #	Vehicle Technology Category
	Normal Emitting Cars
1	No Catalyst
2	2-way Catalyst
3	3-way Catalyst, Carbureted
4	3-way Catalyst, FI, >50K miles, low power/weight
5	3-way Catalyst, FI, >50K miles, high power/weight
6	3-way Catalyst, FI, <50K miles, low power/weight
7	3-way Catalyst, FI, <50K miles, high power/weight
8	Tier 1, >50K miles, low power/weight
9	Tier 1, >50K miles, high power/weight
10	Tier 1, <50K miles, low power/weight
11	Tier 1, <50K miles, high power/weight
24	Tier 1, >100K miles
	Normal Emitting Trucks
12	Pre-1979 (<=8500 GVW)
13	1979 to 1983 (<=8500 GVW)
14	1984 to 1987 (<=8500 GVW)
15	1988 to 1993, <=3750 LVW
16	1988 to 1993, >3750 LVW
17	Tier 1 LDT2/3 (3751-5750 LVW or Alt. LVW)
18	Tier 1 LDT4 (6001-8500 GVW, >5750 Alt. LVW)
25	Gasoline-powered, LDT (> 8500 GVW)
40	Diesel-powered, LDT (> 8500 GVW)
	High Emitting Vehicles
19	Runs lean
20	Runs rich
21	Misfire
22	Bad catalyst
23	Runs very rich

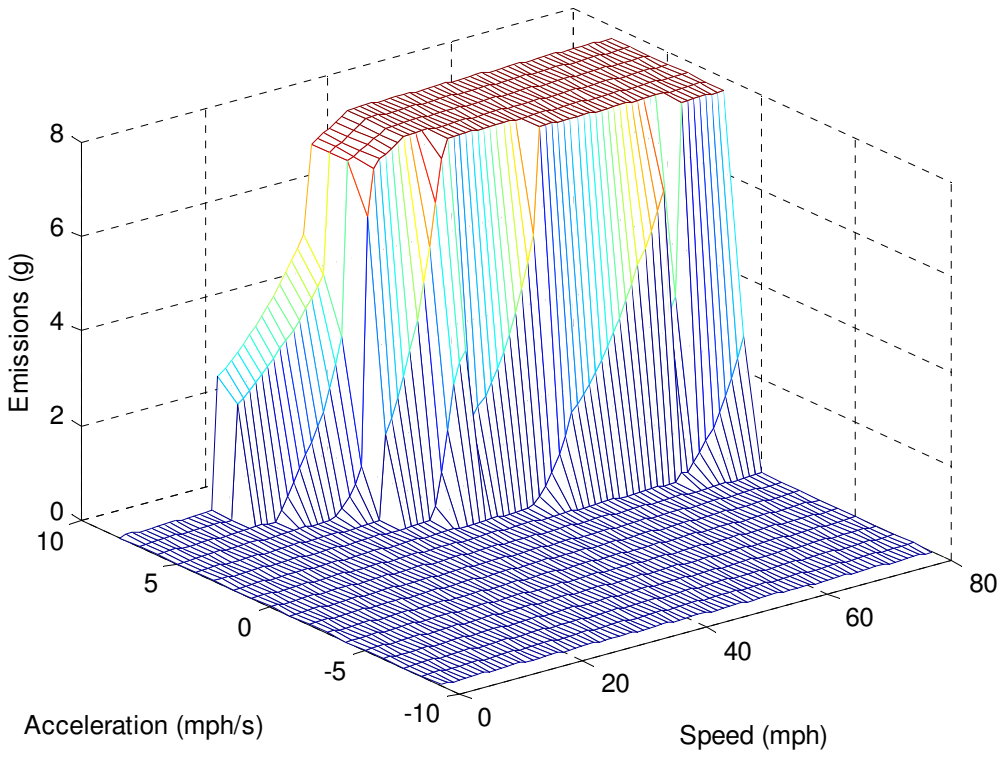

Figure 3 Category 11 speed/acceleration-indexed CO lookup table according to CMEM

CMEM developers suggested integrating these lookup tables with a microscopic traffic simulation model because the computational costs were very low (Barth et al., 2000). Boriboonsomsin and Barth (2008) integrated CMEM with a microscopic traffic simulation model PARAMICS to compare vehicle emissions caused by two types of HOV lane configurations: continuous access and limited access HOV lanes. Simulation results demonstrated that continuous access HOV lanes always performed better in light of emissions. Stevanovic et al. (2010) integrated CMEM with another microscopic traffic simulation model VISSIM to optimize signal timings and minimize fuel

consumptions and emissions. However, CMEM has not been widely used in practices. One reason might be that too many lookup tables needed to be updated periodically corresponding to different CMEM categories and combination situations of speed and acceleration, and such updates needed excessive data and cost.

1.1.3 NCSU Model

North Carolina State University developed another microscopic model, which is referred to as the NCSU model in this study. The NCSU model was sponsored by the North Carolina Department of Transportation. Data were collected on Chapel Hill Road between August and October 2000 (Frey et al., 2003). Over one hundred one-way trips were archived, and onboard systems were used to provide representative real-world emission measurements. The NCSU model determined emission rates of a vehicle according to its operating modes. According to the data availability, the operating modes were classified into 4 categories: idling, acceleration, deceleration, and cruise. In the NCSU model, the driving mode is considered to be idling when both the measured speed and acceleration are zero. The driving mode is acceleration when the measured acceleration is at least 2 mph/s for 1 second or 1 mph/s for 3 consecutive seconds. The driving mode is deceleration when the measured acceleration is at most -2 mph/s for 1 second or -1 mph/s for 3 consecutive seconds. The driving mode that does not belong to any of these three categories is considered to be cruise. Some emission rates according to driving modes are summarized in Table 3.

Table 3 Emission rates according to different driving modes (Coelho et al., 2005a)

Mode	Emission Rate (mg/s)		
	CO	HC	NO
Idling	1.5	0.25	0.1
Acceleration	22.5	1.1	1.5
Deceleration	7.5	0.4	0.5
Cruise	10	0.6	1.25

The data used to develop the NCSU model was limited: only passenger vehicles and road conditions in a small area were considered. Accordingly, not many studies had applied the NCSU model. Ceolho et al. (2005a; 2005b) applied the NCSU model to evaluate emission effects of certain transportation facilities, such as toll stations and speed control signals. However, the concept of operating modes was accepted by EPA and was subsequently applied to the development of MOVES (Environmental Protection Agency, 2002).

1.1.4 MOVES

MOVES is the newest microscopic model. It was recently updated by the EPA in 2010. The EPA recommends replacing MOBILE6.2 with MOVES2010 to estimate on road mobile source emissions. MOVES is also a mode based model, but its classification of vehicle operating modes is more elaborate than the NCSU model. MOVES defines a new parameter, vehicle specific power (VSP), in the classification of modes. Based on VSP and speeds, MOVES classifies 23 vehicle operating modes, as shown in Table 4

(Environmental Protection Agency, 2009). Figure 4 shows an example of emission rates for light duty vehicles (LDVs) at vehicle operating modes.

Table 4 Definition of vehicle operating modes (Environmental Protection Agency, 2009)

Operating Mode	Operating Mode Description	Vehicle-Specific Power (VSP*t*, kW/tonne)	Vehicle Speed (v_t,mi/hr)	Vehicle Acceleration (a, mi/hr-sec)
0	Deceleration/Braking			$a_t \leq$ -2.0 OR ($a_t <$ -1.0 AND $a_{t-1} <$-1.0 AND $a_{t-2} <$-1.0)
1	Idle		-1.0 $\leq v_t <$ 1.0	
11	Coast	$VSP_t < 0$	0 $\leq v_t <$ 25	
12	Cruise/Acceleration	0 $\leq VSP_t <$ 3	0 $\leq v_t <$ 25	
13	Cruise/Acceleration	3 $\leq VSP_t <$ 6	0 $\leq v_t <$ 25	
14	Cruise/Acceleration	6 $\leq VSP_t <$ 9	0 $\leq v_t <$ 25	
15	Cruise/Acceleration	9 $\leq VSP_t <$ 12	0 $\leq v_t <$ 25	
16	Cruise/Acceleration	12 $\leq VSP_t$	0 $\leq v_t <$ 25	
21	Coast	$VSP_t < 0$	25 $\leq v_t <$ 50	
22	Cruise/Acceleration	0 $\leq VSP_t <$ 3	25 $\leq v_t <$ 50	
23	Cruise/Acceleration	3 $\leq VSP_t <$ 6	25 $\leq v_t <$ 50	
24	Cruise/Acceleration	6 $\leq VSP_t <$ 9	25 $\leq v_t <$ 50	
25	Cruise/Acceleration	9 $\leq VSP_t <$ 12	25 $\leq v_t <$ 50	
27	Cruise/Acceleration	12 $\leq$ VSP < 18	25 $\leq v_t <$ 50	
28	Cruise/Acceleration	18 $\leq$ VSP < 24	25 $\leq v_t <$ 50	
29	Cruise/Acceleration	24 $\leq$ VSP < 30	25 $\leq v_t <$ 50	
30	Cruise/Acceleration	30 $\leq$ VSP	25 $\leq v_t <$ 50	
33	Cruise/Acceleration	$VSP_t < 6$	50 $\leq v_t$	
35	Cruise/Acceleration	6 $\leq VSP_t <$ 12	50 $\leq v_t$	
37	Cruise/Acceleration	12 $\leq$ VSP <18	50 $\leq v_t$	
38	Cruise/Acceleration	18 $\leq$ VSP < 24	50 $\leq v_t$	
39	Cruise/Acceleration	24 $\leq$ VSP < 30	50 $\leq v_t$	
40	Cruise/Acceleration	30 $\leq$ VSP	50 $\leq v_t$	

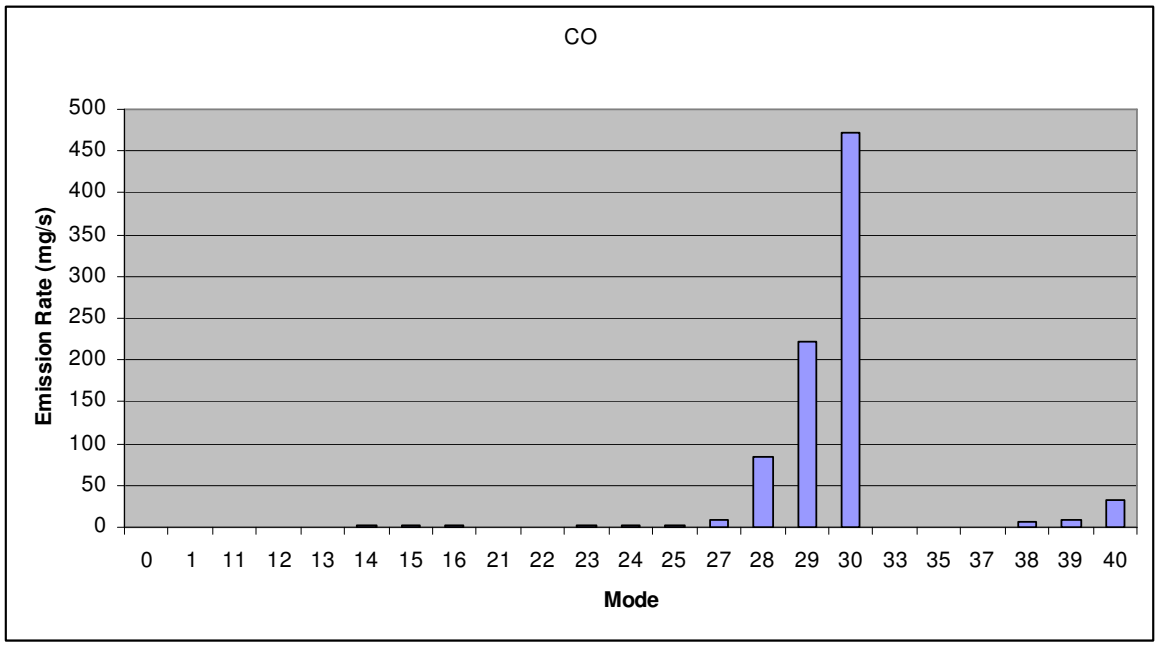

Figure 4 An example of CO emissions (Environmental Protection Agency, 2009)

MOVES is the latest emission model and has been recognized by EAP. As a result, many studies have applied MOVES to emission estimations recently, but these applications are usually simple and need to be further developed. For example, when investigating the effect of signal coordination on traffic emissions, Lv and Zhang (2012) used VISSIM to produce traffic data and then input these data to MOVES for emission estimations. Such a simple application of MOVES could generate excessive computer load. Therefore, advanced applications of MOVES should be developed for those complicated traffic problems considering emissions, e.g., signal optimization at an intersection or along an arterial.

1.2 Emissions at Intersections

Dating back to 1970s, the concerns with emissions at an intersection could be found in the EPA reports (Environmental Protection Agency, 1975; Midurski and Corbin, 1976). There have been many studies on intersection emissions since then. However, most of them computed emissions based on stops, delay, or queue length from macroscopic modeling of traffic. For example, Tarnoff and Parsonson (1979) translated emissions and fuel consumption from vehicle stops and delay when demonstrating the potential environmental benefits at intersections. CAL3QHC, an early computer program for emission predictions by the EPA, only required the number of vehicles involved in the queue as an input (Environmental Protection Agency, 1992). Hurley and Kalus (2007) studied signal timing and air quality using the data from more than one hundred intersections in New York State. The study concluded that improving the level of service (LOS) at those intersections, particularly increasing the number of intersections with LOS C or better, could significantly reduce emissions. TRANSYT-7F and SYNCHRO applied linear combinations of total vehicle mile traveled (VMT), delay, and stops to estimating fuel consumption and CO_2 emissions (Stevanovic et al., 2009).

According to modern emission models such as CMEM, the NCSU model, and MOVES, vehicles produce much more emissions during acceleration than during cruise, deceleration, or idling, so emission estimations from such macroscopic parameters as stops, delay, and queue length lack accuracy, especially in the intersection area involving intensive accelerations.

Therefore, Matzoros and Van Vliet (1992) and Coelho et al. (2005a) applied a more detailed method to emission estimation at an intersection with the consideration of motions of individual vehicles. This microscopic method groups the vehicle operating mode into four categories based on vehicle trajectories: cruise, deceleration, queuing, and acceleration (see Figure 5). Figure 5 illustrates four typical vehicle trajectories at an intersection. Trajectory 1, 2, and 3 represent those vehicles that queue at the intersection to different degrees, while Trajectory 4 represents a vehicle that does not stop when driving through the intersection. Those trajectories impacted by queue (i.e., Trajectory 1, 2, and 3 in Figure 5) are divided into several segments, respectively representing different operating modes in a chronological order: cruise, deceleration, queuing (this segment can be zero), acceleration, and cruise.

As discussed in Section 1.1, however, MOVES further classifies the operating mode into 23 categories (Environmental Protection Agency, 2009), which causes the microscopic method by Matzoros and Van Vliet and Coelho et al. to fail in applying MOVES.

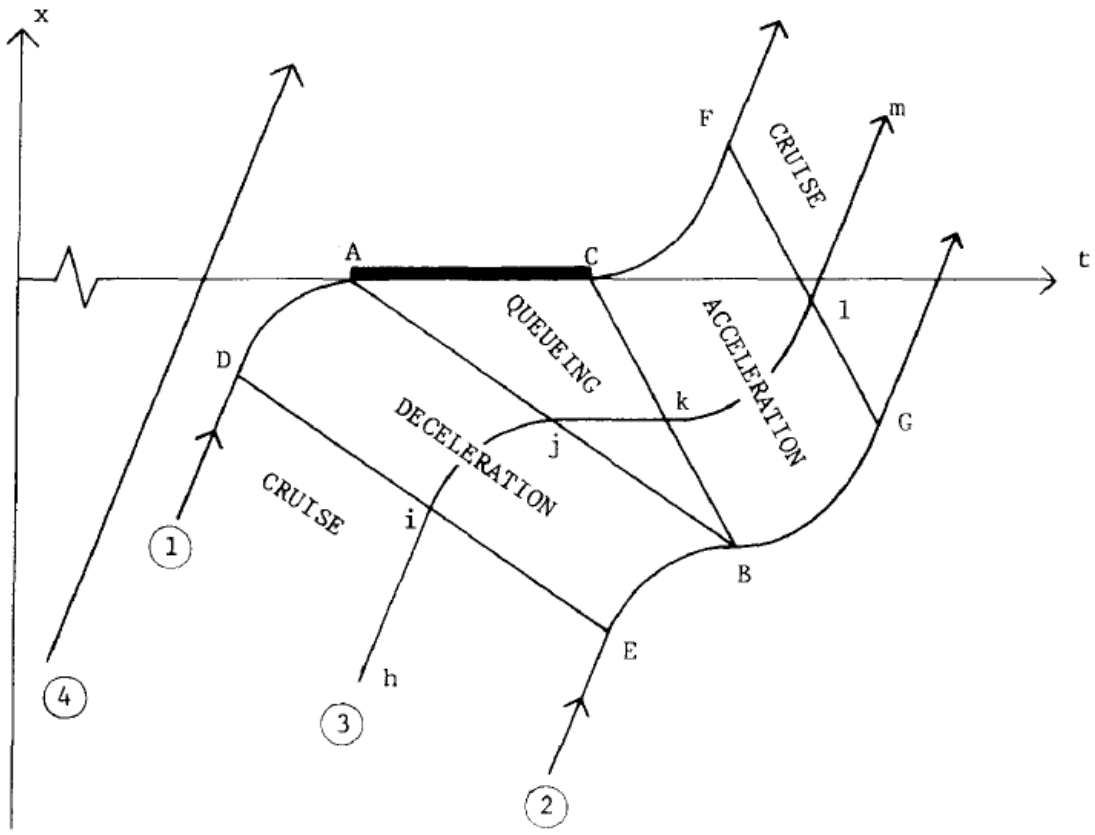

Figure 5 Vehicle trajectories at an intersection (Matzoros and Van Vliet, 1992)

1.3 Research Objective

According to Section 1.1 and 1.2, a major gap in the literature is that the research on signal optimization at intersections lags behind the development of emission models. Therefore, this study develops an optimization methodology for signal timing at intersections to reduce emissions based on MOVES. The methodology development includes four levels: the vehicle level, the movement level, the intersection level, and the arterial level. The objective of each level is described as follows:

At the vehicle level, the emission function with respect to control delay is derived for a vehicle driving through an intersection;

At the movement level, emissions are modeled for a movement if its green time and red time are given;

At the intersection level, an optimization problem is formulated to consider emissions at an intersection; and

At the arterial level, emissions are minimized at multiple intersections along an arterial.

The research activities and results of these four levels are respectively documented in Section 2 though 5. In addition, the summary and conclusions are provided in Section 6.

2. EMISSION FUNCTION AT VEHICLE LEVEL

The objective in the vehicle level modeling is to investigate the relationship between emissions and intersection delay when a vehicle drives through a signalized intersection. First, a general method of generating vehicle trajectories from intersection delay is proposed. This method is mathematically proven to be applicable to any form of acceleration models. Second, multiple acceleration models are evaluated, and the best one is selected in terms of emission estimations at an intersection. By substituting the selected acceleration model to the general method of generating vehicle trajectories, the emissions can be estimated corresponding to each intersection delay value. In addition, piecewise functions are used to describe the relationship between emissions and intersection delay.

2.1 General Method

This section proposes a general method of generating vehicle trajectories from intersection delay. First, a typical vehicle trajectory is illustrated, and relevant parameters are introduced. Second, a proposition is deduced to characterize a special category of vehicle trajectories without idling time. Based on the proposition, the flow chart of generating vehicle trajectories is provided.

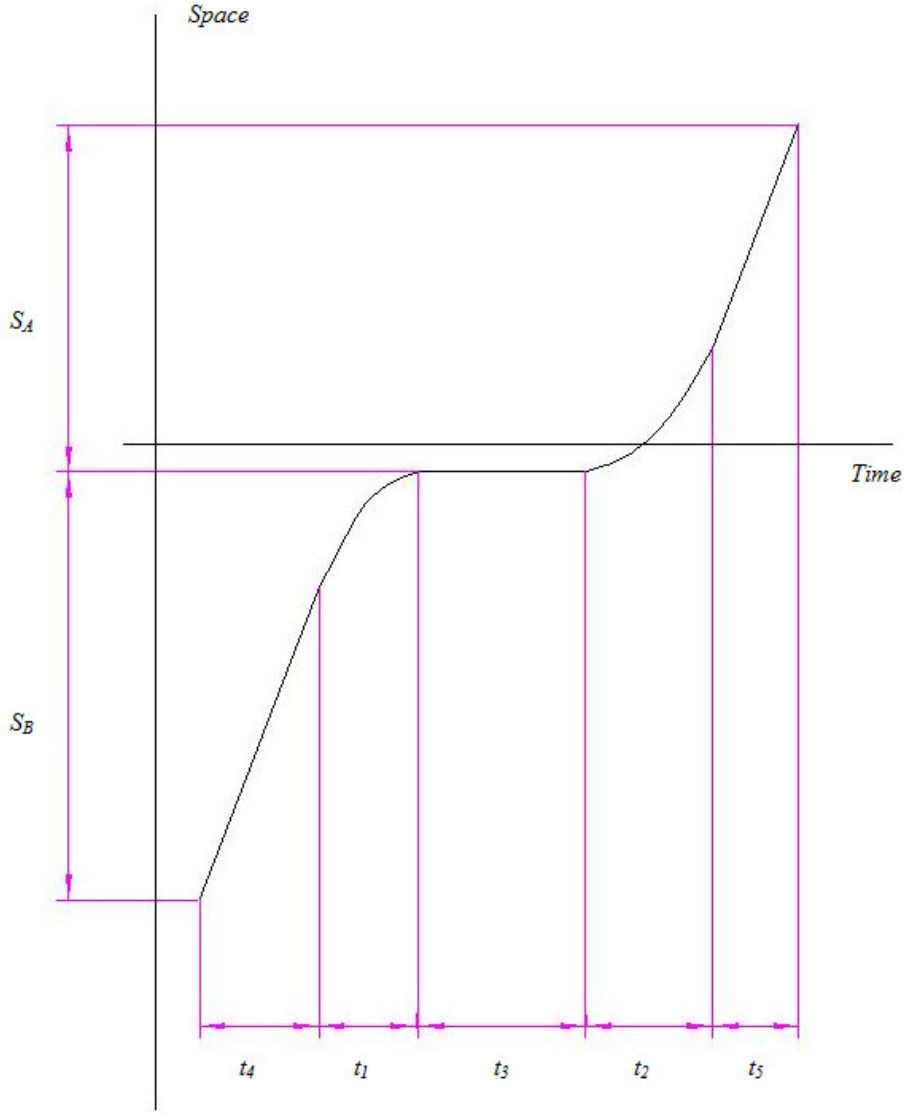

Figure 6 A typical vehicle trajectory at an intersection

Figure 6 shows a typical vehicle trajectory at an intersection. In the study area, a typical vehicle trajectory can be divided into five segments: Segment 1 represents vehicle deceleration; Segment 2 represents vehicle acceleration; Segment 3 represents vehicle idling; Segment 4 represents vehicle cruise before deceleration; Segment 5

represents vehicle cruise after acceleration. Accordingly, t_i and s_i ($i \in \{1, 2, 3, 4, 5\}$) represent the travel time and travel distance in each segment of a vehicle trajectory. The lengths of study areas before and after the intersection are defined as S_B and S_A, so $S_B = s_1 + s_4$ and $S_A = s_2 + s_5$. In addition,

$$s_1 = f_{1s}(t_1) \tag{1}$$

$$s_2 = f_{2s}(t_2) \tag{2}$$

$$s_3 = 0 \tag{3}$$

$$s_4 = v_f * t_4 \tag{4}$$

$$s_5 = v_f * t_5 \tag{5}$$

where v_f is the vehicle cruise speed; f_{1s} and f_{2s} are travel distance functions during deceleration and acceleration process. Furthermore,

$$f_{1v}(t) = \frac{df_{1s}(t)}{dt} \tag{6}$$

$$f_{2v}(t) = \frac{df_{2s}(t)}{dt} \tag{7}$$

where f_{1v} is the vehicle speed function during declaration process, so it is monotone decreasing; f_{2v} is the vehicle speed function during acceleration process, so it is monotone increasing.

When a vehicle trajectory dose not include an idling segment ($t_3 = 0$), the vehicle speed at the end of the deceleration process should be greater than or equal to zero but smaller than or equal to v_f.

$$t_1 = f_{1v}^{-1}(v_m) \tag{8}$$

$$t_2 = f_{2v}^{-1}(v_f) - f_{2v}^{-1}(v_m) \tag{9}$$

where v_m is the vehicle speed at the end of the deceleration process, and $0 \le v_m \le v_f$; f_{1v}^{-1} and f_{2v}^{-1} are inverse functions of f_{1v} and f_{2v}. f_{1v} is monotone decreasing, so f_{1v}^{-1} is monotone decreasing; f_{2v} is monotone increasing, so f_{2v}^{-1} is monotone increasing. According to the definition of S_B and S_A,

$$t_4 = \frac{S_B - s_1}{v_f} = \frac{S_B - f_{1s}(t_1)}{v_f} = \frac{S_B - f_{1s}(f_{1v}^{-1}(v_m))}{v_f} \tag{10}$$

$$t_5 = \frac{S_A - s_2}{v_f} = \frac{S_A - \left[f_{2s}(f_{2v}^{-1}(v_f)) - f_{2s}(f_{2v}^{-1}(v_m))\right]}{v_f} \tag{11}$$

The total travel time, $T = \sum_i t_i$, will be

$$T = f_{1v}^{-1}(v_m) + \left[f_{2v}^{-1}(v_f) - f_{2v}^{-1}(v_m)\right]$$

$$+ \frac{S_B - f_{1s}(f_{1v}^{-1}(v_m))}{v_f} + \frac{S_A - \left[f_{2s}(f_{2v}^{-1}(v_f)) - f_{2s}(f_{2v}^{-1}(v_m))\right]}{v_f} \tag{12}$$

Eq. (12) can be rearranged to the following format:

$$\left[f_{1v}^{-1}(v_m) - \frac{f_{1s}(f_{1v}^{-1}(v_m))}{v_f}\right] + \left[\left[f_{2v}^{-1}(v_f) - f_{2v}^{-1}(v_m)\right] - \frac{f_{2s}(f_{2v}^{-1}(v_f)) - f_{2s}(f_{2v}^{-1}(v_m))}{v_f}\right]$$

$$= T - \frac{S_B + S_A}{v_f} \tag{13}$$

In this equation, the right hand represents the vehicle delay, denoted by D; the left hand is a function with only one variable (v_m), denoted by $F_1(v_m)$.

(*Lemma 1*) $F_1(v_m)$ is monotone decreasing.

Proof: $F_1(v_m)$ has two terms, $F_{11}(f_{1v}^{-1}(v_m))$ and $F_{12}(f_{2v}^{-1}(v_m))$, where

$$F_{11}(x) = x - \frac{f_{1s}(x)}{v_f} \tag{14}$$

$$F_{12}(x) = \left[f_{2v}^{-1}(v_f) - x\right] - \frac{f_{2s}(f_{2v}^{-1}(v_f)) - f_{2s}(x)}{v_f} \tag{15}$$

And considering that vehicle speed during the acceleration or deceleration process should be smaller than the cruise speed,

$$\frac{dF_{11}(x)}{dx} = 1 - \frac{f_{1v}(x)}{v_f} \geq 0 \tag{16}$$

$$\frac{dF_{12}(x)}{dx} = -1 + \frac{f_{2v}(x)}{v_f} \leq 0 \tag{17}$$

Also because f_{1v}^{-1} is monotone decreasing, and f_{2v}^{-1} is monotone increasing, both $F_{11}(f_{1v}^{-1}(v_m))$ and $F_{12}(f_{2v}^{-1}(v_m))$ are monotone decreasing with respect to v_m. Therefore, $F_1(v_m)$ is monotone decreasing.

It should be noted that $F_{11}(f_{1v}^{-1}(v_m))$ and $F_{12}(f_{2v}^{-1}(v_m))$ have physical meanings: they respectively represent the vehicle delay during deceleration and acceleration processes.

(*Proposition 1*) When $0 = F_1(v_f) < F_1(v_m) < F_1(0)$, there is one and only one solution to Eq. (13) in the interval of $(0, v_f)$.

This proposition is obvious according to *Lemma 1*.

(*Definition 1*) A vehicle trajectory is considered critical when a vehicle decelerates its speed to zero and then accelerate but without idling time.

Subscript $_C$ represents critical situations, and the critical delay can be expressed as $D_C = F_1(v_{Cm}) = F_1(0)$.

(*Property 1*) For any trajectory with its intersection delay $D_a < D_C$, its speed at the end of deceleration process $v_{am} > 0$.

Proof: According to *Lemma 1*, $F_1(v_m)$ is monotone decreasing. $D_a < D_C$, that is $F_1(v_{am}) < F_1(v_{Cm})$, so $v_{am} > v_{Cm} = 0$.

(*Property 2*) For any trajectory with its intersection delay $D_a > D_C$, it must include an idling process, and its idling time $t_{a3} > 0$.

Proof (by contradiction): if $t_{a3} = 0$, *Lemma 1* still holds: $F_1(v_m)$ is monotone decreasing, so $D_a > D_C$ leads to $v_{am} = F_1^{-1}(D_a) < F_1^{-1}(D_C) = 0$. However, vehicle speed cannot be negative, so it must be $t_{a3} > 0$.

(*Deduction 1*) Selections of S_B and S_A do not impact the value of Eq. (13) as long as $S_B \geq \max s_1 = f_{s1}(f_{v1}^{-1}(0))$ and $S_A \geq \max s_2 = f_{s2}(f_{v2}^{-1}(v_f))$, so they do not impact the calculation of increased travel time (namely intersection delay) and the generation of vehicle trajectories. In turn, S_B and S_A do not impact the estimation of

increased emissions. In other words, the definition of a study domain (S_B and S_A) dose not change the estimations of emissions caused by intersection delay.

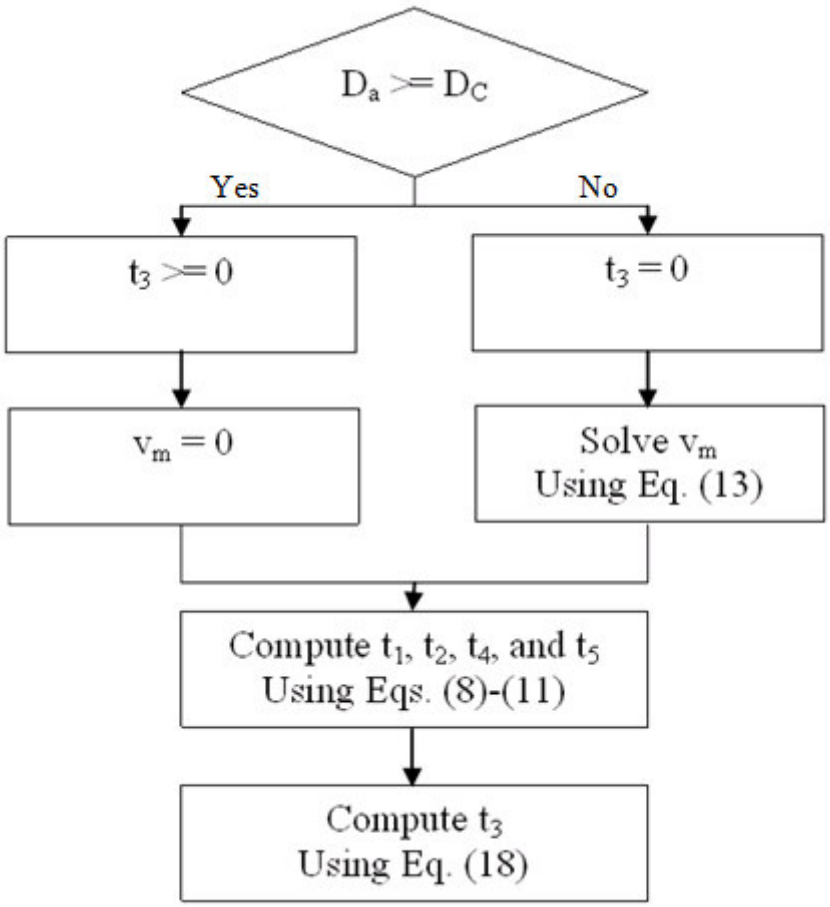

Figure 7 Flow chart of generating vehicle trajectories from intersection delay

Based on *Proposition 1*, Figure 7 provides a flow chart of generating vehicle trajectories from intersection delay for the purpose of estimating emissions. First, the input intersection delay D_a is compared with the critical delay D_C. If $D_a \geq D_C$,

$v_m = 0$; otherwise, v_m is calculated using Eq. (13). Second, t_1, t_2, t_4, and t_5 can be calculated using Eqs. (8)-(11). Third, t_3 is calculated using Eq. (18) if $D_a \geq D_C$. It is noted that Eq. (18) holds when either $D_a \geq D_C$ or $D_a < D_C$. When $D_a < D_C$, $D_a = F_1(v_m)$ and $t_3 = 0$. As a result, a complete vehicle trajectory is generated from its intersection delay.

$$t_3 = D_a - F_1(v_m) \tag{18}$$

2.2 Acceleration Function

This section evaluates three vehicle acceleration models – constant acceleration model, linearly decreasing acceleration model, and aaSIDRA model – in terms of emission estimations during the acceleration process at an intersection. These three models are first calibrated using the field data of vehicle trajectories. With the calibrated models, second-by-second speed and acceleration data are produced. From second-by-second speed and acceleration data, emissions can be estimated using MOVES. After that, emission estimations based on acceleration models are compared with field data to select the best acceleration model for this study.

2.2.1 Field Data

In this study, GPS data are collected in passenger vehicles along University Drive during afternoon peak hours. During data collection, our drives maintain a constant distance from their leading vehicles, so their vehicle trajectories together can

reflect the average driver behavior at the intersection. PC-TRAVEL by JAMAR Technologies is used to record section-by-second speed data. 8 vehicle acceleration trajectories are archived at two different sites (see Figure 8). Site (a) is the intersection of University Drive (East Bound) crossing Texas Avenue, where the speed limit is 40 mph; Site (b) is the intersection of University Drive (West Bound) crossing Lincoln Ave, where the speed limit is 45 mph.

2.2.2 Acceleration Models

Three acceleration models are evaluated in this study. First, the constant acceleration model can be described in Eq. (19):

$$a = C \tag{19}$$

where a represents vehicle acceleration; C is a constant, indicating that acceleration is constant with speed. As a result, the speed profile during the acceleration process, $v_1(t)$, will be

$$v_1(t) = \begin{cases} Ct & Ct \le v_f \\ v_f & Ct > v_f \end{cases} \tag{20}$$

where v_f represents the final cruise speed after the acceleration process. In Eq. , both C and v_f need to be calibrated to determine the speed profile during the acceleration process, $v_1(t)$. C can be estimated by minimizing the value of Eq. (21).

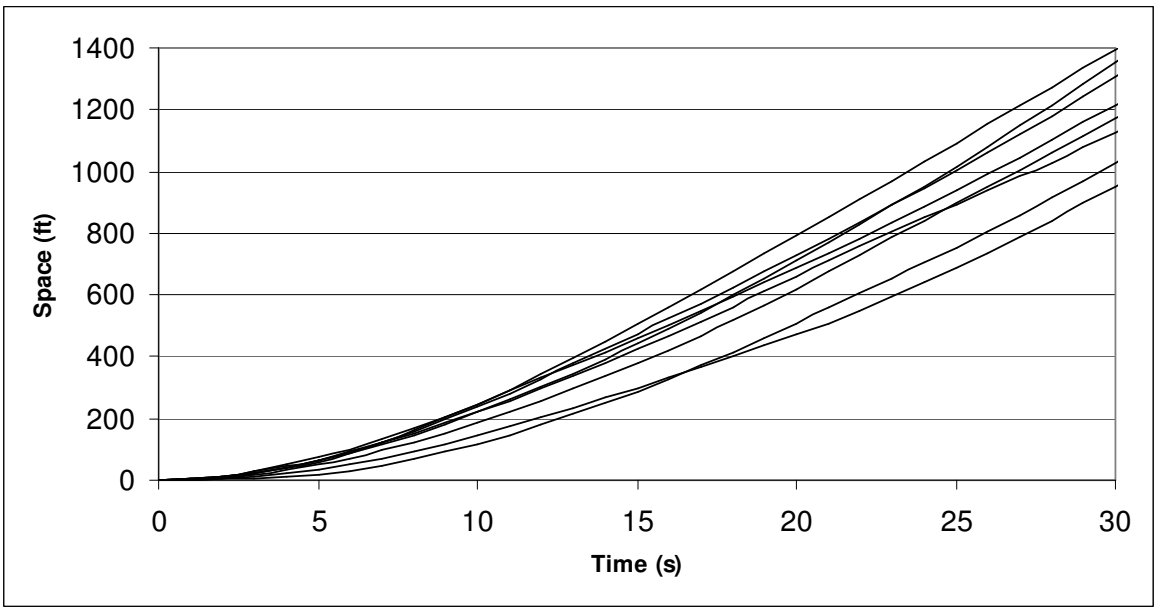

(a) Intersection of University Drive (East Bound) crossing Texas Avenue

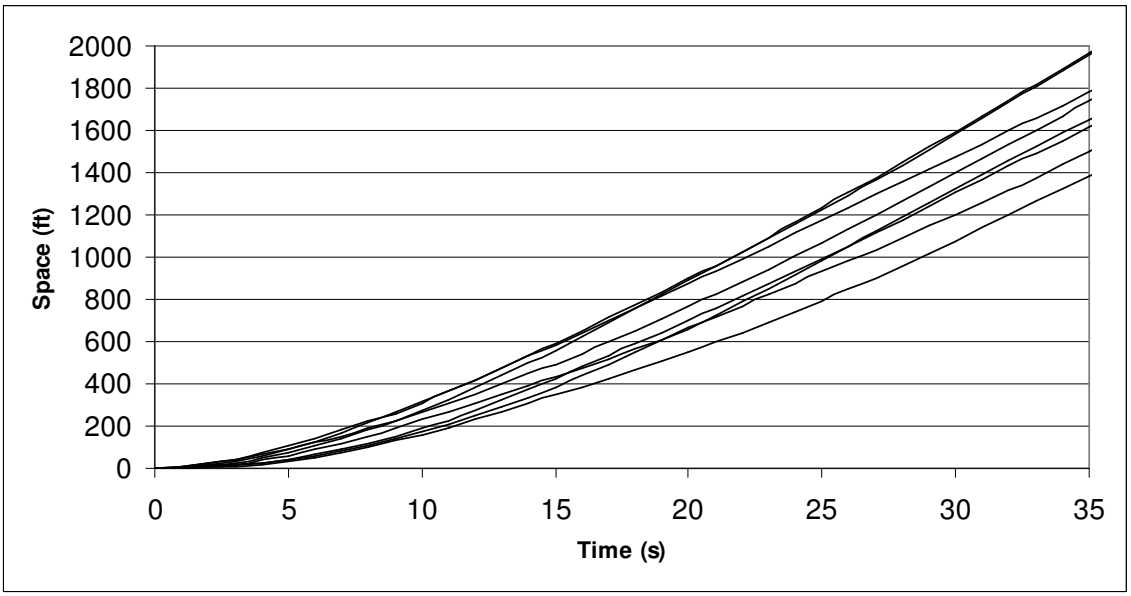

(b) Intersection of University Drive (West Bound) crossing Lincoln Ave

Figure 8 Vehicle trajectories during acceleration

$$RMSE_1(C, v_f) = \sqrt{\frac{\sum_{i=1}^{N}\left[v_1(i) - M(i)\right]^2}{N}} \tag{21}$$

where $RMSE$ represents the root mean squared error; $M(i)$ is the measured speed at the time i during the acceleration process; N is the number of speed measures after a vehicle starts.

Second, the linearly decreasing acceleration model can be described in Eq. (22).

$$a = \beta_0 + \beta_1 v \tag{22}$$

where v represents vehicle speed; β_0 and β_1 are two coefficients. According to $a(t) = \frac{\partial v(t)}{\partial t}$, the speed profile during the acceleration process, $v_2(t)$, can be derived:

$$v_2(t) = \frac{\beta_0}{\beta_1}\left(e^{\beta_1 t} - 1\right) \tag{23}$$

β_0 and β_1 can be estimated by minimizing the value of Eq. (24).

$$RMSE_2(\beta_0, \beta_1) = \sqrt{\frac{\sum_{i=1}^{N}\left[v_2(i) - M(i)\right]^2}{N}} \tag{24}$$

Third, aaSIDRA model was developed by Akcelik et al. (Akcelik and Besley, 2001; Akcelik and Biggs, 1987). Akcelik and Biggs (1987) suggested polynomial functions to represent acceleration and speed profiles, as shown in Eqs. (25) and (26).

$$a_3(t) = ra_m\theta(1 - \theta^m)^2 \tag{25}$$

$$v_3(t) = t_a ra_m \theta^2 [0.5 - 2\theta^m/(m+2) + \theta^{2m}/(2m+2)] \tag{26}$$

where r and m are two parameters, and r depends on the value of m; a_m represents the maximum acceleration; t_a represents acceleration time; θ represents a time ratio, which is t/t_a. r and a_m can be calculated using the following equations:

$$r = [(1+2m)^{2+1/m}]/4m^2 \tag{27}$$

$$a_m = v_f/(rqt_a) \tag{28}$$

where q is a parameter that depends on the value of m:

$$q = m^2/[(2m+2)(m+2)] \tag{29}$$

According to Eqs. (27) through (29), m, t_a, and v_f are those parameters that need to be calibrated to determine the acceleration and speed profiles in Eqs. (25) and (26). These parameters can be estimated by minimizing the value of Eq.(30).

$$RMSE_3(m,t_a,v_f) = \sqrt{\frac{\sum_{i=1}^{N}[v_3(i)-M(i)]^2}{N}} \tag{30}$$

2.2.3 Emission Model

After second-by-second speed and acceleration data are produced according to acceleration models, MOVES is used to estimate vehicle emissions during the acceleration process at an intersection. In addition to second-by-second speed and acceleration, MOVES needs VSP to determine operating modes and to estimate emissions. VSP shall be calculated using Eq. (31) (Environmental Protection Agency, 2004):

$$VSP = 0.3227 * ve * acc + 0.0954 * ve + 0.0000272 * ve^3 \quad (31)$$

where ve is the instantaneous speed in mph, and acc is the instantaneous acceleration in ft/s^2. In this study, the emission calculation and comparison adopt a set of emission rates for the evaluation year 2010 (Environmental Protection Agency, 2009).

2.2.4 Results

In this subsection, emissions based on acceleration models are computed and evaluated. First, acceleration models are calibrated using the field data of vehicle trajectories. Second, with the calibrated acceleration models, second-by-second speed and acceleration data are produced on a 1000 ft road segment after the intersection. After that, the second-by-second data, including those both produced by acceleration models and measured in the field, are input to MOVE for estimating emissions. Those emission estimations are compared with each other to evaluate acceleration models.

Table 5 and Table 6 summarize the result of model calibrations, including estimated parameters, RMSEs, and their means and standard deviations. T-tests are conducted between RMSEs. The constant acceleration model (Model 1) produces a greater RMSE than the other two models, but no statistical difference is found between the decreasing acceleration model and aaSIDRA model (Model 2 and Model 3 linearly) at the significant level of 0.050.

Table 5 Calibration of acceleration models on Site (a)

Vehicle Trajectory	Model 1			Model 2			Model 3			
	C	v_f	$RMSE_1$	β_0	β_1	$RMSE_2$	m	t_a	v_f	$RMSE_3$
1	2.905	33.226	2.799	4.236	-0.112	1.372	0.003	22.073	34.270	2.314
2	2.378	39.236	2.663	3.541	-0.073	1.404	0.000	30.043	40.537	1.594
3	1.695	35.380	2.029	2.064	-0.032	2.025	0.257	35.740	37.604	1.271
4	2.943	40.071	1.293	4.686	-0.104	1.761	0.001	24.425	40.867	0.441
5	1.996	37.133	1.654	3.045	-0.066	1.327	0.001	32.215	37.828	1.112
6	1.359	37.267	2.479	1.882	-0.032	1.608	0.001	44.338	36.384	2.282
7	2.301	42.792	2.638	3.352	-0.060	0.490	0.000	33.839	44.485	1.590
8	2.793	37.188	2.591	4.149	-0.095	1.525	0.000	24.936	38.334	1.883
Mean	2.296	37.787	2.268	3.369	-0.072	1.439	0.033	30.951	38.789	1.561
S.D.	0.582	2.928	0.549	1.010	0.031	0.448	0.091	7.275	3.129	0.625
T-test			$RMSE_1$ vs. $RMSE_2$			$RMSE_2$ vs. $RMSE_3$				$RMSE_3$ vs. $RMSE_1$
P-value			0.027			0.694				0.000

Note: "S.D." stands for "standard deviation."

Table 6 Calibration of acceleration models on Site (b)

Vehicle	Model 1			Model 2			Model 3			
Trajectory	C	v_f	$RMSE_1$	β_0	β_1	$RMSE_2$	m	t_a	v_f	$RMSE_3$
1	2.459	43.228	3.675	4.011	-0.081	1.062	0.000	31.028	44.097	2.854
2	3.570	40.138	2.259	6.422	-0.153	0.662	0.000	19.004	40.318	1.532
3	3.428	45.959	3.733	5.263	-0.102	1.474	0.001	24.766	46.999	2.932
4	1.615	39.891	3.113	2.394	-0.045	1.687	0.000	42.095	40.590	2.208
5	2.232	37.000	3.570	3.575	-0.085	1.572	0.000	29.008	37.641	2.623
6	2.162	44.820	1.565	3.182	-0.056	2.693	0.226	33.145	45.555	1.109
7	3.113	47.870	2.320	4.970	-0.093	1.193	0.000	27.554	48.795	1.250
8	2.438	40.668	1.653	3.678	-0.077	2.260	0.127	28.997	41.709	0.948
Mean	2.627	42.447	2.736	4.187	-0.086	1.575	0.044	29.450	43.213	1.932
S.D.	0.679	3.639	0.899	1.290	0.033	0.653	0.086	6.667	3.786	0.817
T-test			$RMSE_1$ vs. $RMSE_2$			$RMSE_2$ vs. $RMSE_3$				$RMSE_3$ vs. $RMSE_1$
P-value			0.045			0.441				0.000

Note: "S.D." stands for "standard deviation."

Table 7 and Table 8 summarize emission estimations from second-by-second data, including those both produced by acceleration models and measured in the field. Three typical types of emissions, carbon monoxide (CO), hydrocarbon (HC), and nitrogen oxides (NO), are selected to evaluate acceleration models. According to T-tests, the constant acceleration model (Model 1) tends to overestimate emissions because P-values are smaller than 0.050 for all three types of emissions in the comparison with measured data. This overestimation of emissions is caused by the constant acceleration assumed during the acceleration process. In reality, acceleration decreases with the increase of speed; accordingly, the constant acceleration model underestimates acceleration at low speed levels but overestimate it at high speed levels. VSP is very sensitive to acceleration at high speed levels. High speeds and overestimated VSP in turn result in the overestimation of emissions.

Furthermore, in Table 7 and Table 8 the P-values for Model 3 are even greater than those for Model 2, indicating that aaSIDRA model is better than the linearly decreasing acceleration model. However, this better performance of Model 3 over Model 2 is not always supported by T-tests. When comparing these two models in estimating CO, HC, and NO, P-values are 0.443, 0.372, and 0.355 at the speed limit of 40 mph and 0.083, 0.074, and 0.047 at the speed limit of 45 mph.

Table 7 Emission estimations from second-by-second data on Site (a) (unit: mg)

Vehicle	Measured			Model 1			Model 2			Model 3		
Trajectory	CO	HC	NO	CO	HC	NO	CO	HC	NO	CO	HC	NO
1	57.856	0.778	2.764	430.931	5.539	16.056	43.986	0.603	2.375	62.319	0.820	2.639
2	97.042	1.270	3.903	597.875	7.761	24.375	113.153	1.428	4.056	101.764	1.345	3.986
3	88.908	1.147	3.319	86.408	1.103	2.889	91.131	1.067	3.153	54.206	0.667	2.431
4	323.469	4.309	15.444	943.747	12.006	31.972	107.358	1.345	4.042	399.303	5.320	19.444
5	239.022	3.120	11.039	236.169	3.111	10.792	56.467	0.578	2.264	77.281	1.017	3.236
6	79.742	0.939	2.667	79.742	0.956	2.722	53.353	0.508	1.889	43.928	0.528	2.042
7	133.172	1.748	4.764	896.783	11.617	34.833	144.283	1.906	5.014	120.672	1.559	4.361
8	89.283	1.131	3.542	730.394	9.350	26.181	90.394	1.103	3.500	87.061	1.159	3.486
Mean	138.562	1.805	5.930	500.256	6.430	18.727	87.516	1.067	3.286	118.317	1.552	5.203
S.D.	93.276	1.252	4.710	346.217	4.447	12.532	34.477	0.490	1.072	116.296	1.561	5.807
T-test				Measured vs. Model 1			Measured vs. Model 2			Measured vs. Model 3		
P-value				0.015	0.015	0.018	0.164	0.142	0.153	0.420	0.440	0.547

Note: "S.D." stands for "standard deviation."

Table 8 Emission estimations from second-by-second data on Site (b) (unit: mg)

Vehicle	Measured			Model 1			Model 2			Model 3		
Trajectory	CO	HC	NO	CO	HC	NO	CO	HC	NO	CO	HC	NO
1	126.900	1.665	4.694	1030.214	13.220	36.778	133.567	1.742	4.806	120.492	1.573	4.514
2	171.642	2.337	7.986	1425.808	11.590	32.181	171.086	2.270	7.875	385.253	5.134	19.000
3	545.828	7.220	27.153	2297.772	16.437	52.653	516.939	6.887	24.611	1075.272	13.951	43.458
4	107.692	1.392	3.956	253.469	3.328	11.319	56.803	0.567	2.236	71.544	0.817	2.806
5	97.731	1.309	3.942	304.064	4.028	14.597	51.286	0.606	2.444	83.231	1.098	3.458
6	293.806	3.903	12.903	980.472	12.714	38.972	146.028	1.920	5.097	282.992	3.731	12.542
7	785.272	10.279	33.736	2518.883	19.181	58.653	666.939	8.887	32.389	803.328	10.687	39.653
8	384.639	5.084	18.986	811.603	10.426	30.333	105.214	1.326	3.958	106.603	1.398	4.097
Mean	314.189	4.149	14.169	1202.786	11.366	34.436	230.983	3.026	10.427	366.089	4.799	16.191
S.D.	246.648	3.231	11.422	838.534	5.496	16.450	230.084	3.105	11.481	377.171	4.945	16.644
T-test				Measured vs. Model 1			Measured vs. Model 2			Measured vs. Model 3		
P-value				0.006	0.001	0.000	0.044	0.040	0.081	0.551	0.562	0.560

2.3 Relationship between Emissions and Intersection Delay

The previous section identifies aaSIDRA as the best acceleration model in estimating emissions at an intersection. On Site (a), the calibrated aaSIDRA acceleration function is shown in Eq. (32), where $m = 0.033$, $t_a = 30.951$ s, and $v_f = 38.789$ mph are the average values in Table 5.

$$f_{2v}(t) = 78.085t^2 - 137.180t^{2.033} + 60.268^{2.066} \quad (32)$$

where $f_{2v}(t)$ is in terms of mph, and t is in terms of s.

Since vehicle deceleration produces much less emissions than acceleration at an intersection, a simple constant deceleration function is used in this study, as shown in Eq. (33), and the RMSE in comparing with filed data is 5.934 mph.

$$f_{1v}(t) = 38.789 - 2.924t \quad (33)$$

where $f_{1v}(t)$ is in terms of mph, and t is in terms of s.

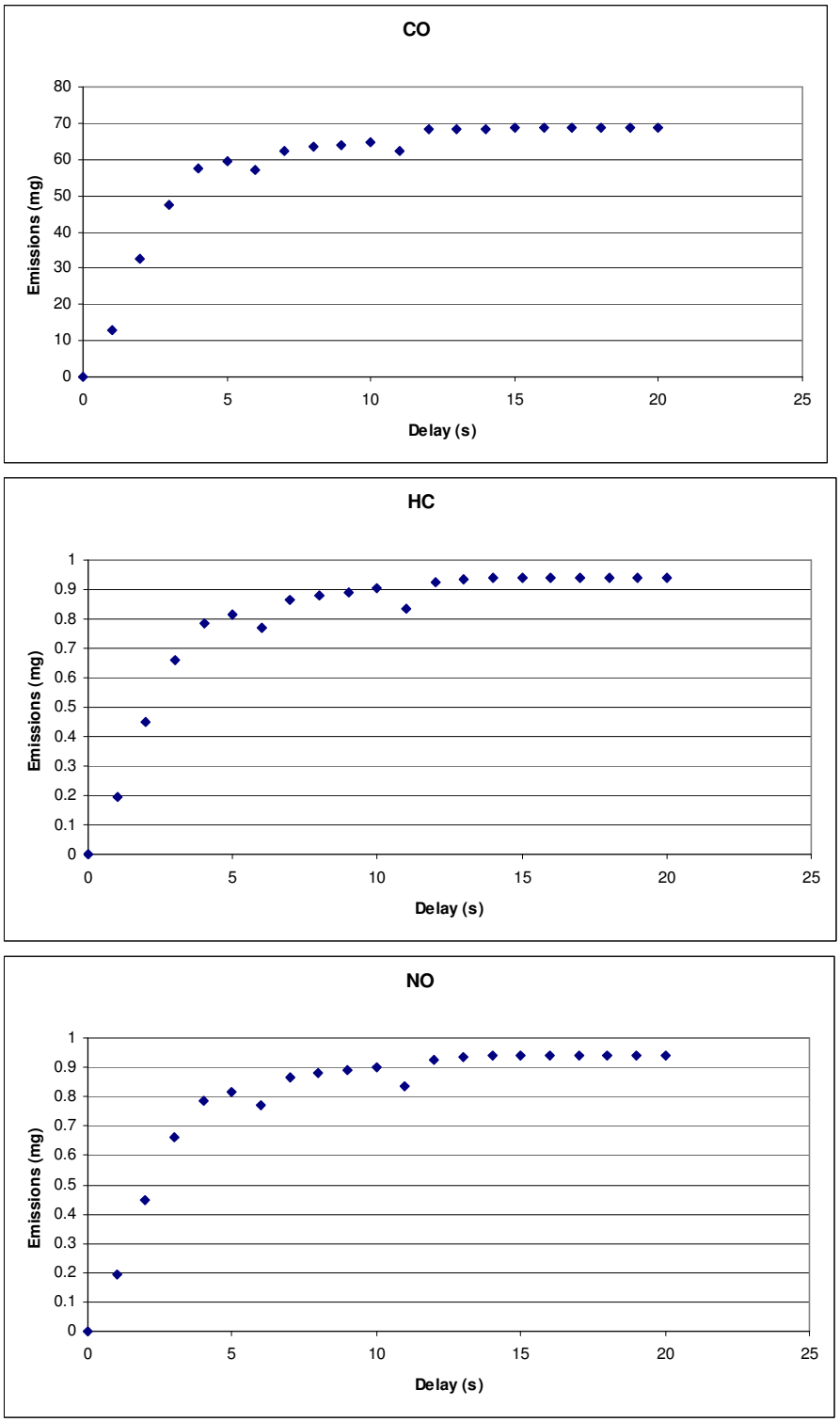

Figure 9 Relationship between emissions and intersection delay on Site (a)

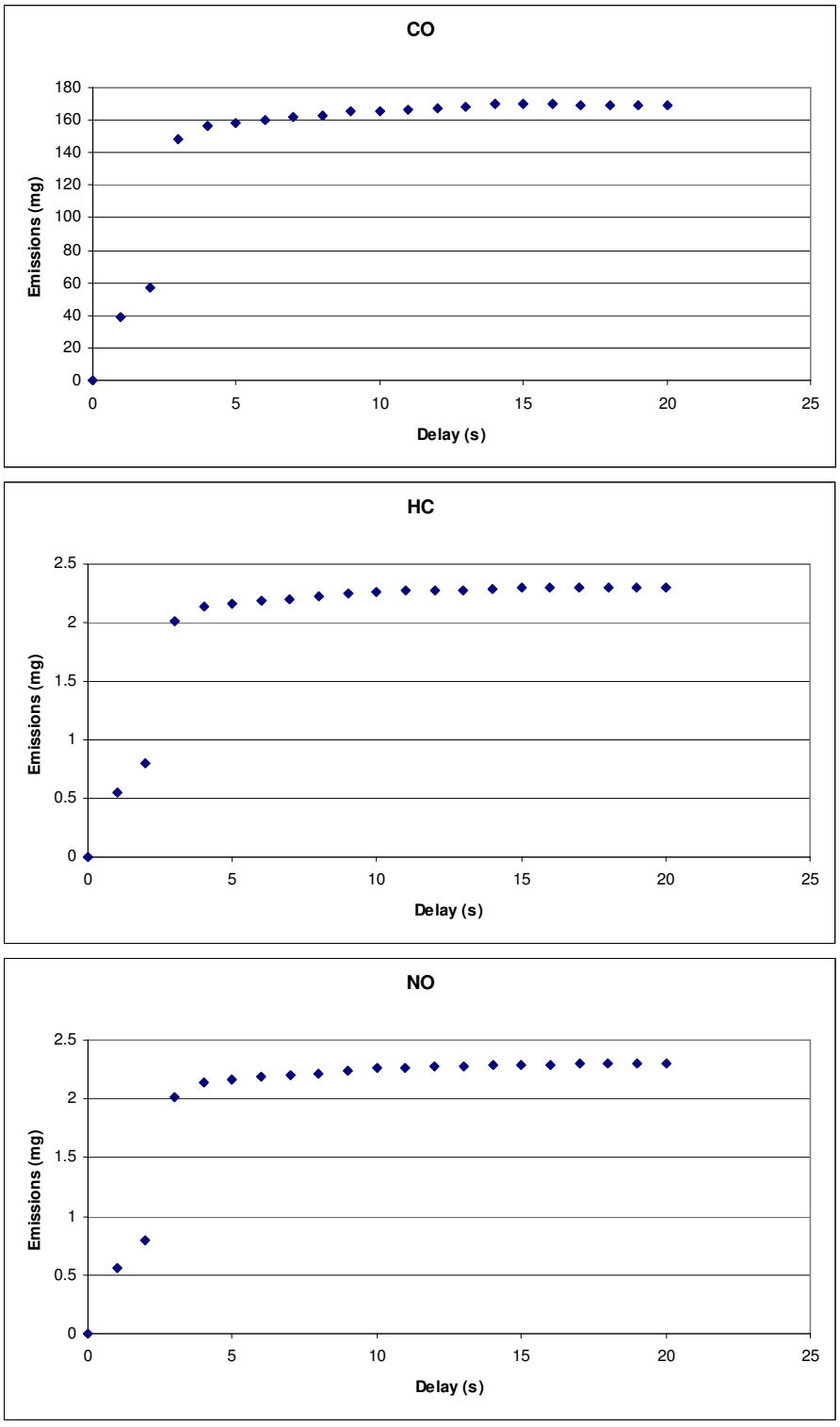

Figure 10 Relationship between emissions and intersection delay on Site (b)

With these two speed functions, Eqs. (32) and (33), second-by-second speed data can be produced from intersection delay, and emissions can be estimated using MOVES. Figure 9 depicts the relationship between emissions and intersection delay on Site (a). Based on the same procedure, the relationship between emissions and intersection delay on Site (b) can be obtained, as shown in Figure 10. Emissions increase very fast as the intersection delay increases from 0, but this increase rate of emissions with intersection delay keeps decreasing. The reason behind this increase trend is that the emission rate for vehicle acceleration is much greater than that of vehicle idling: at the very beginning, increasing intersection delay in turn increases the acceleration process and time; later when intersection delay is greater a threshold value, increasing intersection delay only increases idling time.

The piecewise function is a simple way to describe the plots in Figure 9 and Figure 10:

$$f_{1E}(x) = \alpha_{E,i} + \beta_{E,i} x \quad \text{when } x \in [a_{E,i}, b_{E,i}) \tag{34}$$

where $f_{1E}(x)$ represents the piecewise function of emissions with respect to intersection delay; $[a_{E,i}, b_{E,i})$ represents a subset, and $\alpha_{E,i}$ and $\beta_{E,i}$ are corresponding coefficients of the linear function in this subset. Table 9 and Table 10 provide two piecewise functions of emissions at the speed limits of 40 and 45 mph, respectively.

Table 9 Piecewise function of emissions on Site (a)

Subset	CO		HC		NO	
$[a_{E,i}, b_{E,i})$	$\alpha_{E,i}$	$\beta_{E,i}$	$\alpha_{E,i}$	$\beta_{E,i}$	$\alpha_{E,i}$	$\beta_{E,i}$
[0, 1)	0.000	12.667	0.000	0.194	0.000	0.931
[1, 2)	-7.056	19.722	-0.061	0.256	0.253	0.678
[2, 3)	2.389	15.000	0.028	0.211	0.586	0.511
[3, 4)	17.389	10.000	0.286	0.125	1.211	0.303
[4, 5)	48.500	2.222	0.675	0.028	1.878	0.136
[5, 6)	72.111	-2.500	1.036	-0.044	2.781	-0.044
[6, 7)	27.111	5.000	0.186	0.097	0.947	0.261
[7, 8)	51.806	1.472	0.769	0.014	2.736	0.006
[8, 9)	59.806	0.472	0.792	0.011	2.069	0.089
[9, 10)	56.556	0.833	0.792	0.011	3.269	-0.044
[10, 11)	92.667	-2.778	1.569	-0.067	4.075	-0.125
[11, 12)	-5.111	6.111	-0.142	0.089	0.592	0.192
[12, 13)	68.222	0.000	0.825	0.008	2.058	0.069
[13, 14)	64.611	0.278	0.861	0.006	2.817	0.011
[14, 15)	64.611	0.278	0.900	0.003	2.778	0.014
[15, 16)	68.778	0.000	0.942	0.000	2.986	0.000
[16, +∞)	68.467	0.019	0.941	5.56E-05	2.764	0.014

Table 10 Piecewise function of emissions on Site (b)

Subset	CO		HC		NO	
$[a_{E,i}, b_{E,i})$	$\alpha_{E,i}$	$\beta_{E,i}$	$\alpha_{E,i}$	$\beta_{E,i}$	$\alpha_{E,i}$	$\beta_{E,i}$
[0, 1)	0.000	39.056	0.000	0.556	0.000	1.764
[1, 2)	21.278	17.778	0.317	0.239	1.142	0.622
[2, 3)	-125.722	91.278	-1.650	1.222	-6.453	4.419
[3, 4)	121.944	8.722	1.667	0.117	5.964	0.281
[4, 5)	149.833	1.750	2.033	0.025	6.619	0.117
[5, 6)	148.861	1.944	2.019	0.028	6.592	0.122
[6, 7)	151.028	1.583	2.119	0.011	6.875	0.075
[7, 8)	154.333	1.111	2.042	0.022	6.836	0.081
[8, 9)	147.667	1.944	2.019	0.025	6.725	0.094
[9, 10)	159.417	0.639	2.069	0.019	7.025	0.061
[10, 11)	158.306	0.750	2.208	0.006	7.303	0.033
[11, 12)	157.389	0.833	2.147	0.011	8.158	-0.044
[12, 13)	157.389	0.833	2.281	0.000	7.792	-0.014
[13, 14)	142.944	1.944	2.208	0.006	7.286	0.025
[14, 15)	170.167	0.000	2.169	0.008	6.664	0.069
[15, 16)	169.875	0.019	2.294	0.000	7.497	0.014
[16, 17)	192.408	-1.389	2.250	0.003	7.986	-0.017
[17, +∞)	168.467	0.019	2.296	5.56E-05	7.467	0.014

2.4 Adjustment for Turning Vehicles

In the process of emission estimation described above, those vehicles that are not impacted by red signal or traffic queue are assumed to maintain their operating speeds. However, it is observed that turning vehicles reduce their speeds to 10 ~ 20 mph at an intersection even when they are not hindered by any leading vehicle (Fitzpatrick et al., 2003; Fitzpatrick & Schneider, 2005). Therefore, the relationship between emissions and intersection delay identified in Eq. needs to be adjusted for turning vehicles. Let v_{f0} denote the lowest speed of turning vehicles driving through an intersection at the free flow condition. By substituting $v_m = v_{f0}$, $F_1(v_m) = F_1(v_{f0})$ provides the delay of turning vehicles compared to through vehicles, denoted by D_0. Corresponding to this delay an emission value is calculated using Eq. , $Em_0 = f_{1E}(D_0)$. By substituting these two constants in Eq. , $x = x + D_0$ and $f_{1E}(x) = f_{2E}(x) + Em_0$, the relationship between delay and emissions caused by the intersection signal for turning vehicles can be described in Eq. (35).

$$f_{2E}(x) = f_{1E}(x + D_0) - Em_0 \tag{35}$$

It is noted that Eq. (35) can be considered a generalized equation for both through vehicles and turning vehicles. For through vehicles, $D_0 = 0$, and $Em_0 = 0$.

For example, on a road with the speed limit of 45 mph, turning vehicles reduce their speeds to 15 mph at an intersection, and the corresponding delay is $D_0 = 7.154$ s. The emissions can be calculated using Eq. : Em_0 is 162.282 mg, 2.200 mg, and 7.412

mg for CO, HC, and NO. With the values of D_0 and Em_0, all parameters in Eq. (35) can be determined.

3. EMISSION MODELING AT MOVEMENT LEVEL

The objective of this section is to model emissions for a movement when its green and red times are given. Section 2 investigates the relationship between emissions and intersection delay when a vehicle drives through a signalized intersection. In order to model emissions of a group of vehicles, the distribution of intersection delay of this group of vehicles needs to be estimated. However, conventional methods of intersection delay such as Webster (1958) and HCM (Transportation Research Board, 2010) only estimate a value of average intersection delay for a movement.

Therefore, this section first develops a stochastic model based on the Markov chain to estimate the distribution of intersection delay of individual vehicles at a movement. A state of the Markov chain is defined as the number of vehicles at the beginning of red time in a signal cycle. To account for randomness, the number of vehicle arrivals during a cycle is assumed to follow Poisson distributions. Second, a numerical study is conducted considering a variety of cycle lengths, green times, saturation flow rates, and demands. Third, emission estimations are compared with and without considering randomness.

3.1 Stochastic Model

The stochastic model is based on the development of a Markov chain. For a movement, a state of the Markov chain is defined as the number of vehicles at the beginning of red time in a signal cycle. The number of vehicle arrivals during a cycle is

assumed to follow Poisson distributions to account for randomness, while within a cycle vehicles are assumed to arrive at the intersection uniformly. In this section, the transition matrix of the Markov chain is first established. Based on the transition matrix, stationary probabilities, as well as the probability of each transition situation, can be calculated. After that, for each transition situation, the distribution of intersection delay is modeled. Accordingly, the distribution of intersection delay considering all transition situations can be estimated.

3.1.1 Transition Matrix

The number of vehicle arrivals during a cycle is assumed to follow Poisson distributions, which can be expressed as Eq. (36):

$$p_k = P\{X = k\} = e^{-\lambda} \frac{\lambda^k}{k\ !} \tag{36}$$

where p_k is the probability that k vehicles arrive in a cycle; λ is the expected number of vehicle arrivals in a cycle. With Eq. (36), the transition matrix of the Markov chain (P) can be established:

$P =$

	0	1	2	3	…	j
0	$\sum_{n=0}^{C_C} p_n$	p_{C_C+1}	p_{C_C+2}	p_{C_C+3}		
1	$\sum_{n=0}^{C_C-1} p_n$	p_{C_C}	p_{C_C+1}	p_{C_C+2}		

2	$\sum_{n=0}^{C_C-2} p_n$	p_{C_C-1}	…	…
3	$\sum_{n=0}^{C_C-3} p_n$	p_{C_C-2}	…	…
…				
i	$\begin{cases} \sum_{n=0}^{C_C-i} p_n & C_C - i \geq 0 \\ 0 & C_C - i < 0 \end{cases}$		$\begin{cases} p_{C_C-i+j} & C_C - i + j \geq 0 \\ 0 & C_C - i + j < 0 \end{cases}$	

where C_C is the capacity during a cycle (unit: number of vehicles); i is the number of vehicles at the beginning of this cycle; and j is the number of vehicles at the beginning of the next cycle.

By definition, the stationary probability (π) and transition matrix have such a relationship:

$$\pi^T P = \pi^T \text{ or } P^T \pi = \pi \tag{37}$$

where π is a column vector, with its element π_i representing the probability of i vehicles appearing at the beginning of a cycle; π^T is the transpose of π; P^T is the transpose of P. Moreover, the sum of all elements in π is equal to 1:

$$1_{[\ ]}\pi = 1_{[\ ]} \tag{38}$$

where $1_{[\ ]}$ represents a matrix with all elements equal to 1, and its dimensions are adaptive to the matrixes for multiplications. The stationary probability (π) can be calculated using the following equation:

$$\pi = (P^T - I + 1_{[\,]})^{-1} 1_{[\,]} \tag{39}$$

where I represents the identity matrix. From the stationary probability, the probability of each transition situation can further be estimated:

$$q_{ik} = \pi_i p_k \tag{40}$$

where q_{ik} is the probability of such a transition situation that the number of vehicles at a beginning of a cycle is i, and another k vehicles arrive during the cycle.

3.1.2 Distribution of Intersection Delay

In addition to probabilities of transition situations, distributions of intersection delay under different transition situations are modeled. As illustrated in Figure 11, transition situations can be categorized according to their characteristics of delay distributions: $j = 0$ and $j \neq 0$. R represents the red time; G represents the green time; and $C = G + R$ is equal to the cycle length. The delay distributions for these two categories of transition situations are modeled separately.

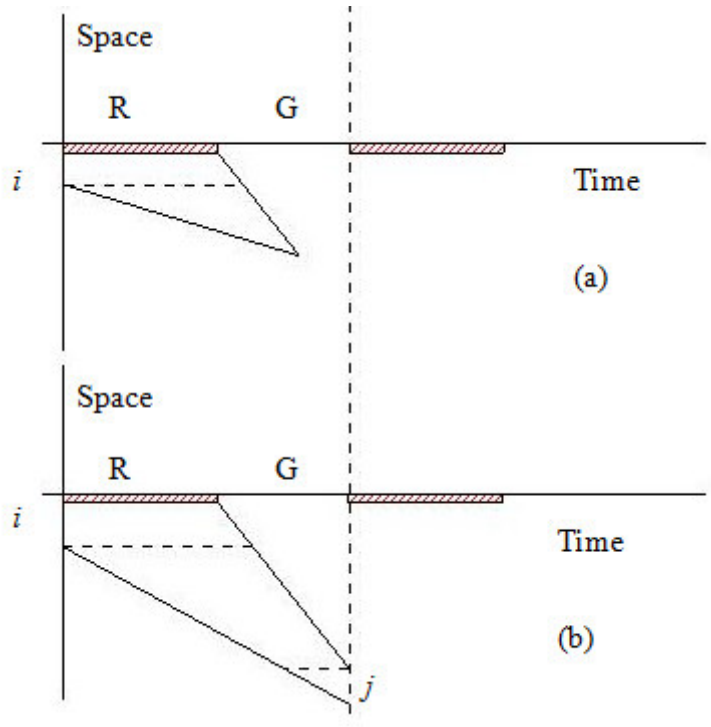

Figure 11 Transition situations when $j = 0$ and $j \neq 0$

In the first category of transition situations, $j = 0$, as shown in Figure 11(a) . The blockage time (T_B) is a function of k and i:

$$T_B = \frac{sR + i}{s - k/C} \tag{41}$$

where s is the saturation flow rate. Since vehicle arrivals within a cycle are assumed to be uniformly distributed, the percentage of vehicles with delay (pd_{ik}) can be expressed as Eq. (42), and the cumulative distribution function (CDF) of intersection delay Eq. (43).

$$pd_{ik} = \frac{T_B}{C} \tag{42}$$

$$F_{ik}^{(1)}(x) = \begin{cases} 0 & x \in (-\infty,\ 0) \\ \dfrac{x}{R + i/s} & x \in [0,\ R + i/s) \\ 1 & x \in [R + i/s,\ +\infty) \end{cases} \tag{43}$$

In the second category of transition situations, $j \neq 0$, as shown in Figure 11(b). $j \neq 0$ indicates that a certain number of vehicles arriving at the intersection cannot be discharged at the end of the current cycle. All vehicles in this cycle are involved in queue, and the percentage of vehicles with delay is pd_{ik} = 1.0. Vehicles discharged in the current cycle and in the following cycle have different distributions of intersection delay, respectively represented by the two trapezoids (S1 and S2) in Figure 12.

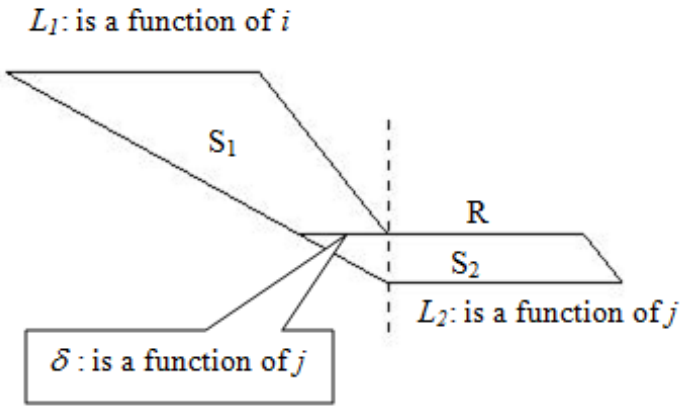

Figure 12 Modeling delay distribution when $j \neq 0$

The percentage of vehicles in S1 is $\frac{k-j}{k}$. Lengths of upper and lower sides of S1 can be calculated:

$$L_1 = \frac{i}{s} + R \tag{44}$$

$$\delta = \frac{j}{k} * C \tag{45}$$

where L_1 is the length of upper side of S1; δ is the length of lower side of S1.

Accordingly, the CDF for S1 is

$$F_{ik}^{(2,1)}(x) = \begin{cases} 0 & x \in (-\infty,\ \delta) \\ \dfrac{x-\delta}{L_1-\delta} & x \in [\delta,\ L_1) \\ 1 & x \in [L_1,\ +\infty) \end{cases} \tag{46}$$

The percentage of vehicles in S2 is $\frac{j}{k}$. $\delta + R$ is the length of upper side of S2, and the length of lower sides of S2 is

$$L_2 = \frac{j}{s} + R \tag{47}$$

where L_2 is the length of lower side of S2. Since the arrival rate cannot be greater than the saturation flow rate, in S2 the absolute value of the slope of the left side is smaller than the right side. Accordingly, $\delta + R \geq L_2$, and the CDF for S2 is

$$F_{ik}^{(2,2)}(x)=\begin{cases}0 & x\in(-\infty,\ L_2)\\ \dfrac{x-L_2}{\delta+R-L_2} & x\in[L_2,\ \delta+R)\\ 1 & x\in[\delta+R,\ +\infty)\end{cases} \tag{48}$$

According to Eqs. (46) and (48), the CDF for the second category of transition situations can be expressed in Eq. (49):

$$F_{ik}^{(2)}(x)=\frac{k-j}{k}F_{ik}^{(2,1)}(x)+\frac{j}{k}F_{ik}^{(2,2)} \tag{49}$$

Combining Eqs. (43) and (49), the CDF of the two categories of transition situations can be expressed using a single equation:

$$F_{ik}(x)=\begin{cases}F_{ik}^{(1)}(x) & j=0\\ F_{ik}^{(2)}(x) & j\neq 0\end{cases} \tag{50}$$

Therefore, the number of vehicles with delay, N_d, is

$$N_d=\sum_{i=0}^{\infty}\sum_{k}^{\infty} q_{ik}*pd_{ik}*k \tag{51}$$

And in this movement, the CDF of intersection delay is

$$F(x)=\frac{\sum_{i=0}^{\infty}\sum_{k}^{\infty} q_{ik}*pd_{ik}*k*F_{ik}(x)}{N_d} \tag{52}$$

Accordingly, the average delay and emissions in this movement can be estimated:

$$D_A = \frac{\int_0^{\infty} \left(\frac{\partial F(x)}{\partial x} * x \right) dx * N_d}{\lambda} \tag{53}$$

$$E_A = \frac{\int_0^{\infty} \left(\frac{\partial F(x)}{\partial x} * f_{2E}(x) \right) dx * N_d}{\lambda} \tag{54}$$

where D_A is the average delay in terms of seconds per vehicle (s/veh); E_A is the average emissions; $f_{2E}(x)$ is the emission function with respect to intersection delay developed in Section 2.

3.2 Numerical Study

In the numerical study, the developed model is used to estimate the average intersection delay and emissions for an unsaturated movement considering a variety of cycle lengths, green times, saturation flow rates, and demands.

Table 11 Average intersection delay based on the stochastic model

X		G/C = 0.3 C			G/C = 0.4 C			G/C = 0.5 C		
	s	90 s	120 s	150 s	90 s	120 s	150 s	90 s	120 s	150 s
0.5	1600 vph	27.11	35.64	44.23	21.18	27.89	34.62	15.77	20.75	25.73
	1800 vph	27.03	35.50	44.13	21.06	27.78	34.52	15.68	20.66	25.65
	3200 vph	26.45	35.09	43.73	20.70	27.44	34.19	15.38	20.38	25.37
	3600 vph	26.39	35.04	43.68	20.65	27.40	34.14	15.34	20.34	25.34
0.7	1600 vph	31.48	40.13	48.99	24.91	32.23	39.56	19.13	24.90	30.31
	1800 vph	31.83	39.59	48.92	24.49	31.65	38.94	19.07	24.38	30.10
	3200 vph	29.01	38.11	47.30	23.30	30.75	38.16	17.97	23.69	29.44
	3600 vph	28.81	37.96	47.17	23.17	30.60	38.06	17.88	23.61	29.36
0.9	1600 vph	54.73	63.48	72.21	42.99	54.85	65.81	34.01	46.40	47.88
	1800 vph	66.86	60.41	77.38	40.61	47.88	55.32	37.22	37.95	46.65
	3200 vph	40.69	49.77	59.02	32.55	42.46	48.81	25.88	32.71	39.43
	3600 vph	39.18	48.34	57.67	31.47	39.21	47.09	25.06	31.32	37.70

Table 11 summarizes the numerical results of average delay based on the proposed stochastic model. The unit of average delay is s/veh. Generally, as the G/C ratio increases, intersection delay decreases. As the degree of saturation (X) increases, intersection delay increases. As the cycle length increases, intersection delay increases due to the longer red time and vehicle waiting time. Once a vehicle cannot be discharged in the current cycle, it has to wait until the next green signal and suffers the longer time caused by a greater cycle length. As the saturation flow rate increases, intersection delay decreases. Its physical meaning can be interpreted in a comparison between one lane and two lane roads. At the same value of X , the probability of one lane falling into oversaturated conditions in a cycle is higher than that of both two lanes doing so. Therefore, on a two lane road, vehicles encountering oversaturated conditions on one lane can switch to the other lane; accordingly, the average delay on a two lane road is smaller than that on a one lane road.

To estimate emissions, this numerical study adopts the emission functions derived in Section 2 for Site (a). Table 12, Table 13, and Table 14 summarize the numerical results of average emissions of CO, HC, and NO. Compared with Table 11, the change of average emissions with respect to the G/C ratio, the degree of saturation (X), the cycle length, and the saturation flow rate has the similar trend to that of average delay; however, the change range of average emissions is much smaller than that of average delay.

Table 12 Average emissions (CO) based on the stochastic model

X	s	G/C = 0.3 C 90 s	120 s	150 s	G/C = 0.4 C 90 s	120 s	150 s	G/C = 0.5 C 90 s	120 s	150 s
0.5	1600 vph	56.20	56.53	56.80	50.94	51.27	51.52	44.97	45.31	45.55
	1800 vph	56.02	56.36	56.67	50.70	51.09	51.38	44.74	45.13	45.41
	3200 vph	55.19	55.78	56.20	49.90	50.49	50.90	43.91	44.52	44.92
	3600 vph	55.08	55.70	56.13	49.79	50.41	50.83	43.80	44.43	44.85
0.7	1600 vph	60.86	61.12	61.35	57.14	57.48	57.69	52.68	53.05	53.08
	1800 vph	60.95	60.92	61.28	56.85	57.15	57.39	52.53	52.62	52.87
	3200 vph	59.63	60.18	60.59	55.75	56.35	56.73	51.09	51.68	52.08
	3600 vph	59.48	60.07	60.50	55.59	56.20	56.63	50.91	51.54	51.96
0.9	1600 vph	66.60	66.77	66.93	65.00	65.69	66.16	63.09	64.32	63.70
	1800 vph	67.60	66.61	67.34	64.78	64.97	65.15	63.86	62.98	63.62
	3200 vph	65.54	65.88	66.16	63.77	64.58	64.55	61.57	62.15	62.51
	3600 vph	65.38	65.74	66.04	63.57	63.96	64.27	61.33	61.75	62.05

Table 13 Average emissions (HC) based on the stochastic model

X	s	G/C = 0.3 C 90 s	120 s	150 s	G/C = 0.4 C 90 s	120 s	150 s	G/C = 0.5 C 90 s	120 s	150 s
0.5	1600 vph	0.77	0.77	0.77	0.70	0.70	0.70	0.61	0.62	0.62
	1800 vph	0.76	0.77	0.77	0.69	0.70	0.70	0.61	0.62	0.62
	3200 vph	0.75	0.76	0.76	0.68	0.69	0.69	0.60	0.61	0.61
	3600 vph	0.75	0.76	0.76	0.68	0.69	0.69	0.60	0.61	0.61
0.7	1600 vph	0.83	0.83	0.83	0.78	0.78	0.78	0.72	0.72	0.72
	1800 vph	0.83	0.83	0.83	0.78	0.78	0.78	0.72	0.72	0.72
	3200 vph	0.81	0.82	0.82	0.76	0.77	0.77	0.70	0.70	0.71
	3600 vph	0.81	0.82	0.82	0.76	0.76	0.77	0.70	0.70	0.71
0.9	1600 vph	0.90	0.90	0.90	0.88	0.89	0.89	0.86	0.87	0.86
	1800 vph	0.91	0.90	0.91	0.88	0.88	0.88	0.87	0.86	0.86
	3200 vph	0.89	0.89	0.89	0.87	0.88	0.87	0.84	0.85	0.85
	3600 vph	0.89	0.89	0.89	0.87	0.87	0.87	0.84	0.84	0.84

Table 14 Average emissions (NO) based on the stochastic model

X	s	G/C = 0.3 C 90 s	120 s	150 s	G/C = 0.4 C 90 s	120 s	150 s	G/C = 0.5 C 90 s	120 s	150 s
0.5	1600 vph	2.65	2.77	2.89	2.36	2.46	2.55	2.05	2.12	2.20
	1800 vph	2.64	2.76	2.89	2.35	2.45	2.55	2.04	2.12	2.19
	3200 vph	2.60	2.73	2.86	2.31	2.42	2.52	2.00	2.09	2.16
	3600 vph	2.60	2.73	2.86	2.31	2.42	2.52	2.00	2.08	2.16
0.7	1600 vph	2.89	3.02	3.14	2.66	2.77	2.87	2.41	2.49	2.56
	1800 vph	2.90	3.00	3.13	2.64	2.75	2.85	2.40	2.47	2.55
	3200 vph	2.81	2.95	3.09	2.59	2.70	2.81	2.33	2.42	2.51
	3600 vph	2.81	2.95	3.08	2.58	2.69	2.81	2.32	2.42	2.50
0.9	1600 vph	3.42	3.54	3.67	3.21	3.39	3.55	3.01	3.22	3.22
	1800 vph	3.62	3.50	3.75	3.17	3.27	3.37	3.09	3.06	3.20
	3200 vph	3.20	3.33	3.46	3.02	3.18	3.26	2.85	2.96	3.06
	3600 vph	3.17	3.31	3.44	3.00	3.12	3.23	2.83	2.93	3.02

3.3 Comparison between with and without Considering Randomness

Without considering the randomness of vehicle arrivals, the average delay can be expressed as Eq. (55) (Transportation Research Board, 2010).

$$D_U = \frac{0.5 * C * (1 - G/C)^2}{1 - X * G/C} \tag{55}$$

where D_U represents the uniform delay. The delay are uniformly distributed on the domain $[0, R)$, and the percentage of vehicles with delay will be:

$$pd_{ik} = \frac{T_B}{C} = \frac{\frac{sR + i}{s - k/C}}{C} \xrightarrow{i=0, k=\lambda} \frac{R/C}{1 - \frac{\lambda/C}{s}} = \frac{1 - G/C}{1 - X * G/C} \tag{56}$$

Substituting the uniform distribution and Eq. (56) to Eq. (54), the average emissions for a movement of uniform vehicle arrivals can be estimated. Table 15 through Table 18 summarizes average delay and average emissions assuming uniform vehicle arrivals. Compared with Table 11 through Table 14, where the saturation flow rate impacts delay and emissions by causing oversaturated situations in certain cycles, Table 15 through Table 18 indicates no impact of the saturation flow rate on delay and emissions. That is because without considering the randomness of vehicle arrivals, the oversaturated conditions will not happen in any cycle as long as the degree of saturation (X) is smaller than 1.0.

Table 15 Average intersection delay based on the uniform arrival

X	s	G/C = 0.3 C 90 s	120 s	150 s	G/C = 0.4 C 90 s	120 s	150 s	G/C = 0.5 C 90 s	120 s	150 s
0.5	1600 vph	25.94	34.59	43.24	20.25	27.00	33.75	15.00	20.00	25.00
	1800 vph	25.94	34.59	43.24	20.25	27.00	33.75	15.00	20.00	25.00
	3200 vph	25.94	34.59	43.24	20.25	27.00	33.75	15.00	20.00	25.00
	3600 vph	25.94	34.59	43.24	20.25	27.00	33.75	15.00	20.00	25.00
0.7	1600 vph	27.91	37.22	46.52	22.50	30.00	37.50	17.31	23.08	28.85
	1800 vph	27.91	37.22	46.52	22.50	30.00	37.50	17.31	23.08	28.85
	3200 vph	27.91	37.22	46.52	22.50	30.00	37.50	17.31	23.08	28.85
	3600 vph	27.91	37.22	46.52	22.50	30.00	37.50	17.31	23.08	28.85
0.9	1600 vph	30.21	40.27	50.34	25.31	33.75	42.19	20.45	27.27	34.09
	1800 vph	30.21	40.27	50.34	25.31	33.75	42.19	20.45	27.27	34.09
	3200 vph	30.21	40.27	50.34	25.31	33.75	42.19	20.45	27.27	34.09
	3600 vph	30.21	40.27	50.34	25.31	33.75	42.19	20.45	27.27	34.09

Table 16 Average emissions (CO) based on the uniform arrival

X	s	G/C = 0.3 C 90 s	120 s	150 s	G/C = 0.4 C 90 s	120 s	150 s	G/C = 0.5 C 90 s	120 s	150 s
0.5	1600 vph	54.22	55.05	55.61	48.92	49.75	50.30	42.92	43.77	44.32
	1800 vph	54.22	55.05	55.61	48.92	49.75	50.30	42.92	43.77	44.32
	3200 vph	54.22	55.05	55.61	48.92	49.75	50.30	42.92	43.77	44.32
	3600 vph	54.22	55.05	55.61	48.92	49.75	50.30	42.92	43.77	44.32
0.7	1600 vph	58.34	59.23	59.84	54.35	55.28	55.89	49.53	50.50	51.13
	1800 vph	58.34	59.23	59.84	54.35	55.28	55.89	49.53	50.50	51.13
	3200 vph	58.34	59.23	59.84	54.35	55.28	55.89	49.53	50.50	51.13
	3600 vph	58.34	59.23	59.84	54.35	55.28	55.89	49.53	50.50	51.13
0.9	1600 vph	63.14	64.10	64.76	61.14	62.19	62.87	58.53	59.68	60.43
	1800 vph	63.14	64.10	64.76	61.14	62.19	62.87	58.53	59.68	60.43
	3200 vph	63.14	64.10	64.76	61.14	62.19	62.87	58.53	59.68	60.43
	3600 vph	63.14	64.10	64.76	61.14	62.19	62.87	58.53	59.68	60.43

Table 17 Average emissions (HC) based on the uniform arrival

X	s	G/C = 0.3 C 90 s	120 s	150 s	G/C = 0.4 C 90 s	120 s	150 s	G/C = 0.5 C 90 s	120 s	150 s
0.5	1600 vph	0.74	0.75	0.75	0.67	0.68	0.68	0.59	0.60	0.60
	1800 vph	0.74	0.75	0.75	0.67	0.68	0.68	0.59	0.60	0.60
	3200 vph	0.74	0.75	0.75	0.67	0.68	0.68	0.59	0.60	0.60
	3600 vph	0.74	0.75	0.75	0.67	0.68	0.68	0.59	0.60	0.60
0.7	1600 vph	0.80	0.80	0.81	0.74	0.75	0.76	0.68	0.69	0.70
	1800 vph	0.80	0.80	0.81	0.74	0.75	0.76	0.68	0.69	0.70
	3200 vph	0.80	0.80	0.81	0.74	0.75	0.76	0.68	0.69	0.70
	3600 vph	0.80	0.80	0.81	0.74	0.75	0.76	0.68	0.69	0.70
0.9	1600 vph	0.86	0.87	0.88	0.83	0.85	0.85	0.80	0.81	0.82
	1800 vph	0.86	0.87	0.88	0.83	0.85	0.85	0.80	0.81	0.82
	3200 vph	0.86	0.87	0.88	0.83	0.85	0.85	0.80	0.81	0.82
	3600 vph	0.86	0.87	0.88	0.83	0.85	0.85	0.80	0.81	0.82

Table 18 Average emissions (NO) based on the uniform arrival

X	s	G/C = 0.3 C 90 s	120 s	150 s	G/C = 0.4 C 90 s	120 s	150 s	G/C = 0.5 C 90 s	120 s	150 s
0.5	1600 vph	2.56	2.70	2.83	2.27	2.38	2.49	1.96	2.05	2.14
	1800 vph	2.56	2.70	2.83	2.27	2.38	2.49	1.96	2.05	2.14
	3200 vph	2.56	2.70	2.83	2.27	2.38	2.49	1.96	2.05	2.14
	3600 vph	2.56	2.70	2.83	2.27	2.38	2.49	1.96	2.05	2.14
0.7	1600 vph	2.75	2.90	3.05	2.52	2.65	2.77	2.26	2.37	2.46
	1800 vph	2.75	2.90	3.05	2.52	2.65	2.77	2.26	2.37	2.46
	3200 vph	2.75	2.90	3.05	2.52	2.65	2.77	2.26	2.37	2.46
	3600 vph	2.75	2.90	3.05	2.52	2.65	2.77	2.26	2.37	2.46
0.9	1600 vph	2.98	3.14	3.30	2.83	2.98	3.12	2.67	2.80	2.91
	1800 vph	2.98	3.14	3.30	2.83	2.98	3.12	2.67	2.80	2.91
	3200 vph	2.98	3.14	3.30	2.83	2.98	3.12	2.67	2.80	2.91
	3600 vph	2.98	3.14	3.30	2.83	2.98	3.12	2.67	2.80	2.91

To explore the impact of random vehicle arrivals, Table 19 through Table 22 provides the relative increases of delay and emissions caused by random vehicle arrivals. The relative increase (RI) is computed as described in Eq. (57).

$$RI = \frac{Val_1 - Val_2}{Val_2} \tag{57}$$

where RI represents the relative increase, which represents the contribution of random vehicle arrivals to delay (or missions); Val_1 represents the value of delay (or missions) estimated by the stochastic model; Val_2 represents the corresponding value of delay (or missions) estimated by the uniform vehicle arrival model. According to Table 19 through Table 22, as the G/C ratio increases, RI increases; as the degree of saturation (X) increases, RI increases; as the cycle length increases, RI decreases; as the saturation flow rate increases, RI decreases.

In addition, the change range of emission RI is much smaller than that of delay RI . The delay RI can be greater than 1.000 when X is 0.9; the emission RI is normally smaller than 0.150. The large delay RI is caused by longer waiting time when oversaturated conditions happen at certain cycles; on the other hand, modern emission models like MOVES recognize low emission rates for idling vehicles, so the emission RI is much smaller. In particular, at a typical major intersection of two urban arterials, where the cycle length is longer than 90 s and the saturation flow rate is greater than 3200 vph, the emission RI is even smaller than 0.050.

Table 19 Relative increase of average delay

X	s	G/C = 0.3 C 90 s	120 s	150 s	G/C = 0.4 C 90 s	120 s	150 s	G/C = 0.5 C 90 s	120 s	150 s
0.5	1600 vph	0.045	0.030	0.023	0.046	0.033	0.026	0.051	0.037	0.029
	1800 vph	0.042	0.026	0.021	0.040	0.029	0.023	0.045	0.033	0.026
	3200 vph	0.020	0.014	0.011	0.022	0.016	0.013	0.025	0.019	0.015
	3600 vph	0.017	0.013	0.010	0.020	0.015	0.012	0.023	0.017	0.013
0.7	1600 vph	0.128	0.078	0.053	0.107	0.074	0.055	0.105	0.079	0.051
	1800 vph	0.141	0.064	0.052	0.088	0.055	0.038	0.102	0.057	0.043
	3200 vph	0.039	0.024	0.017	0.036	0.025	0.018	0.038	0.027	0.021
	3600 vph	0.032	0.020	0.014	0.030	0.020	0.015	0.033	0.023	0.018
0.9	1600 vph	0.812	0.576	0.434	0.698	0.625	0.560	0.663	0.701	0.405
	1800 vph	1.214	0.500	0.537	0.604	0.419	0.311	0.819	0.392	0.369
	3200 vph	0.347	0.236	0.172	0.286	0.258	0.157	0.265	0.199	0.156
	3600 vph	0.297	0.200	0.146	0.243	0.162	0.116	0.225	0.148	0.106

Table 20 Relative increase of average emissions (CO)

X	s	G/C = 0.3 C 90 s	120 s	150 s	G/C = 0.4 C 90 s	120 s	150 s	G/C = 0.5 C 90 s	120 s	150 s
0.5	1600 vph	0.036	0.027	0.021	0.041	0.031	0.024	0.048	0.035	0.028
	1800 vph	0.033	0.024	0.019	0.037	0.027	0.021	0.042	0.031	0.025
	3200 vph	0.018	0.013	0.011	0.020	0.015	0.012	0.023	0.017	0.014
	3600 vph	0.016	0.012	0.009	0.018	0.013	0.011	0.020	0.015	0.012
0.7	1600 vph	0.043	0.032	0.025	0.051	0.040	0.032	0.064	0.050	0.038
	1800 vph	0.045	0.029	0.024	0.046	0.034	0.027	0.061	0.042	0.034
	3200 vph	0.022	0.016	0.013	0.026	0.019	0.015	0.032	0.023	0.018
	3600 vph	0.020	0.014	0.011	0.023	0.017	0.013	0.028	0.021	0.016
0.9	1600 vph	0.055	0.042	0.034	0.063	0.056	0.052	0.078	0.078	0.054
	1800 vph	0.071	0.039	0.040	0.059	0.045	0.036	0.091	0.055	0.053
	3200 vph	0.038	0.028	0.022	0.043	0.039	0.027	0.052	0.041	0.034
	3600 vph	0.036	0.026	0.020	0.040	0.029	0.022	0.048	0.035	0.027

Table 21 Relative increase of average emissions (HC)

X	s	G/C = 0.3 C 90 s	120 s	150 s	G/C = 0.4 C 90 s	120 s	150 s	G/C = 0.5 C 90 s	120 s	150 s
0.5	1600 vph	0.035	0.026	0.021	0.040	0.030	0.024	0.046	0.034	0.027
	1800 vph	0.032	0.023	0.019	0.035	0.026	0.021	0.041	0.030	0.024
	3200 vph	0.017	0.013	0.010	0.020	0.015	0.012	0.022	0.017	0.013
	3600 vph	0.015	0.012	0.009	0.017	0.013	0.010	0.020	0.015	0.012
0.7	1600 vph	0.040	0.030	0.024	0.048	0.038	0.031	0.059	0.048	0.037
	1800 vph	0.042	0.027	0.023	0.044	0.033	0.026	0.057	0.040	0.033
	3200 vph	0.021	0.016	0.012	0.025	0.019	0.015	0.031	0.023	0.018
	3600 vph	0.019	0.014	0.011	0.022	0.016	0.013	0.027	0.020	0.016
0.9	1600 vph	0.045	0.034	0.027	0.054	0.048	0.043	0.068	0.067	0.048
	1800 vph	0.056	0.032	0.031	0.052	0.039	0.031	0.079	0.049	0.047
	3200 vph	0.034	0.024	0.019	0.039	0.035	0.024	0.048	0.038	0.032
	3600 vph	0.032	0.023	0.018	0.036	0.026	0.020	0.044	0.032	0.025

Table 22 Relative increase of average emissions (NO)

X	s	G/C = 0.3 C 90 s	120 s	150 s	G/C = 0.4 C 90 s	120 s	150 s	G/C = 0.5 C 90 s	120 s	150 s
0.5	1600 vph	0.036	0.027	0.021	0.040	0.030	0.024	0.046	0.034	0.027
	1800 vph	0.033	0.023	0.019	0.035	0.026	0.021	0.041	0.030	0.024
	3200 vph	0.017	0.013	0.010	0.020	0.015	0.012	0.022	0.017	0.013
	3600 vph	0.015	0.012	0.009	0.017	0.013	0.010	0.020	0.015	0.012
0.7	1600 vph	0.050	0.037	0.029	0.053	0.042	0.035	0.062	0.050	0.038
	1800 vph	0.053	0.033	0.028	0.047	0.035	0.028	0.060	0.041	0.034
	3200 vph	0.023	0.017	0.013	0.026	0.019	0.015	0.031	0.023	0.018
	3600 vph	0.020	0.015	0.011	0.023	0.017	0.013	0.027	0.020	0.016
0.9	1600 vph	0.131	0.114	0.100	0.116	0.120	0.122	0.115	0.132	0.095
	1800 vph	0.178	0.102	0.121	0.105	0.088	0.076	0.135	0.086	0.089
	3200 vph	0.070	0.057	0.048	0.063	0.064	0.046	0.064	0.055	0.048
	3600 vph	0.062	0.050	0.042	0.056	0.044	0.036	0.058	0.044	0.036

4. SIGNAL OPTIMIZATION AT INTERSECTION LEVEL

The objective of this section is to formulate an optimization problem of signal timing at an intersection considering traffic emissions. Section 3 models emissions for a movement when the green and red times are given, so the decision variables of the optimization problem are green times of all movements during a cycle. The objective function is a linear combination of delay and emissions at an intersection, so that the tradeoff between the two could be examined with the optimization problem. Moreover, various factors that impact this tradeoff are investigated, such as the cycle length, the percentage of turning vehicles, and the ratio of traffic volumes on major roads over minor roads.

The emission model developed in Section 2 and Section 3 has complex structures, so two steps of approximations are made to simplify the optimization problem. First, emissions are estimated for a movement without considering random vehicle arrivals. Section 3 models emissions at a movement with and without considering randomness, respectively: the emission model considering randomness is based on the development of Markov chains and numerical simulations; the emission model without considering randomness can be expressed with mathematic formulations. Without considering randomness, the emission model underestimates emissions at a movement, but this underestimation is very small. For example, at a typical urban intersection, the underestimated emissions can be smaller than 5% of the total emissions

at a movement. Therefore, uniform vehicle arrivals are assumed in formulating the optimization problem, which is referred to Optimization Problem-1 (OP1).

Genetic Algorithm (GA) is used to solve OP1 because emission functions developed in Section 2 are piecewise. To solve the optimization problem more efficiently, the second step of approximations is to replace those piecewise functions with smooth ones. Parabolic functions are adopted in this step, and the new optimization problem is referred to Optimization Problem-2 (OP2). The convexity of OP2 is discussed, and a more efficient solution approach is used to solve OP2. Furthermore, the optimal results of OP2 are compared with those to OP1.

4.1 Optimization Problem-1 (OP1)

This section first develops OP1, and based on the solutions to OP1 the tradeoff between delay and emissions is discussed. First, OP1 is formulized with the green times as decision variables and the linear combination of delay and emissions as the objective function; second, a case study is conducted at a typical intersection; third, the tradeoff between delay and emissions is discussed in a variety of scenarios with different cycle lengths, percentages of turning vehicles, and ratios of traffic volumes on major roads over minor roads.

4.1.1 Formulation

OP1 adopts the green times as its decision variables and the linear combination of delay and emissions as its objective function. The delay equations in HCM (2010) are used in this study.

$$H_D(G) = D_U(G) + D_R(G) \tag{58}$$

where $H_D(G)$ represents the function of average delay with respect to green time; $D_U(G)$ and $D_R(G)$ represents uniform and random delay, respectively:

$$D_U(G) = \frac{0.5 * C * (1 - G/C)^2}{1 - X * G/C} \tag{59}$$

$$D_R(G) = 900 * T_D * \left[(X - 1) + \sqrt{(X - 1)^2 + \frac{4 * X}{s * G/C * T_D}} \right] \tag{60}$$

where T_D is the duration of analysis period, whose default value is 0.25 indicated by Highway Capacity Software (HCS).

OP1 assumes uniform vehicle arrivals when modeling emissions. The delay are uniformly distributed on the domain $[0, R)$, and recall the percentage of vehicles with delay:

$$pd = \frac{1 - G/C}{1 - X * G/C} \tag{61}$$

$G + R = C$, and the emission function can be expressed as follows:

$$H_E(G) = \int_0^R \left(\frac{1}{R} * f_{2E}(x) \right) dx * pd = \int_0^{C-G} \left(\frac{1}{C - G} * f_{2E}(x) \right) dx * pd \tag{62}$$

where $H_E(G)$ represents the function of average emissions with respect to green time.

With the functions of delay and emissions, OP1 can be formulized:

$$\text{Min } \alpha * \frac{\dfrac{\sum_i \left[H_D^{(i)}(G^{(i)}) * \lambda^{(i)}\right]}{\sum_i \lambda^{(i)}}}{BDe} + (1-\alpha) * \frac{\dfrac{\sum_i \left[H_E^{(i)}(G^{(i)}) * \lambda^{(i)}\right]}{\sum_i \lambda^{(i)}}}{BEm} \tag{63}$$

$$\text{Subject to } sG^{(i)} \geq \lambda^{(i)} \qquad \text{for each movement } i$$

$$\sum_{critial} (G^{(i)} + Lost) = C$$

In Eq. (63), the superscript $^{(i)}$ represents the movement i; α is a fraction between 0 and 1, considering different relative weights between delay and emissions. BDe and BEm are base values to normalize delay and emissions. In this study, BDe and BEm are equal to the average delay and emissions under the best signal timing plan when only delay is minimized. $sG^{(i)} \geq \lambda^{(i)}$ ensures that the demand is not over the capacity to avoid oversaturated conditions. For all critical movements during a cycle, the summation of their effective green time plus lost time ($Lost$) is equal to the cycle length.

4.1.2 Case Study

The case study intersection is designed based on Example 3 in Chapter 16 of the Highway Capacity Manual (2000). The data regarding this intersection is presented in Table 23. North-South (N-S) directions are major roads, which have larger demand flow rates, more lanes, and higher operating speeds than minor roads along East-West (E-W) directions. At the free flow condition, through vehicles are assumed to maintain their

normal operating speeds when driving through the intersection, but turning vehicles reduce their speeds to 15 mph. The cycle length is 120 seconds (s). Only CO is considered in the objective function in the case study.

Table 23 Intersection information in the case study

Approach		**EB**	**WB**	**NB**	**SB**
Traffic Volume (vph)	LT	60	100	120	175
	TH	270	510	1480	840
	RT	90	20	80	70
Number of Lanes	Exclusive LT	1	1	1	1
	RT+TH	2	2	3	3
Normal Operating Speed (mph)		40	40	45	45
Saturation flow Rate (vphpl)		1800	1800	1800	1800
Lost time (s)		4	4	4	4
Cycle length (s)		120			
Phase Diagram		1	2	3	4
		SB LT	SB TH+RT	EB LT	EB TH+RT
		NB LT	NB TH+RT	WB LT	NB TH+RT

NOTE: LT stands for left turn, TH stands for through, and RT stands for right turn.

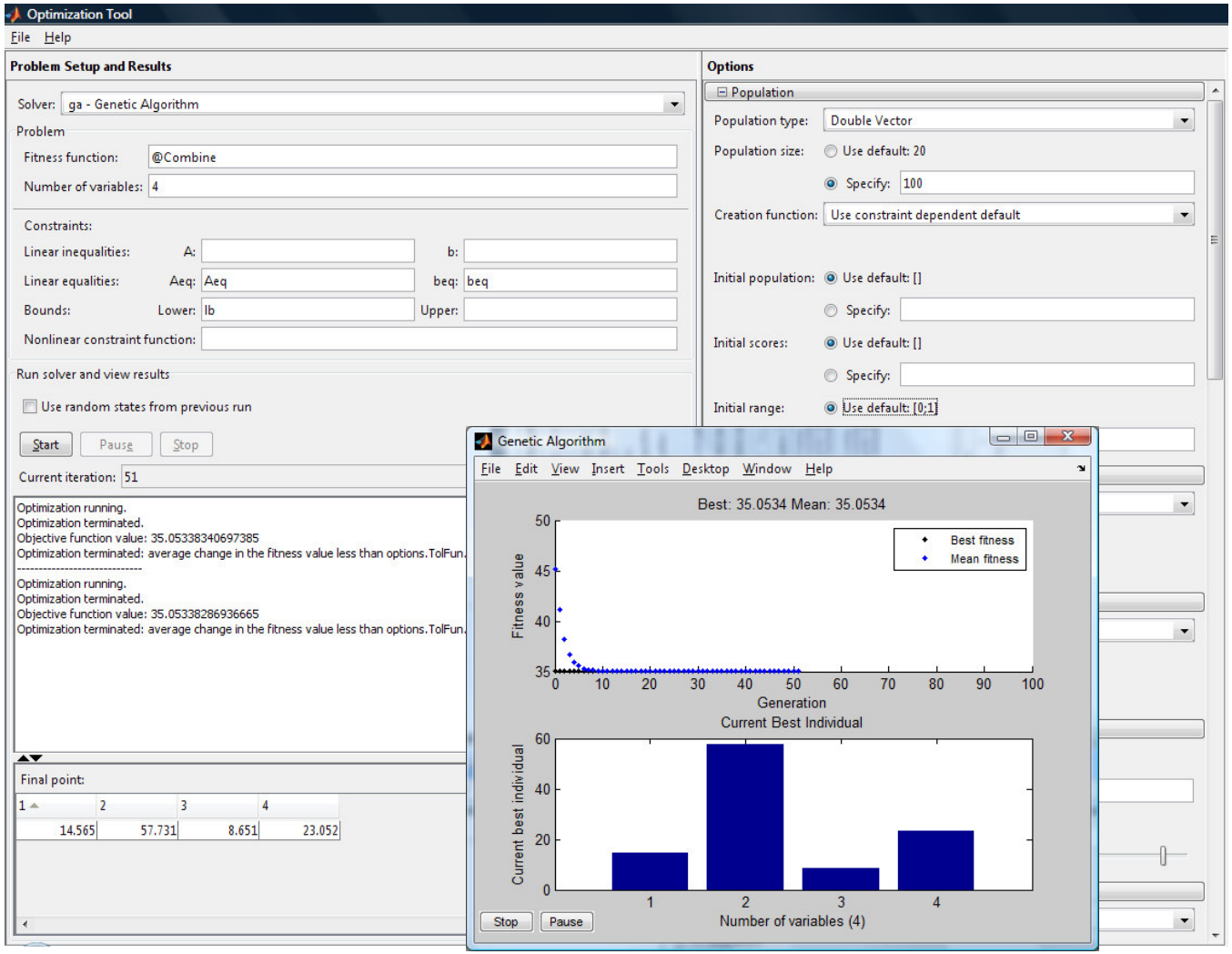

Figure 13 Process of GA searching optimal solution in MATLAB

In this case study, GA is used to solve the proposed optimization problem because the piecewise functions of emissions are involved. GA is a heuristic method for solving optimization problems. Borrowing the concept of biological evolution, GA repeatedly modifies a population of individual solutions, also named chromosomes. During every evolution, based on the fitness function values, the parent chromosomes produce their children through the selection, crossover and mutation rules. Figure 13 illustrates the process of GA searching optimal solution in MATLAB. The population size is set to be 100; other GA parameters such as the selection, crossover, and mutation adopt the default values in MATLAB.

Table 24 Summary of optimization results

α	Optimal solution				Optimal value	Delay	Emissions	Ratios over base values	
								Delay	Emissions
1.0	14.6	57.7	8.7	23.1	1.000	35.05	82.46	1.000	1.000
0.8	14.0	59.5	8.3	22.2	0.998	35.15	80.51	1.003	0.976
0.6	13.3	61.8	7.8	21.1	0.988	35.62	78.01	1.016	0.946
0.4	12.2	64.8	7.1	19.9	0.967	37.07	74.77	1.058	0.907
0.2	11.7	67.3	6.7	18.4	0.925	39.48	72.12	1.126	0.875
0.0	11.7	68.0	6.7	17.7	0.866	40.72	71.41	1.162	0.866

The optimization results of the case study are summarized in Table 24. The optimal solution provides the green times of all phases during a cycle. When α = 1.0, i.e., only delay is considered in the objective function, more green time is assigned to major roads than minor roads. The average delay is 35.05 seconds per vehicle (s/veh), and the average emissions are 82.46 mg per vehicle (mg/veh). By definition, at this

optimal solution when α = 1.0, the delay and emissions are equal to BDe and BEm, so the optimal objective value is 1.000, and ratios of both delay and emissions over base values are also 1.000. When α = 0.0, only emissions are considered in the objective function. The average delay is 40.72 s/veh, and the average emissions are 71.41 mg/veh. As a result, from the delay minimization to emission minimization, a 13.4% reduction of emissions accompanies a 16.2% rise of delay. Meanwhile, as α decreases from 1.0 to 0.0 more and more green time is assigned to major roads for the phase of TH+RT, which has the highest demand. The green time of this major phase increases by 17.9%, while green times of the other phases decrease by 19.9~23.4%, which drives the ratios of flow rate to capacity for these phases close to 1.0. Due to the calculation method of incremental delay in HCM (2010) (see Eq. (60)), the closer to 1.0 these ratios the faster the total delay increases. Therefore, as α decreases, the same value of emissions reduced corresponds to an increasing value of the delay rise. For example in Table 2, from α = 1.0 to 0.8, emissions decrease by 2.4% while delay increases by 0.3%; from α = 0.2 to 0.0, emissions decrease by 0.9% while delay increases by 3.6%. In other words, as α decreases, the marginal value of the emission change with respect to delay decreases. Eq. (64) shows a function of this marginal value, $MV(\alpha)$.

$$MV(\alpha) = \left| \frac{\dfrac{\partial Em^*(\alpha)}{\partial \alpha} \Big/ Em^*(\alpha)}{\dfrac{\partial De^*(\alpha)}{\partial \alpha} \Big/ De^*(\alpha)} \right| \tag{64}$$

where $MV(\alpha)$ represents the marginal value of the emission change with respect to delay; and $Em^*(\alpha)$ and $De^*(\alpha)$ represent emissions and delay at the optimal condition, which are functions with respect to α.

4.1.3 Discussion

Section 4.1.2 has demonstrated air quality benefit by reducing vehicle emissions through signal timing optimization. This subsection further investigates this benefit under different scenarios of cycle lengths, percentages of turning vehicles, and traffic demands on major/minor roads. Table 25 provides a list of scenarios considered in this study.

Table 25 A list of scenarios

Scenario	Description
No. 1	Base case when cycle length is 120 s
No. 2	Cycle length is 60 s
No. 3	Cycle length is 90 s
No. 4	Cycle length is 150 s
No. 5	Percentage of turning vehicles is 10%
No. 6	Percentage of turning vehicles is 30%
No. 7	Percentage of turning vehicles is 50%
No. 8	Percentage of turning vehicles is 70%
No. 9	Flow ratio on major roads is 0.1; Flow ratio on minor roads is 0.1
No. 10	Flow ratio on major roads is 0.1; Flow ratio on minor roads is 0.2
No. 11	Flow ratio on major roads is 0.1; Flow ratio on minor roads is 0.3
No. 12	Flow ratio on major roads is 0.2; Flow ratio on minor roads is 0.1
No. 13	Flow ratio on major roads is 0.2; Flow ratio on minor roads is 0.2
No. 14	Flow ratio on major roads is 0.2; Flow ratio on minor roads is 0.3
No. 15	Flow ratio on major roads is 0.3; Flow ratio on minor roads is 0.1
No. 16	Flow ratio on major roads is 0.3; Flow ratio on minor roads is 0.2
No. 17	Flow ratio on major roads is 0.3; Flow ratio on minor roads is 0.3

Moreover, two measures of effectiveness (MOEs) are used to assess benefit. The first one is the emission reduction when α decreases from 1.0 to 0.0, ER_{1-0}, which is defined in Eq. (65). The other one is the marginal value of the emission change with respect to delay when α decreases from 1.0 to 0.0, MV_{1-0}, which is defined in Eq. (64). ER_{1-0} indicates the effectiveness of reducing emissions through retiming intersection signals, while MV_{1-0} indicates the effectiveness of reducing emissions by paying excess delay.

$$ER_{1-0} = \frac{Em^*(0) - Em^*(1)}{Em^*(0)} \tag{65}$$

$$MV_{1-0} = \left| \frac{\dfrac{Em^*(0) - Em^*(1)}{Em^*(0)}}{\dfrac{De^*(0) - De^*(1)}{De^*(0)}} \right| \tag{66}$$

To assess the impact of cycle lengths, C, which is a parameter in the constraint in Eq. (63), is changed from 60 to 150 s with an interval of 30 s. The Pareto front lines of these four scenarios are generated by changing α between 0.0 and 1.0 (see Figure 14). In these four scenarios (as C increases), ER_{1-0} are 0.099, 0.131, 0.134 and 0.131, and MV_{1-0} are 0.459, 0.655, 0.829, and 1.002. This indicates that more air quality benefit can be achieved at an intersection with a larger cycle length.

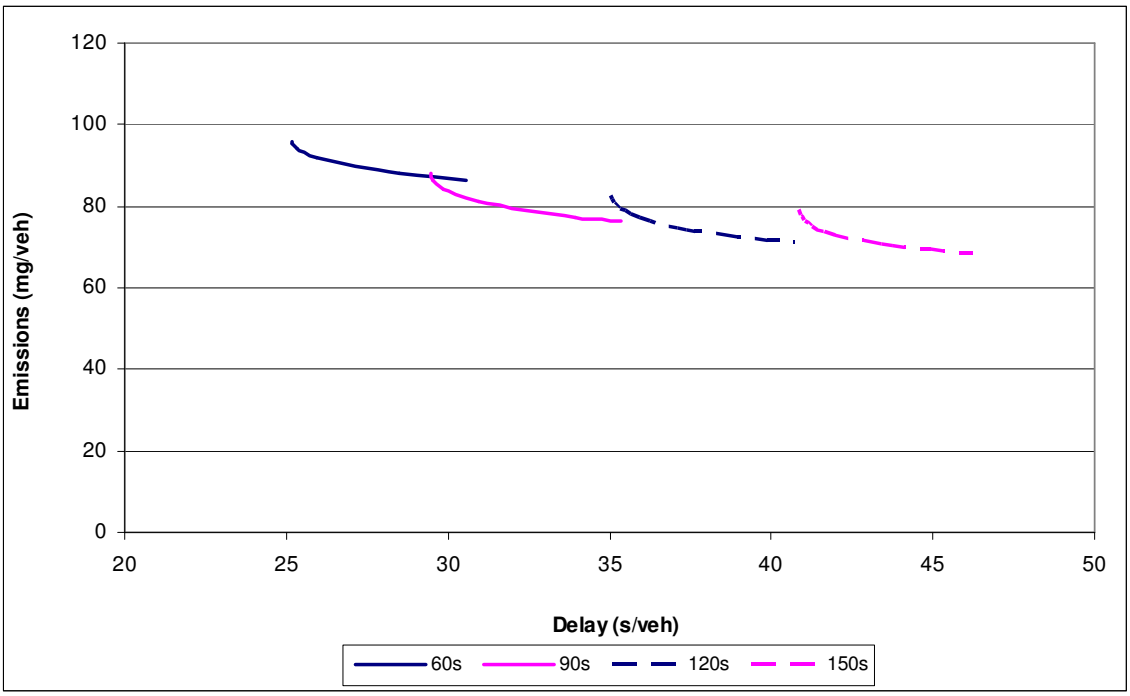

Figure 14 Impact of cycle length

Moreover, Figure 14 illustrates change tendencies of delay and emissions with respect to the cycle length. As the cycle length increases delay increases, but emissions decrease. The delay increase is caused by increasing idling time; however, the impact of idling time on total emissions can be ignored because emission rates for acceleration are much greater than those for idling. The primary reason for the emission decrease is that due to the existence of lost time, the total effective green time for a movement in an hour increases as the cycle length increases, causing less vehicles to stop and accelerate and hence less emissions. Nevertheless, the total effective green time in an hour is not linear with the cycle length, so emissions reduced by increasing the cycle length tends to be insignificant when the cycle length is greater than 150 s.

Table 26 Input table for different percentage of turning vehicles

Approach		**EB**	**WB**	**NB**	**SB**
Traffic Volume (vph)	LT	17	53	101	78
	TH	378	567	1512	977
	RT	25	11	67	31
Turning vehicles (%)		10%			
Approach		**EB**	**WB**	**NB**	**SB**
Traffic Volume (vph)	LT	50	158	302	233
	TH	294	441	1176	760
	RT	76	32	202	93
Turning vehicles (%)		30%			
Approach		**EB**	**WB**	**NB**	**SB**
Traffic Volume (vph)	LT	84	263	504	388
	TH	210	315	840	543
	RT	126	53	336	155
Turning vehicles (%)		50%			
Approach		**EB**	**WB**	**NB**	**SB**
Traffic Volume (vph)	LT	118	368	706	543
	TH	126	189	504	326
	RT	176	74	470	217
Turning vehicles (%)		70%			

To assess the impact of turning vehicles, different sets of traffic demand inputs are generated to represent various percentages of turning vehicles (see Table 26). Based on the case study, in each approach the total volume and the ratio of LT to RT vehicles remain unchanged, but the percentage of turning vehicles (LT + RT) increases from 10% to 70% with an interval of 20%. The Pareto front lines of these four scenarios are generated by changing α between 0.0 and 1.0 (see Figure 15). In these four scenarios

(as the percentage of turning vehicles increases), ER_{1-0} are 0.141, 0.121, 0.077 and 0.003, and MV_{1-0} are 0.733, 0.838, 0.653, and 4.785. As the percentage of turning vehicles increases ER_{1-0} keeps decreasing and approaches to zero, which makes the large MV_{1-0} (e.g., 4.785) meaningless considering that both the emission reduction and the delay rise are too small. The decreasing ER_{1-0} can be reflected in Figure 15 in that the Pareto front line becomes shorter and shorter with the increase of the percentage of turning vehicles, almost degrading to a point when the percentage of turning vehicles increases to 70%. This means that when the percentage of turning vehicles is 70%, minimizing delay and minimizing emissions produce about the same signal timing plan.

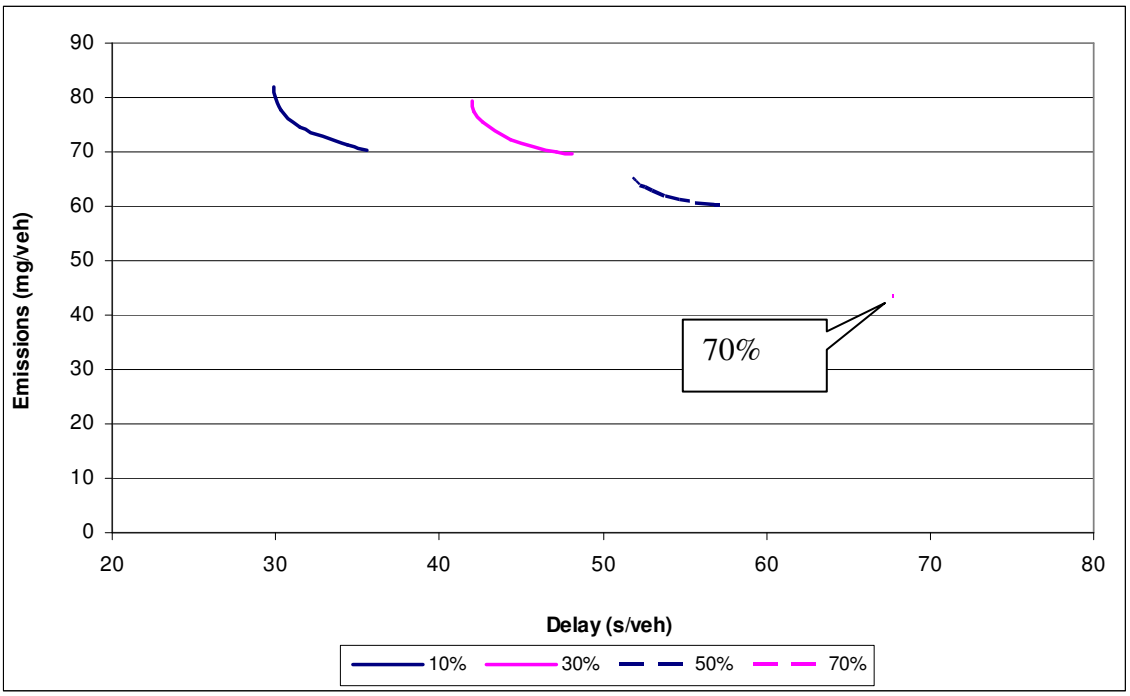

Figure 15 Impact of percentage of turning vehicles

There are two reasons for this degradation of Pareto front line. First, a turning vehicle has to reduce its speed and accelerate at an intersection whether it is hindered by its leading vehicle; therefore, compared with a through vehicle, a turning vehicle experiences a smaller difference of acceleration and emissions between with and without its leading vehicle hindering it. To this end, increasing turning vehicles weakens the impact of signal timing optimization on reducing acceleration and emissions. Second, increasing the percentage of turning vehicles increases traffic flows in turning movements and decreases the counterparts in through movements. Since the saturation flow rate in turning movements is smaller than that in through movements, the increase rate of flow ratios in turning movements is greater than the decrease rate of flow ratios in through movements. To this end, increasing turning vehicles increases the sum of flow ratios of critical movements, which in turn reduces the scope of adjusting signal timing under the unsaturated condition.

Table 27 Input table for different traffic demands on major roads and minor roads

Approach		**EB**	**WB**	**NB**	**SB**
Traffic Volume (vph)	LT	31	52	39	56
	TH	141	266	477	271
	RT	47	10	26	23
Average flow ratio		0.1		0.1	
Approach		**EB**	**WB**	**NB**	**SB**
Traffic Volume (vph)	LT	63	104	77	113
	TH	282	533	955	542
	RT	94	21	52	45
Average flow ratio		0.2		0.2	
Approach		**EB**	**WB**	**NB**	**SB**
Traffic Volume (vph)	LT	94	157	116	169
	TH	432	799	1432	813
	RT	141	31	77	68
Average flow ratio		0.3		0.3	

To assess the impact of traffic demands, different sets of traffic demand inputs are generated to represent various flow ratios on major and minor roads (see Table 27). Based on the case study, in each approach the volume ratios among movements (i.e., LT: TH: RT) remain unchanged, but the total volume changes to increase the average flow ratio from 0.1 to 0.3. Nine scenarios are simulated, and results are summarized in Table 28.

Table 28 Impact of traffic demand levels

Flow Ratio	Major Road					
	0.1		0.2		0.3	
Minor Road	ER_{1-0}	MV_{1-0}	ER_{1-0}	MV_{1-0}	ER_{1-0}	MV_{1-0}
0.1	0.285	0.388	0.211	0.623	0.174	0.748
0.2	0.212	0.319	0.178	0.601	0.134	0.814
0.3	0.082	0.321	0.135	0.556	0.094	0.770

In general, ER_{1-0} decreases when flow ratios on either major or minor roads increase. That is because increasing flow ratios increases the sum of flow ratios of critical movements, which in turn reduces the air quality benefit from adjusting signal timing under the unsaturated condition. However, MV_{1-0} increases with the flow ratios on major roads but decreases with the flow ratios on minor roads. Therefore, it is more beneficial to reduce emissions at an intersection with more traffic on the major road since the delay increases at a slower rate compared to emissions.

4.2 Optimization Problem-2 (OP2)

GA is used to solve OP1. GA is a heuristic method for solving optimization problems, which repeatedly produces a new generation of chromosomes through the selection, crossover and mutation operators; accordingly, GA causes intensive computation load during the process of solving OP1. To solve the optimization problem more efficiently, OP2 makes an approximation to replace the piecewise emission functions with smooth ones. First, parabolic functions are used in the regression analysis

to generate the smooth emission function. Second, the convexity of OP2 is discussed. Furthermore, the optimal solutions to OP2 are compared with those to OP1.

4.2.1 Regression

Section 2 develops relationships between emission and delay, and Table 29 provides delay and its corresponding emission values. This section adopts parabolic functions to represent these relationships because the parabolic function is differentiable and monotone increasing when the argument ≥ 0.

$$f_{1E}(x) = b_0 x^{b_1} \tag{67}$$

where $f_{1E}(x)$ represents emission function with respect to delay in the parabolic format, and b_0 and b_1 are constants. Table 30 summarizes the results of regression analyses. Moreover, considering the adjustment of turning movement Eq. (67) can be extended as follows:

$$f_{2E}(x) = f_{1E}(x + D_0) - Em_0 = b_0 (x + D_0)^{b_1} - Em_0 \tag{68}$$

Table 29 Relationships between emission and delay

Delay	Site (a)			Site (b)		
	CO	HC	NO	CO	HC	NO
0	0	0	0	0	0	0
1	12.667	0.194	0.931	39.056	0.556	1.764
2	32.389	0.450	1.608	56.833	0.794	2.386
3	47.389	0.661	2.119	148.111	2.017	6.806
4	57.389	0.786	2.422	156.833	2.133	7.086
5	59.611	0.814	2.558	158.583	2.158	7.203
6	57.111	0.769	2.514	160.528	2.186	7.325
7	62.111	0.867	2.775	162.111	2.197	7.400
8	63.583	0.881	2.781	163.222	2.219	7.481
9	64.056	0.892	2.869	165.167	2.244	7.575
10	64.889	0.903	2.825	165.806	2.264	7.636
11	62.111	0.836	2.700	166.556	2.269	7.669
12	68.222	0.925	2.892	167.389	2.281	7.625
13	68.222	0.933	2.961	168.222	2.281	7.611
14	68.500	0.939	2.972	170.167	2.286	7.636
15	68.778	0.942	2.986	170.167	2.294	7.706
16	68.778	0.942	2.986	170.186	2.295	7.719
17	68.797	0.942	3.000	168.797	2.297	7.703
18	68.817	0.942	3.014	168.817	2.297	7.717
19	68.836	0.942	3.028	168.836	2.297	7.731
20	68.856	0.942	3.042	168.856	2.297	7.744
21	68.875	0.942	3.056	168.875	2.298	7.758
22	68.894	0.942	3.069	168.894	2.298	7.772
23	68.914	0.942	3.083	168.914	2.298	7.786
24	68.933	0.942	3.097	168.933	2.298	7.800
25	68.953	0.942	3.111	168.953	2.298	7.814
26	68.972	0.942	3.125	168.972	2.298	7.828
27	68.992	0.942	3.139	168.992	2.298	7.842
28	69.011	0.942	3.153	169.011	2.298	7.856
29	69.031	0.942	3.167	169.031	2.298	7.869
30	69.050	0.942	3.181	169.050	2.298	7.883
31	69.069	0.943	3.194	169.069	2.298	7.897
32	69.089	0.943	3.208	169.089	2.298	7.911
33	69.108	0.943	3.222	169.108	2.298	7.925
34	69.128	0.943	3.236	169.128	2.298	7.939
35	69.147	0.943	3.250	169.147	2.298	7.953
36	69.167	0.943	3.264	169.167	2.298	7.967
37	69.186	0.943	3.278	169.186	2.298	7.981
38	69.206	0.943	3.292	169.206	2.298	7.994
39	69.225	0.943	3.306	169.225	2.299	8.008
40	69.244	0.943	3.319	169.244	2.299	8.022

Table 30 Regression results

Emission Functions		b_0	b_1	RMSE
Site (a)	CO	40.800	0.163	6.374
	HC	0.568	0.158	0.086
	NO	1.761	0.179	0.184
Site (b)	CO	110.770	0.134	19.106
	HC	1.513	0.132	0.255
	NO	4.913	0.148	0.086

4.2.2 Convexity

Compared with OP1, OP2 does not include piecewise functions. All functions in OP2 are differentiable, and this subsection further investigates their convexity. First, functions of both uniform and random delays are examined; second, the emission expression in Eq. (62) is revisited by substituting the parabolic functions developed in Section 4.2.1.

When the cycle length and demand are given, the function of uniform delay has only one argument, the green time:

$$D_U(G) = \frac{0.5 * C * (1 - G/C)^2}{1 - X * G/C} = \frac{0.5 * C * (1 - G/C)^2}{1 - \frac{\lambda}{s * C}} \tag{69}$$

The first and second order derivatives of Eq. (69) can be expressed as follows:

$$\frac{\partial D_U(G)}{\partial G} = \frac{C * (1 - G/C)}{1 - \frac{\lambda}{s * C}} * (-\frac{1}{C}) = -\frac{1 - G/C}{1 - \frac{\lambda}{s * C}} \tag{70}$$

$$\frac{\partial^2 D_U(G)}{\partial G^2} = -\frac{-1/C}{1-\frac{\lambda}{s*C}} = \frac{1/C}{1-\frac{\lambda}{s*C}} \tag{71}$$

where λ/C is equal to the flow rate of the demand, which should be smaller than the saturation flow rate, s. As a result, $1-\frac{\lambda}{s*C}>0$, and $\frac{\partial^2 D_U(G)}{\partial G^2}>0$. The function of uniform delay is convex.

Compared with uniform delay, the function of random delay has a more complicated structure, which can be considered a function with respect to the degree of saturation, X:

$$\begin{aligned} D_R(X) &= 900*T_D*\left[(X-1)+\sqrt{(X-1)^2+\frac{4*X}{s*G/C*T_D}}\right] \\ &= 900*T_D*\left[(X-1)+\sqrt{(X-1)^2+\frac{4*X^2}{\lambda/C*T_D}}\right] \end{aligned} \tag{72}$$

The derivative of Eq. (72) can be expressed as follows:

$$\begin{aligned} &\frac{\partial D_R(X)}{\partial X} = \\ &900*T_D*\left[1+\frac{1}{2}\left((X-1)^2+\frac{4*X^2}{\lambda/C*T_D}\right)^{-1/2}*\left(2(X-1)+\frac{8X}{\lambda/C*T_D}\right)\right] \\ &= 900*T_D*\left[1+\frac{(X-1)+\frac{4X}{\lambda/C*T_D}}{\sqrt{(X-1)^2+\frac{4*X^2}{\lambda/C*T_D}}}\right] \end{aligned} \tag{73}$$

It is obvious that $\frac{\partial D_R(X)}{\partial X} > 0$ when $(X-1)+\frac{4X}{\lambda/C*T_D} > 0$. To demonstrate $\frac{\partial D_R(X)}{\partial X} > 0$ when $(X-1)+\frac{4X}{\lambda/C*T_D} \le 0$, we here prove $\left|\frac{(X-1)+\frac{4X}{\lambda/C*T_D}}{\sqrt{(X-1)^2+\frac{4*X^2}{\lambda/C*T_D}}}\right| < 1$:

$$\left[(X-1)+\frac{4X}{\lambda/C*T_D}\right]^2 - \left[\sqrt{(X-1)^2+\frac{4*X^2}{\lambda/C*T_D}}\right]^2 = \frac{4X}{\lambda/C*T_D}\left(\frac{4X}{\lambda/C*T_D}+X-2\right) \tag{74}$$

Because $(X-1)+\frac{4X}{\lambda/C*T_D} \le 0$, $\frac{4X}{\lambda/C*T_D}+X-2 = (X-1)+\frac{4X}{\lambda/C*T_D}-1 < 0$.

Accordingly, $\left|\frac{(X-1)+\frac{4X}{\lambda/C*T_D}}{\sqrt{(X-1)^2+\frac{4*X^2}{\lambda/C*T_D}}}\right| < 1$, and $\frac{\partial D_R(X)}{\partial X} > 0$.

The second order derivative of Eq. (72) can be expressed as follows:

$$\begin{aligned}\frac{\partial^2 D_R(X)}{\partial X^2} &= 900*T_D*\frac{1}{2} \\ &*\left[-\frac{1}{2}\left((X-1)^2+\frac{4*X^2}{\lambda/C*T_D}\right)^{-3/2}*\left(2(X-1)+\frac{8X}{\lambda/C*T_D}\right)^2\right. \\ &\left.+\left((X-1)^2+\frac{4*X^2}{\lambda/C*T_D}\right)^{-1/2}*\left(2+\frac{8}{\lambda/C*T_D}\right)\right] \\ &= 900*T_D*\frac{1}{2}\left((X-1)^2+\frac{4*X^2}{\lambda/C*T_D}\right)^{-3/2}\left(\frac{8}{\lambda/C*T_D}\right)\end{aligned} \tag{75}$$

where all multipliers in the right hand is greater than zero, so $\frac{\partial^2 D_R(X)}{\partial X^2} > 0$. To sum up, $D_R(X)$ is monotone increasing and convex.

In addition, the degree of saturation, X, is a function of green time:

$$X(G) = \frac{\lambda / C}{s * G / C} = \frac{\lambda}{s} * \frac{1}{G} \tag{76}$$

Obvious, $X(G)$ is convex. Therefore, the function of random delay with respect to green time, $D_R(X(G))$, is convex.

By substituting the parabolic functions developed in Section 4.2.1 into the emission expression in Eq. (62):

$$\begin{aligned} H_E(G) &= \int_0^{C-G} \frac{1}{1-G} * \left[b_0 (x + D_0)^{b_1} - Em_0 \right] dx * pd \\ &= \int_0^{C-G} \frac{1}{1-G} * \left[b_0 (x + D_0)^{b_1} - Em_0 \right] dx * \frac{1 - G/C}{1 - X * G/C} \\ &= \frac{s}{sC - \lambda} \left[\frac{b_0}{b_1 + 1} (C - G + D_0)^{b_1 + 1} - \frac{b_0}{b_1 + 1} D_0^{b_1 + 1} \right] - \frac{s(C-G)}{sC - \lambda} Em_0 \end{aligned} \tag{77}$$

The first and second order derivatives of Eq. (77) can be expressed as follows:

$$\frac{\partial H_E(G)}{\partial G} = \frac{s}{sC - \lambda} \left[b_0 (C - G + D_0)^{b_1} \right] + \frac{s}{sC - \lambda} Em_0 \tag{78}$$

$$\frac{\partial^2 H_E(G)}{\partial G^2} = \frac{s}{sC - \lambda} \left[b_0 b_1 (C - G + D_0)^{b_1 - 1} \right] \tag{79}$$

where $C - G > 0$, and $sC - \lambda > 0$, so $\frac{\partial^2 H_E(G)}{\partial G^2} > 0$, and $H_E(G)$ is convex.

Because the functions of uniform delay, random delay, and emissions are all convex, the objective function of OP2, which is the linear combination of these convex functions, is also convex. Moreover, the constraints of OP2 are in the linear format. Therefore, OP2 is convex. The interior point algorithm (IPA) is used to solve OP2, and the default set of barrier functions (logarithmic barrier) in MATLAB is adopted.

4.2.3 Comparison of Optimal Solutions

The complete optimization results for OP1 and OP2 under different scenarios are provided in Section 4.3, including the green times, average delay, average emissions, ER_{1-0}, and MV_{1-0}. Paired T-tests are conducted to compare the optimization results of OP1 with OP2, as shown in Table 31. The P-value for the emission comparison is close to zero, indicating a significant difference of emission estimations between OP1 and OP2. Compared with OP1, OP2 overestimates emissions because at the high level of delay the parabolic function of emissions has a steeper slope than its corresponding piecewise function. However, the P-values for all other comparisons are very large, implying that statistically OP1 and OP2 generate the same optimal solution, reach the same optimal values, and estimate the same delay, ER_{1-0}, and MV_{1-0}. In conclusion, with a convex approximation OP2 can still produce appropriate optimal signal timing plans when considering traffic emissions.

Table 31 Comparison between OP1 and OP2

T-tests	Green time	Optimal value	Delay	Emissions	ER_{1-0}	MV_{1-0}
P-value	0.996	0.086	0.216	0.000	0.551	0.259

4.3 Detailed Optimization Results

This subsection provided detailed optimization results for OP1 and OP2 under different scenarios. For OP1, Table 32 summarizes the impact of cycle length; Table 33 the impact of turning vehicles; Table 34, Table 35, and Table 36 the impact of minor road flow ratio when the major road flow ratio is fixed. Correspondingly, the five tables from Table 37 to Table 41 summarize the results for OP2. For each scenario when α changes between 0 and 1, six sets of optimization solutions, optimal values, and delay and emission values are obtained, but only one set of ER_{1-0} and MV_{1-0} are computed.

Table 32 Optimization results of OP1 when cycle length changes

Scenario	α	Optimal solution				Optimal value	Delay	Emissions	ER_{1-0}	MV_{1-0}
	1.0	7.2	21.6	4.3	11.0	1.000	25.18	95.99		
	0.8	7.0	21.9	4.2	10.8	0.999	25.20	95.23		
No. 2	0.6	6.8	22.5	4.1	10.6	0.996	25.34	94.05	0.099	0.459
	0.4	6.5	23.5	3.8	10.2	0.987	25.95	91.87		
	0.2	5.8	25.3	3.4	9.5	0.960	28.50	87.94		
	0.0	5.9	26.0	3.4	8.8	0.902	30.59	86.53		
	1.0	11.1	38.9	6.6	17.3	1.000	29.46	87.98		
	0.8	10.7	40.1	6.4	16.8	0.998	29.53	86.30		
No. 3	0.6	10.2	41.6	6.1	16.1	0.990	29.86	84.12	0.131	0.655
	0.4	9.5	43.7	5.6	15.2	0.973	30.93	81.08		
	0.2	8.8	46.3	5.0	13.9	0.933	33.92	77.28		
	0.0	8.8	47.0	5.0	13.3	0.869	35.37	76.42		
	1.0	14.6	57.7	8.7	23.1	1.000	35.05	82.46		
	0.8	14.0	59.5	8.3	22.2	0.998	35.15	80.51		
No. 1	0.6	13.3	61.8	7.8	21.1	0.988	35.62	78.01	0.134	0.829
(Base)	0.4	12.2	64.8	7.1	19.9	0.967	37.07	74.77		
	0.2	11.7	67.3	6.7	18.4	0.925	39.48	72.12		
	0.0	11.7	68.0	6.7	17.7	0.866	40.72	71.41		
	1.0	17.9	76.9	10.5	28.6	1.000	40.86	78.82		
	0.8	17.1	79.5	10.0	27.4	0.997	40.99	76.59		
No. 4	0.6	16.1	82.5	9.4	26.0	0.986	41.59	74.01	0.131	1.002
	0.4	14.8	86.3	8.5	24.5	0.963	43.40	70.68		
	0.2	14.6	89.0	8.3	22.1	0.922	46.21	68.47		
	0.0	14.6	89.0	8.3	22.1	0.869	46.22	68.46		

Table 33 Optimization results of OP1 when percentage of turning vehicle changes

Scenario	α	Optimal solution				Optimal value	Delay	Emissions	ER_{1-0}	MV_{1-0}
	1.0	9.2	64.1	4.9	25.8	1.000	29.87	82.02		
	0.8	8.8	65.9	4.6	24.6	0.997	29.96	79.96		
No. 5	0.6	8.3	68.0	4.3	23.4	0.988	30.33	77.62	0.141	0.733
	0.4	7.6	70.6	3.9	22.0	0.967	31.47	74.62		
	0.2	6.7	73.6	3.5	20.1	0.925	34.38	71.21		
	0.0	6.8	74.3	3.6	19.4	0.859	35.60	70.48		
	1.0	24.3	46.5	12.6	20.7	1.000	42.01	79.22		
	0.8	23.5	48.4	12.2	20.0	0.998	42.12	77.52		
No. 6	0.6	22.4	50.9	11.6	19.1	0.989	42.64	75.33	0.121	0.838
	0.4	21.0	54.3	10.7	18.0	0.970	44.34	72.28		
	0.2	20.1	57.1	10.5	16.3	0.931	47.19	69.97		
	0.0	20.1	57.5	10.5	15.8	0.879	48.09	69.61		
	1.0	37.2	32.1	19.1	15.6	1.000	51.81	65.28		
	0.8	36.8	32.9	18.9	15.5	0.999	51.86	64.78		
No. 7	0.6	36.0	34.5	18.4	15.1	0.996	52.22	63.80	0.077	0.653
	0.4	34.4	37.6	17.5	14.5	0.984	53.81	61.90		
	0.2	33.6	39.5	17.5	13.4	0.960	55.63	60.80		
	0.0	33.6	40.5	17.6	12.3	0.922	57.95	60.23		
	1.0	47.1	22.0	24.5	10.4	0.999	67.67	43.63		
	0.8	47.1	22.1	24.5	10.3	0.998	67.64	43.59		
No. 8	0.6	47.1	22.2	24.5	10.2	0.998	67.65	43.56	0.003	4.785
	0.4	47.1	22.3	24.5	10.1	0.998	67.67	43.53		
	0.2	47.1	22.3	24.5	10.1	0.997	67.68	43.53		
	0.0	47.1	22.3	24.5	10.1	0.996	67.71	43.51		

Table 34 Optimization results of OP1 when flow ratio on major roads is 0.1

Scenario	α	Optimal solution				Optimal value	Delay	Emissions	ER_{1-0}	MV_{1-0}
	1.0	7.9	61.7	7.2	27.2	1.000	29.34	61.43		
	0.8	7.5	67.4	6.8	22.3	0.993	29.55	57.70		
No. 9	0.6	6.8	73.0	6.2	18.0	0.972	30.31	54.00	0.285	0.388
	0.4	6.0	77.7	5.5	14.8	0.931	31.90	50.77		
	0.2	4.9	82.3	4.5	12.2	0.863	35.70	47.57		
	0.0	3.7	87.6	3.5	9.2	0.715	50.93	43.91		
	1.0	7.0	34.4	11.6	51.0	1.000	33.01	67.20		
	0.8	6.7	38.4	11.1	47.8	0.998	33.09	65.80		
No. 10	0.6	6.3	44.9	10.5	42.3	0.989	33.59	63.57	0.212	0.319
	0.4	5.8	54.7	9.6	33.9	0.965	35.30	60.19		
	0.2	4.8	65.8	8.3	25.1	0.912	40.07	56.23		
	0.0	3.7	74.6	7.0	18.7	0.787	54.99	52.95		
	1.0	6.3	22.0	15.5	60.2	1.000	33.52	64.26		
	0.8	6.2	21.9	14.8	61.1	0.999	33.53	63.97		
No. 11	0.6	5.9	23.3	14.2	60.6	0.997	33.64	63.50	0.082	0.321
	0.4	5.4	26.4	13.3	58.8	0.992	34.08	62.71		
	0.2	4.7	37.4	11.8	50.2	0.976	36.68	60.82		
	0.0	3.8	49.4	10.8	40.0	0.917	42.14	58.96		

Table 35 Optimization results of OP1 when flow ratio on major roads is 0.2

Scenario	α	Optimal solution				Optimal value	Delay	Emissions	ER_{1-0}	MV_{1-0}
	1.0	11.9	70.2	6.0	15.8	1.000	26.85	63.14		
	0.8	11.2	72.6	5.6	14.5	0.996	26.97	60.64		
No. 12	0.6	10.3	75.2	5.2	13.3	0.981	27.47	58.00	0.211	0.623
	0.4	9.3	78.1	4.6	12.0	0.952	28.78	55.04		
	0.2	7.9	81.8	3.8	10.5	0.894	33.03	51.13		
	0.0	7.7	83.2	3.5	9.6	0.789	35.95	49.79		
	1.0	11.0	53.4	10.1	29.5	1.000	34.54	73.80		
	0.8	10.5	56.6	9.6	27.3	0.997	34.67	71.44		
No. 13	0.6	9.8	60.1	9.0	25.0	0.985	35.22	68.81	0.178	0.601
	0.4	9.0	63.9	8.2	22.9	0.960	36.64	65.87		
	0.2	7.7	68.8	7.0	20.5	0.911	41.14	62.03		
	0.0	7.5	70.7	7.0	18.7	0.822	44.76	60.67		
	1.0	10.3	38.7	13.7	41.3	1.000	38.82	78.77		
	0.8	10.0	41.4	13.3	39.3	0.998	38.90	77.28		
No. 14	0.6	9.5	45.1	12.7	36.8	0.991	39.36	75.24	0.135	0.556
	0.4	8.8	49.6	11.7	33.9	0.973	40.69	72.64		
	0.2	7.6	55.1	10.5	30.8	0.935	44.60	69.36		
	0.0	7.6	57.7	10.5	28.2	0.866	48.23	68.15		

Table 36 Optimization results of OP1 when flow ratio on major roads is 0.3

Scenario	α	Optimal solution				Optimal value	Delay	Emissions	ER_{1-0}	MV_{1-0}
	1.0	15.1	70.3	5.3	13.4	1.000	26.61	70.48		
	0.8	14.3	72.1	5.0	12.7	0.997	26.71	68.27		
No. 15	0.6	13.5	74.0	4.6	11.9	0.985	27.13	65.76	0.174	0.748
	0.4	12.4	76.5	4.1	11.0	0.959	28.38	62.61		
	0.2	11.3	79.4	3.6	9.7	0.906	31.64	58.90		
	0.0	11.3	80.0	3.5	9.3	0.826	32.81	58.21		
	1.0	14.2	56.6	9.0	24.2	1.000	35.51	82.21		
	0.8	13.6	58.4	8.6	23.3	0.997	35.61	80.26		
No. 16	0.6	12.9	60.8	8.1	22.2	0.988	36.08	77.81	0.134	0.814
	0.4	11.9	63.8	7.4	20.9	0.967	37.51	74.64		
	0.2	11.3	66.9	6.9	18.9	0.925	40.62	71.53		
	0.0	11.3	67.2	6.9	18.5	0.866	41.36	71.19		
	1.0	13.3	44.8	12.3	33.7	1.000	42.15	88.90		
	0.8	12.9	46.2	11.9	33.0	0.999	42.22	87.67		
No. 17	0.6	12.4	48.3	11.4	31.9	0.993	42.61	85.81	0.094	0.770
	0.4	11.5	51.5	10.6	30.5	0.978	44.03	82.99		
	0.2	11.3	54.5	10.5	27.7	0.949	47.24	80.57		
	0.0	11.3	54.6	10.5	27.7	0.906	47.29	80.54		

Table 37 Optimization results of OP2 when cycle length changes

Scenario	α	Optimal solution				Optimal value	Delay	Emissions	ER_{1-0}	MV_{1-0}
	1.0	7.2	21.6	4.3	11.0	1.000	25.18	98.51		
	0.8	7.0	21.9	4.2	10.8	0.999	25.20	97.72		
No. 2	0.6	6.8	22.5	4.0	10.6	0.996	25.35	96.43	0.101	0.462
	0.4	6.5	23.5	3.8	10.2	0.986	25.97	94.15		
	0.2	5.8	25.3	3.3	9.5	0.958	28.69	89.94		
	0.0	5.8	26.0	3.3	8.8	0.899	30.68	88.56		
	1.0	11.1	38.9	6.6	17.3	1.000	29.46	93.39		
	0.8	10.7	40.1	6.4	16.8	0.998	29.54	91.53		
No. 3	0.6	10.2	41.6	6.0	16.1	0.990	29.88	89.13	0.134	0.661
	0.4	9.5	43.7	5.5	15.2	0.972	30.96	85.85		
	0.2	8.8	46.3	5.0	13.9	0.931	33.89	81.86		
	0.0	8.8	47.0	5.0	13.3	0.866	35.43	80.89		
	1.0	14.6	57.7	8.7	23.1	1.000	35.05	90.02		
	0.8	14.0	59.6	8.3	22.1	0.997	35.16	87.76		
No. 1	0.6	13.2	61.9	7.8	21.1	0.988	35.63	85.04	0.136	0.835
(Base)	0.4	12.2	64.8	7.1	19.9	0.966	37.09	81.48		
	0.2	11.7	67.6	6.7	18.1	0.924	39.94	78.29		
	0.0	11.7	68.0	6.7	17.7	0.864	40.75	77.82		
	1.0	17.8	77.0	10.5	28.6	1.000	40.86	88.07		
	0.8	17.1	79.5	10.0	27.4	0.997	41.00	85.60		
No. 4	0.6	16.1	82.5	9.4	26.0	0.986	41.60	82.69	0.132	1.001
	0.4	14.7	86.3	8.5	24.5	0.963	43.43	78.93		
	0.2	14.6	89.0	8.3	22.1	0.921	46.23	76.49		
	0.0	14.6	89.0	8.3	22.1	0.868	46.23	76.49		

Table 38 Optimization results of OP2 when percentage of turning vehicle changes

Scenario	α	Optimal solution				Optimal value	Delay	Emissions	ER_{1-0}	MV_{1-0}
	1.0	9.2	64.2	4.9	25.8	1.000	29.87	87.02		
	0.8	8.8	66.0	4.6	24.6	0.997	29.96	84.73		
No. 5	0.6	8.2	68.1	4.3	23.3	0.987	30.36	82.11	0.146	0.724
	0.4	7.5	70.7	3.8	21.9	0.966	31.52	78.88		
	0.2	6.7	73.8	3.5	20.0	0.922	34.59	75.13		
	0.0	6.7	74.5	3.5	19.3	0.854	35.89	74.32		
	1.0	24.2	46.5	12.6	20.6	1.000	42.01	89.24		
	0.8	23.5	48.4	12.2	20.0	0.998	42.12	87.34		
No. 6	0.6	22.4	50.9	11.6	19.1	0.989	42.64	84.87	0.122	0.827
	0.4	21.0	54.3	10.7	18.0	0.970	44.35	81.42		
	0.2	20.1	57.0	10.5	16.4	0.931	47.01	78.92		
	0.0	20.1	57.6	10.5	15.8	0.878	48.18	78.39		
	1.0	37.2	32.1	19.1	15.6	1.000	51.81	78.95		
	0.8	36.8	32.9	18.9	15.5	0.999	51.86	78.38		
No. 7	0.6	36.1	34.3	18.4	15.2	0.996	52.18	77.33	0.074	0.614
	0.4	34.5	37.4	17.5	14.5	0.986	53.69	75.18		
	0.2	33.6	39.6	17.5	13.2	0.962	55.87	73.70		
	0.0	33.6	40.6	17.5	12.3	0.926	58.07	73.09		
	1.0	47.1	22.1	24.5	10.3	1.000	67.64	59.46		
	0.8	47.1	22.1	24.5	10.3	1.000	67.64	59.45		
No. 8	0.6	47.1	22.2	24.5	10.2	1.000	67.65	59.42	0.001	1.404
	0.4	47.1	22.3	24.5	10.1	1.000	67.71	59.38		
	0.2	47.1	22.3	24.5	10.1	0.999	67.71	59.38		
	0.0	47.1	22.3	24.5	10.1	0.999	67.71	59.38		

Table 39 Optimization results of OP2 when flow ratio on major roads is 0.1

Scenario	α	Optimal solution				Optimal value	Delay	Emissions	ER_{1-0}	MV_{1-0}
	1.0	7.9	61.7	7.2	27.2	1.000	29.34	68.48		
	0.8	7.4	67.2	6.8	22.5	0.994	29.53	64.62		
No. 9	0.6	6.8	72.5	6.3	18.4	0.974	30.22	60.92	0.265	0.357
	0.4	6.0	77.2	5.6	15.2	0.937	31.66	57.63		
	0.2	5.0	82.0	4.6	12.5	0.874	35.27	54.26		
	0.0	3.7	87.6	3.5	9.2	0.735	51.09	50.35		
	1.0	7.0	34.4	11.6	51.0	1.000	33.01	76.41		
	0.8	6.7	38.3	11.1	47.9	0.998	33.09	74.84		
No. 10	0.6	6.3	44.3	10.5	42.8	0.989	33.54	72.55	0.194	0.277
	0.4	5.7	53.5	9.7	35.1	0.968	35.03	69.25		
	0.2	4.9	64.4	8.4	26.3	0.922	39.27	65.29		
	0.0	3.7	74.9	6.9	18.5	0.806	56.08	61.61		
	1.0	6.4	21.1	15.3	61.2	1.000	33.51	73.85		
	0.8	6.2	21.9	14.8	61.1	1.000	33.53	73.50		
No. 11	0.6	5.9	23.3	14.2	60.6	0.998	33.63	72.99	0.087	0.127
	0.4	5.4	26.4	13.4	58.8	0.992	34.06	72.11		
	0.2	4.7	35.5	11.9	52.0	0.978	36.29	70.25		
	0.0	3.7	62.1	10.5	27.7	0.913	56.49	67.42		

Table 40 Optimization results of OP2 when flow ratio on major roads is 0.2

Scenario	α	Optimal solution				Optimal value	Delay	Emissions	ER_{1-0}	MV_{1-0}
	1.0	11.9	70.2	6.0	15.8	1.000	26.85	68.61		
	0.8	11.2	72.6	5.6	14.6	0.996	26.97	65.94		
No. 15	0.6	10.3	75.1	5.2	13.3	0.982	27.45	63.15	0.216	0.526
	0.4	9.3	78.0	4.6	12.1	0.953	28.70	60.07		
	0.2	7.9	81.7	3.8	10.6	0.897	32.82	55.96		
	0.0	7.5	83.8	3.5	9.2	0.784	37.89	53.78		
	1.0	11.0	53.4	10.1	29.5	1.000	34.54	82.05		
	0.8	10.5	56.6	9.6	27.3	0.997	34.67	79.44		
No. 16	0.6	9.9	60.0	9.0	25.1	0.985	35.19	76.61	0.177	0.551
	0.4	9.0	63.8	8.3	23.0	0.961	36.58	73.45		
	0.2	7.6	68.8	7.0	20.6	0.913	41.16	69.20		
	0.0	7.5	71.1	6.9	18.5	0.823	45.62	67.54		
	1.0	10.3	38.8	13.7	41.2	1.000	38.82	88.62		
	0.8	10.0	41.4	13.3	39.4	0.998	38.90	86.97		
No. 17	0.6	9.5	44.9	12.7	36.9	0.991	39.34	84.77	0.135	0.490
	0.4	8.7	49.4	11.8	34.1	0.973	40.63	81.94		
	0.2	7.5	55.2	10.5	30.8	0.936	44.64	78.23		
	0.0	7.5	58.3	10.5	27.7	0.865	49.51	76.67		

Table 41 Optimization results of OP2 when flow ratio on major roads is 0.3

Scenario	α	Optimal solution				Optimal value	Delay	Emissions	ER_{1-0}	MV_{1-0}
	1.0	15.1	70.3	5.3	13.3	1.000	26.61	75.39		
	0.8	14.3	72.1	5.0	12.7	0.997	26.71	73.00		
No. 15	0.6	13.5	74.1	4.6	11.9	0.985	27.14	70.26	0.176	0.732
	0.4	12.3	76.5	4.1	11.0	0.959	28.39	66.88		
	0.2	11.3	79.5	3.5	9.8	0.906	31.69	62.89		
	0.0	11.3	80.1	3.5	9.2	0.824	33.00	62.13		
	1.0	14.2	56.6	9.0	24.2	1.000	35.51	90.01		
	0.8	13.6	58.5	8.6	23.3	0.997	35.61	87.76		
No. 16	0.6	12.9	60.8	8.1	22.2	0.988	36.09	85.06	0.137	0.805
	0.4	11.9	63.8	7.4	20.9	0.967	37.53	81.56		
	0.2	11.3	66.8	6.9	19.0	0.924	40.50	78.28		
	0.0	11.3	67.3	6.9	18.5	0.863	41.53	77.71		
	1.0	13.3	44.7	12.3	33.7	1.000	42.15	98.65		
	0.8	12.9	46.2	11.9	33.0	0.999	42.22	97.22		
No. 17	0.6	12.4	48.3	11.4	31.9	0.993	42.62	95.15	0.095	0.774
	0.4	11.5	51.5	10.5	30.6	0.978	44.04	92.02		
	0.2	11.3	54.0	10.5	28.2	0.948	46.41	89.78		
	0.0	11.3	54.6	10.5	27.7	0.905	47.31	89.30		

5. EMISSION MINIMIZATION AT ARTERIAL LEVEL

The objective of this section is to propose a methodology to minimize emissions at multiple signal intersections along an arterial. Previous sections indicate that with the same level of intersection delay, on average a through vehicle generates much more excess emissions than a turning one when driving through an intersection. Therefore, the methodology proposed in this section only consider through vehicles when minimizing emissions.

First, discrete models are developed to describe the bandwidth, stops, delay, and emissions at a particular intersection. The parameters of these discrete models include second-by-second vehicle arrivals, the cycle length, the start of red time, and the duration of red time. Second, based on these discrete models, an optimization problem is formulized with the intersection offsets as the decision variables. The objective function can be the bandwidth, stops, delay, or emissions along an arterial. Third, a case study is conducted on an arterial to demonstrate the application the proposed methodology. By comparing the delay minimization with the emission minimization along an arterial, the benefit of emission reduction from the proposed methodology is recognized. The changes of other MOEs such as the bandwidth, stops, and delay are also investigated. In addition, a series of arterial scenarios is simulated to discuss this benefit of emission reduction in various situations of red time durations, intersection spacing, and intersection numbers.

5.1 Discrete Models at a Particular Intersection

This section first develops discrete models to describe the bandwidth, delay, stops, and emissions at a particular intersection. The parameters of the discrete models include vehicle arrivals, the cycle length, the start of red time, and the duration of red time. The model is called "discrete" because its parameters are discretized: the cycle length, the start of red time, and the duration of red time are all integers; and vehicle arrivals are represented by a vector with its length equal to the cycle length.

5.1.1 Bandwidth

At a particular intersection i, the vector $GW_{B,i}$ represents the green window before this intersection, with each of its elements $GW_{B,i}(j) \in \{0,1\}$. "1" represents the green window. The length of this vector is equal to the cycle length (C), i.e., $j \in \{1,2,...,C\}$.

The vector GW_i represents the green window allowed by this intersection, with each of its element $GW_i(j) \in \{0,1\}$:

$$GW_i(REM^+(j,C)) = \begin{cases} 0 & j = \{R_{S,i}+1,...,R_{S,i}+R_{D,i}\} \\ 1 & otherwise \end{cases} \quad (80)$$

where $R_{S,i}$ is the start of red time at the intersection i, and $R_{D,i}$ is the duration of red time at the intersection i. $REM^+(\cdot)$ is a function of remainder, and $REM^+(\cdot)$ is always positive. For example, when dividing j by C, $REM^+(j,C)$ is equal to the remainder if this remainder is greater than zero; otherwise, $REM^+(j,C)$ is equal to C instead of

zero. Accordingly, the green window after this intersection can be represented by vector $GW_{A,i}$ in Eq. (81).

$$GW_{A,i}(j) = \min\{GW_{B,i}(j), GW_i(j)\} \tag{81}$$

Along an arterial with I intersections, the bandwidth of this arterial can be expressed by $GW_{A,I}$, the green window after the last intersection of this arterial.

$$BA = \sum_{j=1}^{C} GW_{A,I}(j) \tag{82}$$

where BA represents the bandwidth.

5.1.2 Stops

In addition to the signal timing plan, traffic arrivals are required to estimate stops. $NV_{B,i}$ is a vector, with its j th element representing the average number of vehicles arriving at the intersection at the j th second during a cycle. The value of each element can be a continuous number. The blockage time can be estimated by solving the following problem:

$$\begin{aligned} &\text{Max} \quad B_{t,i} \\ &\text{Subject to } B_{t,i} * s_i \le \sum_{j=R_{S,i}+1}^{R_{S,i}+R_{D,i}+B_{t,i}} NV_{B,i}(REM^{+}(j,C)) \end{aligned} \tag{83}$$

where $B_{t,i}$ is a integer, representing the blockage time, and s_i is the saturation flow rate at this intersection.

With the blockage time, the vector representing the number of vehicles discharged from the intersection at the j th second, $NV_{A,i}$, can be estimated. When $B_{t,i} \geq 1$ and $B_{t,i} = 0$, the calculations of $NV_{A,i}$ are slightly different, as shown in Eqs. (84) and (85).

When $B_{t,i} \geq 1$,

$$NV_{A,i}(REM^{+}(j,C)) = \begin{cases} 0 & \\ s_i & \\ N_{B,i}(REM^{+}(j,C)) + \left[\sum_{k=R_{S,i}+1}^{R_{S,i}+R_{D,i}+B_{t,i}} NV_{B,i}(REM^{+}(k,C)) - B_{t,i} * s \right] & \\ N_{B,i}(REM^{+}(j,C)) & \end{cases}$$

$$\begin{array}{l} j \in \{R_{S,i}+1,...,R_{S,i}+R_{D,i}\} \\ j \in \{R_{S,i}+R_{D,i}+1,...,R_{S,i}+R_{D,i}+B_{t,i}\} \\ j \in R_{S,i}+R_{D,i}+B_{t,i}+1 \\ otherwise \end{array} \quad (84)$$

When $B_{t,i} = 0$,

$$NV_{A,i}(REM^{+}(j,C)) = \begin{cases} 0 & \\ N_{B,i}(REM^{+}(j,C)) + \left[\sum_{k=R_{Si}+1}^{R_{S,i}+R_{D,i}+B_{t,i}} NV_{B,i}((REM^{+}(k,C)) - B_{t,i} * s \right] & \\ N_{B,i}(REM^{+}(j,C)) & \end{cases}$$

$$j = \{R_{S,i} + 1, ..., R_{S,i} + R_{D,i}\}$$
$$j = R_{S,i} + R_{D,i} + 1 \qquad (85)$$
$$otherwise$$

To estimate stops, another vector, STV_i, is defined with its element as a indicator of stops. $STV_i(j) \in \{0,1\}$, and "1" indicates that all vehicles at the j th second of a cycle need to stop.

$$STV_i(REM^+(j,C)) = \begin{cases} 1 & j = \{R_{S,i} + 1, ..., R_{S,i} + R_{D,i} + B_{t,i}\} \\ 0 & otherwise \end{cases} \qquad (86)$$

Therefore, the number of stops at this intersection will be:

$$STOP_i = \sum_{j=1}^{C} STV_{B,i}(j) * NV_{B,i}(j) \qquad (87)$$

5.1.3 Delay and Emissions

Compared with stops, the estimation of delay and emissions are even more complicated. In addition to the vehicle arrival at each second, its corresponding departure situation is required to estimate delay and emissions. Vehicle arrivals are described by $NV_{B,i}$, and vehicle departure situations can be expressed by solving the following problem:

$$\text{Max} \quad Y_n$$

$$\text{Subject to} \sum_{j=R_{S,i}+1}^{Y_n} NV_{B,i}(REM^+(j,C)) \le s_i * n \tag{88}$$

where $n \in \{1,2,...,B_{t,i}\}$, representing the time after the end of red time (in terms of seconds); Y_n is an integer, indicating that $NV_{B,i}(REM^+(j,C))$ when $j \le Y_n$ can be discharged from the intersection within n s after the end of red time.

With both vehicle arrival and departure situations, delay can be estimated:

$$DEV_i(REM^+(j,C)) = \begin{cases} R_{S,i} + R_{D,i} + 1 - j & j \in \{R_{S,i}+1,...,Y_1\} \\ R_{S,i} + R_{D,i} + 2 - j & j \in \{Y_1+1,...,Y_2\} \\ ... & ... \\ R_{S,i} + R_{D,i} + n - j & j \in \{Y_{n-1}+1,...,Y_n\} \\ 0 & otherwise \end{cases} \tag{89}$$

where $DEV_i(j)$ is a delay vector, representing the average delay per vehicle at the j th second during a cycle. According, the total delay at this intersection, $DELAY_i$, will be:

$$DELAY_i = \sum_{j=1}^{C} DEV_{B,i}(j) * NV_{B,i}(j) \tag{90}$$

Substituting the emission function, $f_{E1}(x)$, into Eq. (90), the total emission at this intersection can be estimated as follows:

$$EMISSION_i = \sum_{j=1}^{C} f_{E1}(DEV_{B,i}(j)) * NV_i(j) \tag{91}$$

5.2 Signal Coordination Optimization

The discrete models of bandwidth, stops, delay, and emissions require such inputs as the start of red time, the duration of red time, second-by-second vehicle arrivals. Based on these discrete models, an optimization problem is formulized with the intersection offsets as its decision variables in this subsection. Denote by OFF_i the offset between the intersections of i and $i+1$, and $R_{S,i+1}$ can be computed from $R_{S,i}$.

$$R_{S,i+1} = REM^{+}(R_{S,i} + OFF_i) \tag{92}$$

In addition, denote by SP_i the travel time (i.e., time spacing) between the intersections of i and $i+1$, and $GW_{B,i+1}(j)$ and $NV_{B,i+1}(j)$ can be computed from $GW_{A,i}(j)$ and $NV_{A,i}(j)$.

$$GW_{B,i+1}(REM^{+}(j + SP_i, C)) = GW_{A,i}(j) \tag{93}$$

$$NV_{B,i+1}(REM^{+}(j + SP_i, C)) = NV_{A,i}(j) \tag{94}$$

On an arterial including I intersections, when the red time durations of all intersections and the spacing between intersections are given, the total bandwidth, stops, delay, and emissions along one direction of the arterial (e.g., inbound) can be estimated.

$$TBA = \sum_{j=1}^{CL} GW_{A,I}(j) \tag{95}$$

$$TMOE = \sum_{i=1}^{I} MOE_i \tag{96}$$

where TBA represents the total bandwidth. $TMOE$ represents the total value of a MOE, which can be stops, delay, or emissions.

To consider the performance of signal coordination in both directions of the arterial, the offsets and spacing along the outbound direction are computed from those along the inbound direction.

$$OFF_i^{(2)} = C - OFF_{I-i}^{(1)} \tag{97}$$

$$SP_i^{(2)} = SP_{I-i}^{(1)} \tag{98}$$

where the superscript $^{(k)}$ is the indicator of direction. $^{(1)}$ indicates inbound, and $^{(2)}$ outbound. As a result, the total bandwidth, stops, delay, and emissions along the outbound direction can also be computed. Therefore, the objective function of the optimization problem can be the bandwidth, delay, stops, or emissions along the arterial. The problem requires such inputs as the traffic arrivals, the red time durations, and the spacing, and the decision variables only include offsets. Considering its discrete nature, GA is used to solve this optimization problem. Figure 16 illustrates the application of GA to solving the optimization problem.

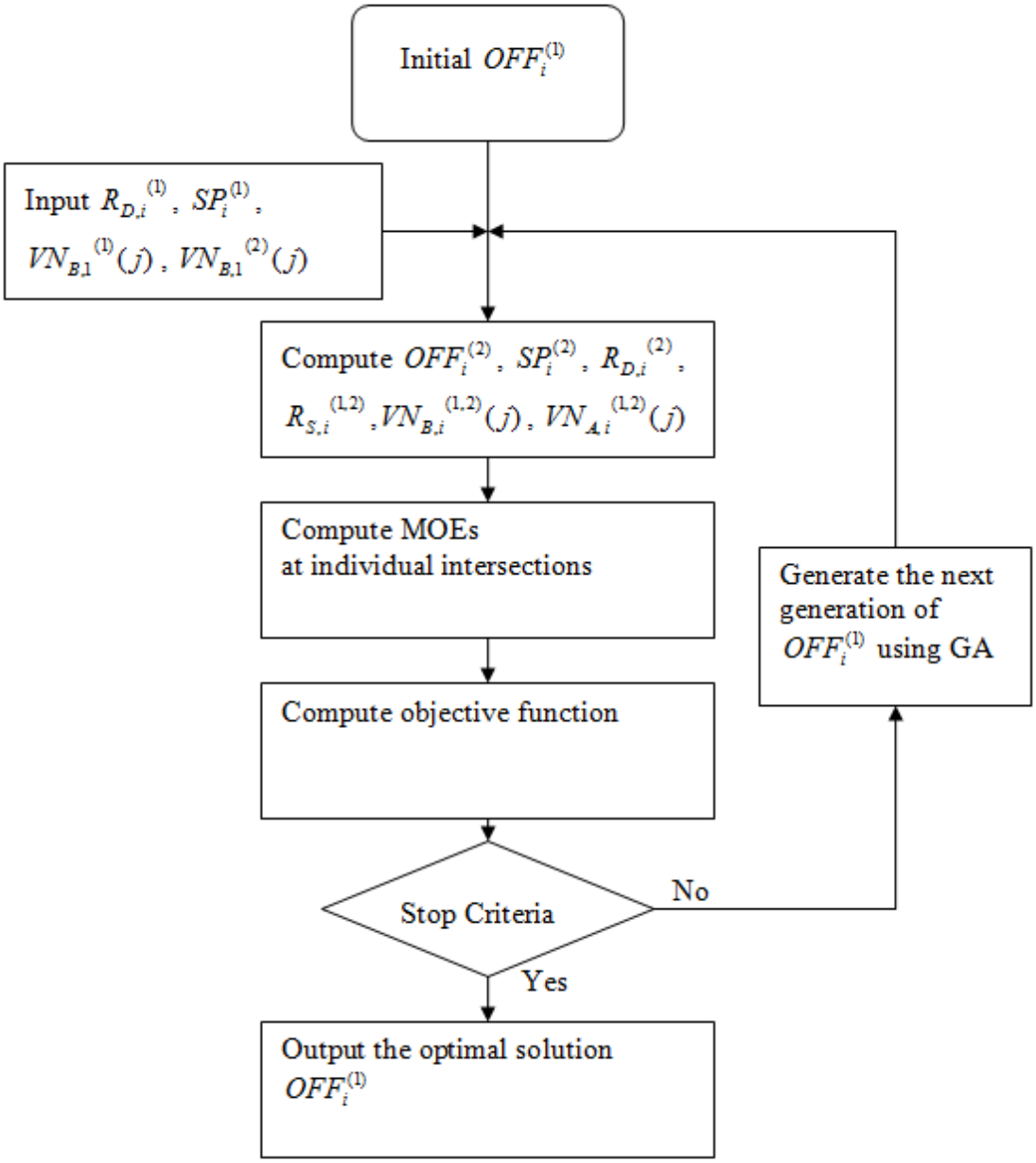

Figure 16 Application of GA to solving the optimization problem

5.3 Case Study

In this subsection, a case study is conducted to demonstrate the application of the proposed model. The benefit of emission reduction is recognized by comparing the delay minimization with the emission minimization along an arterial. The arterial in the case study includes 6 intersections, and their common cycle length is 120 s. Along each direction, there are two through lanes, and the saturation flow rate is 3600 vph. The speed limit on this arterial is 40 mph, and the emission calculation adopts the parabolic function of CO emissions developed in Section 4. The input data of traffic arrivals, red time durations, and intersection spacing are summarized in Table 42.

Table 42 Red durations, intersection spacing, and vehicle arrivals in the case study

Inbound		Red Duration	Spacing		Outbound
	Intersection			Intersection	
$NV_{B,I}^{(0)}(j) = 0.1389$ for each j (Volume = 500 vph)	6	87		1	$NV_{B,I}^{(2)}(j) = 0.1389$ for each j (Volume = 500 vph)
			32		
	5	74		2	
			74		
	4	85		3	
			23		
	3	72		4	
			21		
	2	75		5	
			27		
	1	68		6	

The optimization results are summarized in Table 43 and Table 44. Due to the large number of intersections on the arterial, the bandwidths are very small along both inbound and outbound directions. In particular when minimizing delay, the bandwidths

are equal to zero. In addition to the total values of MOEs on the entire arterial, the average values in terms of per vehicle per intersection are presented. For example, in Table 43 the average stop is 0.624 per vehicle per intersection, indicating that on average a vehicle has a probability of 0.624 to stop when it passes an intersection. Likewise, on average a vehicle causes 14.816 s delay and 39.906 mg additional CO emissions when it passes an intersection. From the delay minimization to the emission minimization, delay is increased by 0.56%, but stops and emissions are reduced by 40.04% and 31.41%, respectively

5.4 Discussion

Section 5.3 identifies the benefit of emission reduction by comparing the delay minimization with emission minimization along an arterial. The emission reduction can be as large as 40.04%. However, such an emission reduction highly depends on the structure of the arterial, such as red time durations, intersection spacing, and the number of intersections. Therefore, this subsection generates a series of arterial scenarios based on the case study in Section 5.3, and with these scenarios the benefit of emission reduction is further discussed.

Table 43 Optimization results when minimizing delay

Decision	Variables	Intersection	$GW_{A,i}$	Stops	Delay	Emissions
Inbound	$OFF_i^{(1)}$	1	52	10.83	373.75	761.17
1	57					
		2	15	16.67	516.53	1173.38
2	8					
		3	15	0.00	0.00	0.00
3	65					
		4	0	16.67	650.00	1235.53
4	73					
		5	0	0.00	0.00	0.00
5	39					
		6	0	16.67	133.33	954.36
		Total	0	60.83	1673.61	4124.44
Outbound	$OFF_i^{(2)}$	1	33	14.03	611.53	1020.32
1	81					
		2	0	16.67	578.75	1211.33
2	47					
		3	0	0.00	0.00	0.00
3	55					
		4	0	16.67	50.00	813.35
4	112					
		5	0	0.00	0.00	0.00
5	63					
		6	0	16.67	50.00	813.35
		Total	0	64.03	1290.28	3858.35
Inbound + Outbound						
		Total	0	125	2964	7983
	Average (per vehicle per intersection)			0.624	14.816	39.906

Table 44 Optimization results when minimizing emissions

Decision	Variables	Intersection	$GW_{A,i}$	Stops	Delay	Emissions
Inbound	$OFF_i^{(1)}$	1	52	10.83	373.75	761.17
1	64					
		2	8	16.67	633.19	1221.07
2	116					
		3	0	0.00	0.00	0.00
3	91					
		4	0	16.67	883.33	1298.87
4	59					
		5	0	0.00	0.00	0.00
5	45					
		6	0	0.00	0.00	0.00
		Total	0	44.17	1890.28	3281.11
Outbound	$OFF_i^{(2)}$	1	33	14.03	611.53	1020.32
1	75					
		2	3	16.67	478.75	1173.90
2	61					
		3	3	0.00	0.00	0.00
3	29					
		4	3	0.00	0.00	0.00
4	4					
		5	3	0.00	0.00	0.00
5	56					
		6	3	0.00	0.00	0.00
		Total	3	30.69	1090.28	2194.21
Inbound + Outbound						
		Total	3	75	2981	5475
	Average (per vehicle per intersection)			0.374	14.900	27.371

As indicated in Figure 16, $R_{D,i}^{(1)}$, $SP_i^{(1)}$, $VN_{B,1}^{(1)}(j)$, and $VN_{B,1}^{(2)}(j)$ are required inputs for the optimization problem. $VN_{B,1}^{(1)}(j)$ and $VN_{B,1}^{(2)}(j)$ are converted from the volume of traffic demand, which is 500 vph in the previous case study. $R_{D,i}^{(1)}$ and $SP_i^{(1)}$ are randomly generated. As shown in Table 45 and Table 46, ten random seeds are used to generate ten scenarios of $R_{D,i}^{(1)}$ and $SP_i^{(1)}$. The range of $R_{D,i}^{(1)}$ is from 60 to 100 s: the minimum value of 60 s indicates that the green ratio at any intersection is smaller than 0.5; the maximum value of 100 s ensures that any intersection does not fall into congested conditions at the demand volume of 500 vph. The range of $SP_i^{(1)}$ is from 20 to 80 s, indicating a range of geometric spacing from 1160 to 4693 ft at the speed of 40 mph. Table 45 describes arterial scenarios with 6 intersections, i.e., $I = 6$. When subsequently this study examines scenarios when $I = 5$, 4, and 3, only the first I columns of data in Table 45 are used.

Table 45 Ten scenarios of red time durations

	Intersection red time duration (s)					
Scenario	1	2	3	4	5	6
1	68	75	72	85	74	87
2	95	74	90	74	61	78
3	73	77	100	64	69	62
4	84	99	78	66	72	100
5	78	98	88	82	71	88
6	61	81	100	87	95	95
7	79	94	99	79	85	81
8	63	84	90	83	98	77
9	66	84	64	60	81	73
10	63	62	91	74	62	72

Table 46 Ten scenarios of intersection spacing

	Spacing (s)				
Scenario	1	2	3	4	5
1	27	21	23	74	32
2	70	25	79	54	63
3	32	79	69	38	21
4	56	73	59	44	29
5	36	76	42	64	46
6	40	30	32	72	38
7	79	32	30	49	61
8	50	45	27	23	51
9	67	64	54	65	30
10	46	30	68	63	29

Table 47 Simulation results on an arterial with 6 intersections

	Delay Minimization			Emission Minimization			Difference		
Scenario	Stops	Delay	Emissions	Stops	Delay	Emissions	Stops	Delay	Emissions
1	0.624	14.816	39.906	0.374	14.900	27.371	-40.04%	0.56%	-31.41%
2	0.460	10.988	22.311	0.457	11.070	18.010	-0.60%	0.74%	-19.28%
3	0.454	12.499	27.942	0.300	12.926	21.833	-34.08%	3.42%	-21.86%
4	0.558	14.233	32.725	0.394	14.512	22.739	-29.47%	1.96%	-30.52%
5	0.665	18.069	38.962	0.563	18.366	27.174	-15.27%	1.64%	-30.25%
6	0.786	19.066	48.276	0.601	19.149	32.483	-23.56%	0.44%	-32.71%
7	0.636	18.085	43.412	0.481	18.105	24.786	-24.31%	0.11%	-42.90%
8	0.751	20.732	51.484	0.663	20.897	36.778	-11.72%	0.80%	-28.56%
9	0.417	9.234	27.164	0.219	9.388	15.498	-47.52%	1.66%	-42.95%
10	0.467	8.568	21.801	0.385	9.018	16.343	-17.52%	5.25%	-25.04%
Average	0.582	14.629	35.398	0.444	14.833	24.302	-24.41%	1.66%	-30.55%
Standard Deviation	0.124	4.056	10.042	0.131	4.000	6.553	13.26%	1.51%	7.41%

Table 48 Simulation results on an arterial with 5 intersections

	Delay Minimization			Emission Minimization			Difference		
Scenario	Stops	Delay	Emissions	Stops	Delay	Emissions	Stops	Delay	Emissions
1	0.456	12.320	30.695	0.369	12.411	21.383	-19.15%	0.74%	-30.34%
2	0.405	10.986	25.974	0.241	11.879	18.144	-40.48%	8.12%	-30.14%
3	0.454	12.494	30.221	0.402	12.494	23.008	-11.47%	0.00%	-23.87%
4	0.428	8.075	21.847	0.435	8.076	18.939	1.79%	0.02%	-13.31%
5	0.516	15.903	34.756	0.488	16.211	25.972	-5.41%	1.93%	-25.27%
6	0.624	16.789	42.056	0.522	16.799	26.837	-16.31%	0.06%	-36.19%
7	0.636	18.085	39.416	0.481	18.085	24.750	-24.38%	0.00%	-37.21%
8	0.692	20.732	46.927	0.521	20.862	32.977	-24.67%	0.63%	-29.73%
9	0.190	5.843	12.656	0.137	5.844	9.929	-27.84%	0.02%	-21.55%
10	0.224	8.003	12.850	0.224	8.003	12.850	0.00%	0.00%	0.00%
Average	0.462	12.923	29.740	0.382	13.067	21.479	-16.79%	1.15%	-24.76%
Standard Deviation	0.157	4.622	11.048	0.130	4.633	6.478	12.62%	2.40%	10.61%

Table 49 Simulation results on an arterial with 4 intersections

	Delay Minimization			Emission Minimization			Difference		
Scenario	Stops	Delay	Emissions	Stops	Delay	Emissions	Stops	Delay	Emissions
1	0.259	10.163	18.785	0.249	10.258	18.210	-4.02%	0.94%	-3.06%
2	0.401	10.989	22.608	0.397	11.036	17.965	-1.21%	0.42%	-20.54%
3	0.378	12.498	25.845	0.268	12.588	19.736	-29.14%	0.73%	-23.64%
4	0.280	8.002	18.785	0.242	8.006	15.604	-13.50%	0.05%	-16.93%
5	0.514	15.903	34.194	0.488	16.200	25.966	-5.03%	1.87%	-24.06%
6	0.521	16.733	31.301	0.511	16.733	26.082	-1.97%	0.00%	-16.68%
7	0.482	15.753	33.942	0.476	15.753	23.963	-1.38%	0.00%	-29.40%
8	0.510	13.317	34.597	0.511	13.317	25.235	0.19%	0.00%	-27.06%
9	0.302	5.703	18.030	0.174	6.314	12.198	-42.30%	10.71%	-32.34%
10	0.224	8.000	12.820	0.224	8.000	12.820	0.00%	0.00%	0.00%
Average	0.387	11.706	25.091	0.354	11.820	19.778	-9.84%	1.47%	-19.37%
Standard Deviation	0.110	3.590	7.595	0.128	3.523	5.043	13.79%	3.13%	10.12%

Table 50 Simulation results on an arterial with 3 intersections

	Delay Minimization			Emission Minimization			Difference		
Scenario	Stops	Delay	Emissions	Stops	Delay	Emissions	Stops	Delay	Emissions
1	0.288	8.820	20.001	0.206	8.890	15.203	-28.43%	0.79%	-23.99%
2	0.395	10.984	22.211	0.387	11.012	17.352	-2.11%	0.25%	-21.88%
3	0.328	12.494	22.934	0.266	12.494	19.600	-18.69%	0.00%	-14.54%
4	0.227	8.002	15.825	0.242	8.003	15.602	6.61%	0.02%	-1.41%
5	0.357	14.003	25.234	0.283	14.353	20.756	-20.56%	2.50%	-17.75%
6	0.367	13.150	25.008	0.358	13.154	20.516	-2.42%	0.03%	-17.96%
7	0.332	12.420	23.159	0.324	12.431	18.766	-2.47%	0.09%	-18.97%
8	0.354	8.402	23.346	0.344	8.472	19.015	-2.98%	0.83%	-18.55%
9	0.239	5.706	15.247	0.135	5.739	9.822	-43.31%	0.58%	-35.58%
10	0.224	7.988	12.814	0.224	7.988	12.814	0.00%	0.00%	0.00%
Average	0.311	10.197	20.578	0.277	10.254	16.945	-11.44%	0.51%	-17.06%
Standard Deviation	0.059	2.627	4.189	0.074	2.668	3.387	14.89%	0.73%	9.82%

The simulation results are summarized in Table 47 through Table 50. Generally, as the number of intersections along an arterial increases, the average delay and its standard deviation both increase; likewise, the average emission and its standard division both increase with the increase of intersection number. This is so because the signal coordination becomes more complicated and difficult when the intersection number increases. In particular, signal coordination cannot favor the traffic flows along both directions of an arterial simultaneously when the number of intersections is large. Nevertheless, when the intersection number increases, the changes of all MOEs from the delay minimization to the emission minimization become more significant. Moreover, the percentages of emission reductions are much greater than those of delay increases, indicating the significant benefit from the proposed methodology in light of reducing emissions.

6. SUMMARY AND CONCLUSIONS

In urban areas, major intersections along arterials typically involve the highest traffic density, the longest vehicle idling time, and the most deceleration and acceleration. Many studies have focused on evaluating and reducing emissions at urban intersections. However, in 2011, EPA released its latest emission model, MOVES, which defines 23 operating modes and requires second-by-second vehicle speed data as an input to estimate emissions. The literature review of this study identifies a gap in the research on the emissions at signalized intersections that the signal optimization method lags behind the development of emissions models. Therefore, this study develops an optimization methodology for signal timing at intersections to reduce emissions based on MOVES. The methodology development includes four levels: the vehicle level, the movement level, the intersection level, and the arterial level. The research activities and results of each level are summarized as follows.

6.1 Vehicle Level

At the vehicle level, the emission function with respect to delay is derived for a vehicle driving through an intersection. First, Section 2.1 proposes a general method of generating vehicle trajectories from intersection delay. A proposition is deduced to prove that once the deceleration and acceleration models are determined, a unique vehicle trajectory will be generated from the intersection delay.

The general method of generating vehicle trajectories can be applicable to any form of acceleration models; therefore, Section 2.2 evaluates multiple acceleration models in terms of the accuracy of emission estimations: constant acceleration model, linearly decreasing acceleration model, and aaSIDRA model. These three models are calibrated using the field data of vehicle trajectories. With the calibrated models, second-by-second speed and acceleration data are produced. From second-by-second speed and acceleration data, emissions are estimated using MOVES. After that, emission estimations based on acceleration models are compared with field data. T-tests indicates that the aaSIDRA model is the best in the context of this study.

By substituting the aaSIDRA model to the general method of generating vehicle trajectories, emissions can be estimated corresponding to each value of intersection delay. According to the numerical results, emissions increase very fast as the intersection delay increases from 0, but the increase rate of emissions with intersection delay keeps decreasing. The reason behind this increase trend is that the emission rate for vehicle acceleration is much greater than that of vehicle idling: at the very beginning, increasing intersection delay implies the increase of acceleration process and time; later when intersection delay is greater than a threshold value, increasing intersection delay only increases idling time. Piecewise functions are used to describe the relationship between emissions and intersection delay. In addition, the adjustment is made in Section 2.4 to estimate emissions of turning vehicles, which reduce their speeds to 10 ~ 20 mph at an intersection even when they are not hindered by red signals or their leading vehicles.

6.2 Movement Level

At the movement level, emissions are modeled for a movement if its green time and red time are given. First, Section 3.1 develops a stochastic model based on Markov chains to estimate the distribution of intersection delay of individual vehicles at a movement. A state of the Markov chain is defined as the number of vehicles at the beginning of red time in a signal cycle. To account for randomness, the number of vehicle arrivals during a cycle is assumed to follow Poisson distributions to account for randomness, while within a cycle vehicles are assumed to arrive at the intersection uniformly. Two transition situations are examined, respectively considering whether all vehicles arriving during a cycle can be discharged within the same cycle.

Section 3.2 conducts numerical study considering a variety of cycle lengths, green times, saturation flow rates, and demands. Generally, as the G/C ratio increases, emissions decrease; as the degree of saturation (X) increases, emissions increase; as the cycle length increases, emissions increase; as the saturation flow rate increases, emissions decrease. The change of average emissions with respect to the G/C ratio, the degree of saturation (X), the cycle length, and the saturation flow rate has the similar trend to that of average delay; however, the change range of average emissions is much smaller than that of average delay.

Section 3.3 compares delay and emission estimations with and without considering randomness. According to the numerical results, the difference of emissions with and without considering random vehicle arrivals is much smaller than that of delay. The relative difference of delay can be greater than 100%; the relative difference of

emissions is normally smaller than 15%. In particular, at a typical major intersection of two urban arterials, where the cycle length is longer than 90 s and the saturation flow rate is greater than 3200 vph, the relative difference of emissions is even smaller than 5%. Therefore, the randomness is not considered in the optimization problem of signal timing at the intersection or arterial levels.

6.3 Intersection Level

At the intersection level, an optimization problem is formulated to consider emissions at an intersection. The objective function is a linear combination of delay and emissions at an intersection, so that the tradeoff between the two could be examined with the optimization problem. In Section 4.1 when the emission functions are piecewise, GA is used to solve the optimization problem due to the complex structure of emission functions. Moreover, the tradeoff between delay and emissions is investigated in various scenarios of cycle lengths, percentages of turning vehicles, and ratios of traffic volumes on major roads over minor roads: as the cycle length at an intersection increases emissions decrease, and more air quality benefit can be achieved; as the percentage of turning vehicles increases, minimizing delay and minimizing emissions would eventually produce the same signal timing plan; the disparity of traffic demands between the major and minor roads leads to a larger emission reduction without incurring a significant cost in delay increase.

GA is a heuristic method, and it causes intensive computation load during the process of solving optimization problems. Therefore, Section 4.2 proposes an

approximation that replaces the piecewise functions with parabolic ones in estimating emissions. It is proven that the optimization problem becomes convex with this approximation. The convex optimization problem can be easily and efficiently solved by IPA. Moreover, T-tests are conducted to compare optimization results with and without the convex approximation. The comparison indicates that although the optimization problem with the convex approximation overestimate emissions, it can still produce appropriate optimal signal timing plans when considering emissions.

6.4 Arterial Level

At the arterial level, emissions are minimized at multiple intersections along an arterial. First, Section 5.1 develops discrete models to describe the bandwidth, stops, delay, and emissions at a particular intersection. The parameters of these discrete models include second-by-second vehicle arrivals, the cycle length, the start of red time, and the duration of red time, and these parameters are discretized.

Based on these discrete models, Section 5.2 formulizes an optimization problem with the intersection offsets as the decision variables. The objective function of the optimization problem can be the bandwidth, delay, stops, or emissions along the arterial. The problem requires such inputs as the traffic arrivals, the red time durations, and the spacing. Another parameter for the discrete model, the start of red time, can be computed from the spacing and offsets. Considering its discrete nature, GA is used to solve this optimization problem. Section 5.3 illustrates the application of this optimization problem to the signal timing along an arterial with 6 intersections. From the delay minimization

to the emission minimization, delay is increased by 0.56%, but stops and emissions are reduced by 40.04% and 31.41%, respectively.

Moreover, Section 5.4 simulates a series of arterial scenarios with different red time durations, intersection spacing, and intersection numbers. Red time durations and intersection spacing are randomly generated; the intersection number increases from 3 to 6. Generally, as the number of intersections along an arterial increases, the average delay and its standard deviation both increase; likewise, the average emission and its standard division both increase with the increase of intersection number. Nevertheless, when the intersection number increases, the changes of both delay and emissions from the delay minimization to the emission minimization become more significant. Moreover, the percentages of emission reductions are much greater than those of delay increases, indicating the significant benefit from the proposed methodology in light of reducing emissions.

6.5 Final Comment and Future Research

Although the results of this study on signal timing at intersections are mainly based on MOVES, the optimization methodology is quite generalized. For example, any form of acceleration models can be used; the methodology still works even when more detailed data of vehicle motions are required in the future emission models. Therefore, future research can be conducted to adopt different acceleration and emission models and to evaluate emissions at different levels (i.e., vehicles, movements, intersections, or

arterials). Additionally, future research can focus on the design of field emission testing to validate and calibrate the signal timing obtained from the optimization problem.

REFERENCES

Akcelik, R., Besley, M., 2001. Acceleration and deceleration models. Proceedings of the 23rd Conference of Australian Institutes for Transport Research, Melbourne, Victoria.

Akcelik, R., Biggs, D., 1987. Acceleration profile models for vehicles in road traffic. Transportation Science 21, 36-54.

Barth, M., An, F., Younglove, T., Scora, G., Levine, C., Ross, M., Wenzel, T., 2000. The development of a comprehensive modal emissions model. National Cooperative Highway Research Program, Transportation Research Board, National Research Council, Washington, D.C.

Boriboonsomsin, K., Barth, M., 2008. Impacts of freeway high-occupancy vehicle lane configuration on vehicle emissions. Transportation Research Part D 13, 112-125.

Coelho, M., Farias, T., Rouphail, N., 2005a. Impact of speed control traffic signals on pollutant emissions. Transportation Research Part D 10, 324-340.

Coelho, M., Farias, T., Rouphail, N., 2005b. Measuring and modeling emission effects for toll facilities. Transportation Research Record: Journal of the Transportation Research Board 1941, 136-144.

Environmental Protection Agency, 1975. Guidelines for air quality maintenance planning and analysis. Volume 9: evaluating indirect sources. Environmental Protection Agency, Washington, D.C.

Environmental Protection Agency, 1992. User's guide to CAL3QHC version 2.0: a modeling methodology for predicting pollutant concentrations near roadway intersections. Environmental Protection Agency, Washington, D.C.

Environmental Protection Agency, 2001. MOBILE6 on-road motor vehicle emissions model 5-day training course. Environmental Protection Agency, Washington, D.C.

Environmental Protection Agency, 2002. Methodology for developing modal emission rates for EPA's multi-scale motor vehicle and equipment emission system. Assessment and Standards Division, Office of Transportation and Air Quality, Environmental Protection Agency, Washington, D.C.

Environmental Protection Agency, 2003. User's guide to MOBILE 6.1 and MOBILE 6.2 - mobile source emission factor model. Assessment and Standards Division, Office of Transportation and Air Quality, Environmental Protection Agency, Washington, D.C.

Environmental Protection Agency, 2004. Guidance on use of remote sensing for evaluation of I/M program performance. Certification and Compliance Division, Office of Transportation and Air Quality, Environmental Protection Agency, Washington, D.C.

Environmental Protection Agency, 2005. Air emission sources. www.epa.gov/air/emissions/. (Last accessed: August 30, 2011).

Environmental Protection Agency, 2009. Development of emission rates for light-duty vehicles in the motor vehicle emissions simulator (MOVES2009). Assessment

and Standards Division, Office of Transportation and Air Quality, Environmental Protection Agency, Washington, D.C.

Fitzpatrick, K., Brewer, M., Parham, A., 2003. Left-turn and in-lane rumble strip treatments for rural intersections. Texas Transportation Institute, The Texas A&M University System, College Station, Texas.

Fitzpatrick, K., Schneider, W. 2005. Turn speeds and crashes within right-turn lane. Texas Transportation Institute, The Texas A&M University System, College Station, Texas.

Frey, H., Unal, A., Rouphail, N., Colyar, J., 2003. On-road measurement of vehicle tailpipe emissions using a portable instrument. Journal of the Air & Waste Management Association 53, 992-1002.

Hurley, T., Kalus, B., 2007. Timely solutions for reducing congestion and improving air quality. Managing Congestion--Can We Do Better? ITE 2007 Technical Conference and Exhibit, San Diego, California.

Lin, J., Ge, Y., 2006. Impacts of traffic heterogeneity on roadside air pollution concentration. Transportation Research Part D 11, 166–170.

Lv, J., Zhang, Y., 2012. Effect of signal coordination on traffic emission Transportation Research Part D 17, 149–153.

Matzoros, A., Van Vliet, D., 1992. A model of air pollution from road traffic, based on the characteristics of interrupted flow and junction control: Part I - model description. Transportation Research Part A 26, 315-330.

Midurski, T., Corbin, V., 1976. Characterization of Washington, D.C., carbon monoxide problem. GCA Corporation, Environmental Protection Agency, Washington, D.C.

Tarnoff, P., Parsonson, P., 1979. Guidelines for selecting traffic signal control at individual intersections. National Cooperative Highway Research Program, Transportation Research Board, National Research Council, Washington, D.C.

Stevanovic, A., Stevanovic, J., Zhang, K., Batterman, S., 2009. Optimizing traffic control to reduce fuel consumption and vehicular emissions. Transportation Research Record: Journal of the Transportation Research Board 2128, 105–113.

Webster, F., 1958. Traffic signal settings. Road Research Technical Paper No. 39, Her Majesty's Stationary Office, London.

Zhang, Y., Ying, Q., Lv, J., Kota, S., 2010. Methodology and guidelines for regulating traffic flows under air quality constraints in metropolitan areas. Texas Transportation Institute, The Texas A&M University System, College Station, Texas.